

Macrocyclic thiourea and thioamide receptor synthesis and utilization

Master's Thesis
University of Jyväskylä
Department of Chemistry
26.4.2020
Ivan Peshev

Abstract

The theoretical part of the thesis discusses the synthetic procedures for thioamide and thiourea macrocyclic receptors and their utilization in supramolecular chemistry research. Covered receptors are organized based on their binding properties towards guests. The focus is on synthetic procedures and conducted complexation studies of macrocyclic thiocarbonyl structures. Theoretical work contains also an introductory part discussing the main principles of supramolecular chemistry that are related to the topic.

The experimental part aimed to synthesize various acyclic and macrocyclic receptors containing several thiourea moieties. Part of the successfully synthesized structures were tested for halogen bonding abilities towards guests containing iodine. Complexation studies were mostly carried in the solid-state by preparation of crystallization samples. Some endeavors also included ^1H and ^{13}C NMR binding studies. Successful attempts for halogen bond formation were achieved between tripodal thiourea receptors and perfluorinated iodobenzene guests. Results showed that the addition of pure iodine caused receptor decomposition and formation of elemental sulfur.

Tiivistelmä

Tutkielman teoreettinen osa käsittelee makrosyklisen tioamidi- ja tioureareseptorien synteessimenetelmiä ja sovelluksia supramolekyyliekemian tutkimuksessa. Käsitellyt reseptorit ovat jaoteltu sitoutumisominaisuuksiensa perusteella. Pääpaino on reseptorien synteettisten proseduurien ja kompleksaatiotutkimusten käsittelyssä. Kirjallinen osa sisältää myös johdantokappaleen, jossa käsitellään tutkielman kannalta relevantteja ilmiöitä supramolekyyliekemian tutkimuksessa.

Kokeellisen osan tavoitteena oli syntetisoida useita tioureayksiköitä sisältäviä asyklisiä ja makrosyklisiä reseptoreita. Lisäksi testattiin osan onnistuneesti syntetisoitujen tuotteiden halogeenisitoutumiskykyä jodia sisältäviä yhdisteitä kohtaan. Kompleksaatiotutkimukset suoritettiin reseptorien kiteytysyritysten kautta analysoimalla muodostuneita rakenteita röntgenkristallografialla. Halogeenisitoutumista seurattiin myös ^1H ja ^{13}C NMR tekniikoiden avulla. Työssä saatiin muodostettua halogeenisidos tripodaalisten tioureareseptorien ja perfluorattujen jodibentseeniyhdisteiden välille. Kompleksaatiotutkimusten tulokset osoittivat, että puhtaan jodin lisäys johtaa reseptorien hajoamiseen ja elementaarisen rikin vapautumiseen.

Table of Contents

Abstract.....	i
Tiivistelmä	ii
Table of Contents	iii
Preface	vi
Abbreviations	vii
Theory section.....	1
1 Introduction.....	1
2 Concepts of supramolecular chemistry.....	2
2.1 Self-assembly and complementarity.....	2
2.2 Host-guest compound classification	3
2.3 Macrocyclic effect and preorganization.....	4
2.4 Supramolecular interactions	7
2.4.1 Hydrogen bonding.....	7
2.4.2 Halogen bonding.....	9
2.5 Crystal engineering.....	11
3 Thioamide macrocycles	13
3.1 Thiocarbonyl structures.....	13
3.2 Thioamide and amide comparison.....	13
3.3 Synthetic methodologies of thioamide macrocycles	14
3.4 Conformational studies	15
3.5 Anion-binding receptors.....	16
3.6 Cation binding receptors	17
4 Thiourea macrocycles.....	19
4.1 Thiourea structures	19
4.2 Synthetic methodologies of thiourea macrocycles	20

4.3 Anion-binding structures.....	21
4.4 Anion pair receptors.....	28
4.5 Cation binding thioureas	31
4.6 Ditopic thiourea receptors	32
4.7 Thioureas as neutral hosts	35
4.8 Thioureas in gelation.....	36
4.9 Thiourea crystalline frameworks	38
5 Conclusion	39
Experimental section	41
6 Objectives.....	41
7 Synthesis of thiourea receptors	42
7.1 Receptors based on 1,3,5-tris(bromomethyl)-2,4,6-trimethylbenzene backbone.....	42
7.2 Receptors based on tris(2-aminoethyl) amine backbone	44
7.3 Dipodal based on 3-(aminomethyl) benzylamine backbone	46
7.4 Tetramethylcalix-[4]-resorcinarene based cavitands	47
7.5 Phenyl sulfone and phenyl ether based thiourea receptors	49
8 Complexation studies and crystal structures	51
8.1 Performed crystallizations.....	53
9 Conclusions	57
10 Experimental procedures	58
10.1 Overall procedures	58
10.2 1,3,5-Trimethyl-2-,4,6-tris(isothiocyanatomethyl) benzene	59
10.3 1,1',1''-((2,4,6-Trimethylbenzene-1,3,5-triyl) tris(methylene))tris(3-(2-methoxyethyl)thiourea).....	60
10.4 1,1',1''-((2,4,6-Trimethylbenzene-1,3,5-triyl) tris(methylene))tris(3-(2-(methylthio)ethyl)thiourea).....	60
10.5 1,1',1''-((2,4,6-Trimethylbenzene-1,3,5-triyl) tris(methylene))tris(3-butylthiourea)....	61

10.6 1,1',1''-((2,4,6-Trimethylbenzene-1,3,5-triyl)tris(methylene))tris(3-(naphthalen-1-yl)thiourea).....	62
10.7 1,1',1''-((2,4,6-Trimethylbenzene-1,3,5-triyl) tris(methylene))tris(3-(naphthalen-1-ylmethyl)thiourea)	62
10.8 Tris(2-isothiocyanatoethyl) amine.....	63
10.9 <i>NI</i> -(4-nitrophenyl)- <i>N2</i> , <i>N2</i> -bis(2-((4-nitrophenyl)amino)ethyl)ethane-1,2-diamine ...	63
10.10 <i>NI</i> -(<i>p</i> -Tolyl)- <i>N2</i> , <i>N2</i> -bis(2-(<i>p</i> -tolylamino)ethyl)ethane-1,2-diamine	64
10.11 <i>NI</i> , <i>NI</i> -Bis(2-aminoethyl)- <i>N2</i> -(4-nitrophenyl)ethane-1,2-diamine	65
10.12 1,3-Bis(isothiocyanatomethyl)benzene	65
10.13 1,3-Bis(isothiocyanatomethyl)benzene	66
10.14 1,1'-(1,3-Phenylenebis(methylene))bis(3-(4-nitrophenyl)thiourea)	66
10.15 1,1'-(1,3-Phenylenebis(methylene))bis(3-(<i>p</i> -tolyl)thiourea)	67
10.16 Tetramethylcalix-[4]-resorcinarene 22.....	68
10.17 Tetramethylcalix-[4]-resorcinarene 23.....	68
10.18 Tetramethylcalix-[4]-resorcinarene 24.....	69
10.19 1,1'-(Sulfonylbis(4,1-phenylene))bis(3-(4-nitrophenyl)thiourea)	70
10.20 1,1'-(Sulfonylbis(4,1-phenylene))bis(3-(<i>p</i> -tolyl)thiourea)	70
10.21 2,8-Dithia-4,6,10,12-tetraaza-1,3,7,9(1,4)-tetrabenzenacyclododecaphane-5,11-dithione 2,2,8,8-tetraoxide	71
10.22 1,1'-(Sulfonylbis(4,1-phenylene))bis(3-(7-amino-9H-fluoren-2-yl)thiourea).....	71
10.23 7H,17H-2,12-Dithia-4,6,8,10,14,16,18,20-octaaza-7,17(2,7)-difluorena-1,3,11,13(1,4)-tetrabenzenacycloicosaphane-5,9,15,19-tetrathione 2,2,12,12-tetraoxide....	72
10.24 2-Thia-4,6,10,12-tetraaza-1,3(1,4),8(1,3)-tribenzenacyclododecaphane-5,11-dithione 2,2-dioxide	73
10.25 2-Oxa-4,6,10,12-tetraaza-1,3(1,4),8(1,3)-tribenzenacyclododecaphane-5,11-dithione	73
11 References	75
Appendix – NMR and MS spectra	83
Appendix – Crystal structures.....	116

Preface

The thesis is conducted at the University of Jyväskylä - Department of Chemistry as a part of Arto Valkonen's project on "Robust S \cdots I $^+$ \cdots S halogen-bonded supramolecular assemblies" (Academy of Finland project no. 314343). The experimental work was done during Fall of 2019 with the collaboration of Kari Rissanen's supramolecular chemistry research group under the close supervision of Arto Valkonen and Lauri Happonen.

Interest towards supramolecular chemistry originated from my master's program in nanoscience that contained a multidisciplinary studying approach in chemical, physical and biological contexts. Hence, I aimed to find a versatile thesis subject, where I can utilize this studying background with an emphasis on synthetic organic chemistry. The opportunity to work in supramolecular research gave me the possibility to combine both. Starting with basic synthetic practices and ending in supramolecular material assembly.

I would like to thank my close supervisors, Arto and Lauri for proper guidance and encouragement during the project. In addition, all other members of Rissanen's group for valuable pieces of advice and inspirational company. Thank you to Toni Metsänen for support and verification of the thesis.

Jyväskylä 1.4.2020

Ivan Peshev

Abbreviations

A	Acceptor atom in an intermolecular interaction
ACN	Acetonitrile
AIBN	Azobisisobutyronitrile
Boc	<i>tert</i> -Butyloxycarbonyl
BSA	Bis(trimethylsilyl)acetamide
<i>cis</i>	Arrangement of functional groups on the same side from the bond or plane
D	Donor atom in an intermolecular interaction
d	Duplet
DBUH	1,8-Diazabicyclo[5.4.0]undec-7-ene
DCC	<i>N,N'</i> -Dicyclohexylcarbodiimide
DCM	Dichloromethane
DMA	Dimethylacetamide
DMF	<i>N,N</i> -Dimethylformamide
DMSO	Dimethyl sulfoxide
DNA	Deoxyribonucleic acid
<i>E</i>	Entgegen, according to Cahn–Ingold–Prelog nomenclature arrangement of substituents on the different sides of the bond
<i>ee</i>	Enantiomeric excess
<i>endo</i>	Refers to the inner part of macrocyclic structure
Et	Ethyl group
EtOAc	Ethyl acetate
EWG	Electron withdrawing group
FT-IR	Fourier transform infrared spectroscopy
HB	Hydrogen bonding
Hex	Hexane

HPLC	High pressure liquid chromatography
LR	Lawesson's reagent
Me	Methyl group
MO	Molecular orbital
MS	Mass spectrometry
n	Orbital occupied with an electron pair
NBS	<i>N</i> -Bromosuccinimide
NMP	<i>N</i> -Methylpyrrolidinone
NMR	Nuclear magnetic resonance
OAc	Acetoxy functional group
ORTEP	The Oak Ridge Thermal Ellipsoid Plot
p	Pentet
q	Quartet
rt	Room temperature
s	Singlet
sx	Sextet
t	Triplet
TBAB	Tetrabutylammonium bromide
THF	Tetrahydrofuran
TLC	Thin layer chromatography
<i>trans</i>	Arrangement of functional groups on the different side from the bond or plane
XB	Halogen bonding
Z	Zusammen, according to Cahn–Ingold–Prelog nomenclature arrangement of substituents on the same side of the bond

Theory section

1 Introduction

In the context of this thesis, a receptor is a molecular structure that expresses a binding affinity toward other compounds via intermolecular (supramolecular) interactions. Natural receptors mostly occur as macromolecular structures, where each part of the molecule plays a role in overall conformation and position of functional groups, which further affects the binding specificity. Hence, when designing synthetic receptors, it is essential to study the nature of supramolecular interactions and rely heavily on the previously published results. Nevertheless, the presence of a trial-and-error approach remains strong in supramolecular chemistry research.¹

This thesis focuses on macrocyclic receptors bearing several thiourea- and thioamide functional groups. Macrocycles are compounds consisting of one or more rings of a minimum of 12 atoms. Thiourea- and thioamide groups can be a part of the macrocycle itself or as a side-chain extension (Figure 1.1). The binding site of these types of receptors is located at the NH-groups or sulfur of thiocarbonyl. It is also typical that other functional groups are involved in the binding process. Overall, there are several chemical and environmental factors that affect the receptor's performance, making it a delicate entity where each atom matters.

The theory section contains examples of macrocyclic thiocarbonyl receptor synthesis and their complexation studies. Receptors are categorized by their binding properties and possible applications. Since there is a vast amount of methodologies for macrocycle synthesis, the focus remains on the insertion of thioamide- and thiourea groups into a macrocyclic backbone.

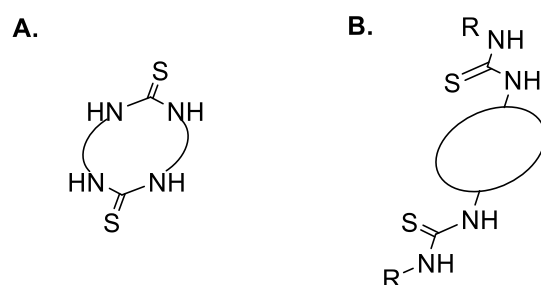


Figure 1.1. Exemplary representation of macrocyclic receptor with **(a)** thiourea-group enclosed and **(b)** outside of the ring.

2 Concepts of supramolecular chemistry

In the early stages of supramolecular chemistry development, it was mainly described through intermolecular non-covalent interactions between a “host” and a “guest” molecule. As the research evolved further, the complexity and diversity of supramolecular structures grew leading to more versatile opportunities for their utilization. In addition to host-guest concepts, modern supramolecular chemistry extends to the design of molecular devices, nanomachines and complex functional materials, which could be utilized in various branches of industry and pharmaceutical development.^{2,3,4} Despite the fast progress in the field, fundamental principles of supramolecular and macrocyclic chemistry have remained relatively unchanged. This chapter discusses core supramolecular concepts in the scope of the thesis project.

2.1 Self-assembly and complementarity

Molecular recognition through noncovalent interactions and self-assembly are fundamental concepts of supramolecular design. The process could be demonstrated as a jigsaw puzzle in [Figure 2.1](#), where only complementary pieces fit together, leading to the most favorable conformation **A**. The pieces could also be forced in conformation **B** if enough energy is applied. However, due to the poor compatibility and tension, the structure would rather prefer the initial disordered arrangement. Since **A** has perfect compatibility between all parts and the lowest energy, it appears to be the most favorable conformation.⁵ Phenomena, where product formation is driven by its energetics, is called thermodynamic control and is one of the key concepts of supramolecular assembly. Descriptive examples of thermodynamic control and self-assembly can be found in various biological systems and processes, which have been a huge inspiration for supramolecular structure development.

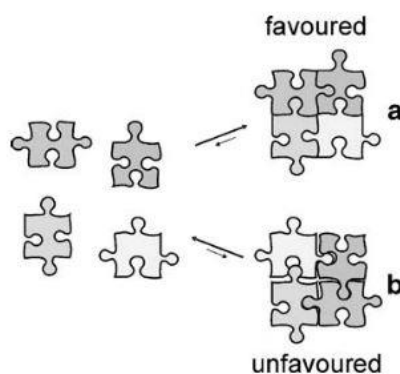


Figure 2.1. Simplified representation of supramolecular self-assembly. *With permission of Copyright © 2007, Springer Nature.*⁵

2.2 Host-guest compound classification

Supramolecular structures can be roughly divided into three groups (Figure 2.2). Cavitands that possess permanent molecular cavities, making its host-acting ability as a permanent molecule's feature. Since cavitand has an intrinsic molecular cavity, it forms complexes in both liquid and solid states. On the contrary, clathrands possess extramolecular cavities in the gaps located between the molecules, which are arranged in a crystalline lattice. These types of structures usually exist only in the crystalline or solid-state. The third group holds the supramolecular self-assembly aggregates that do not fit either of the previous descriptions. These form large supramolecular assemblies through weak interactions but do not express any host-guest characteristics, like cavitands and clathrands.⁴

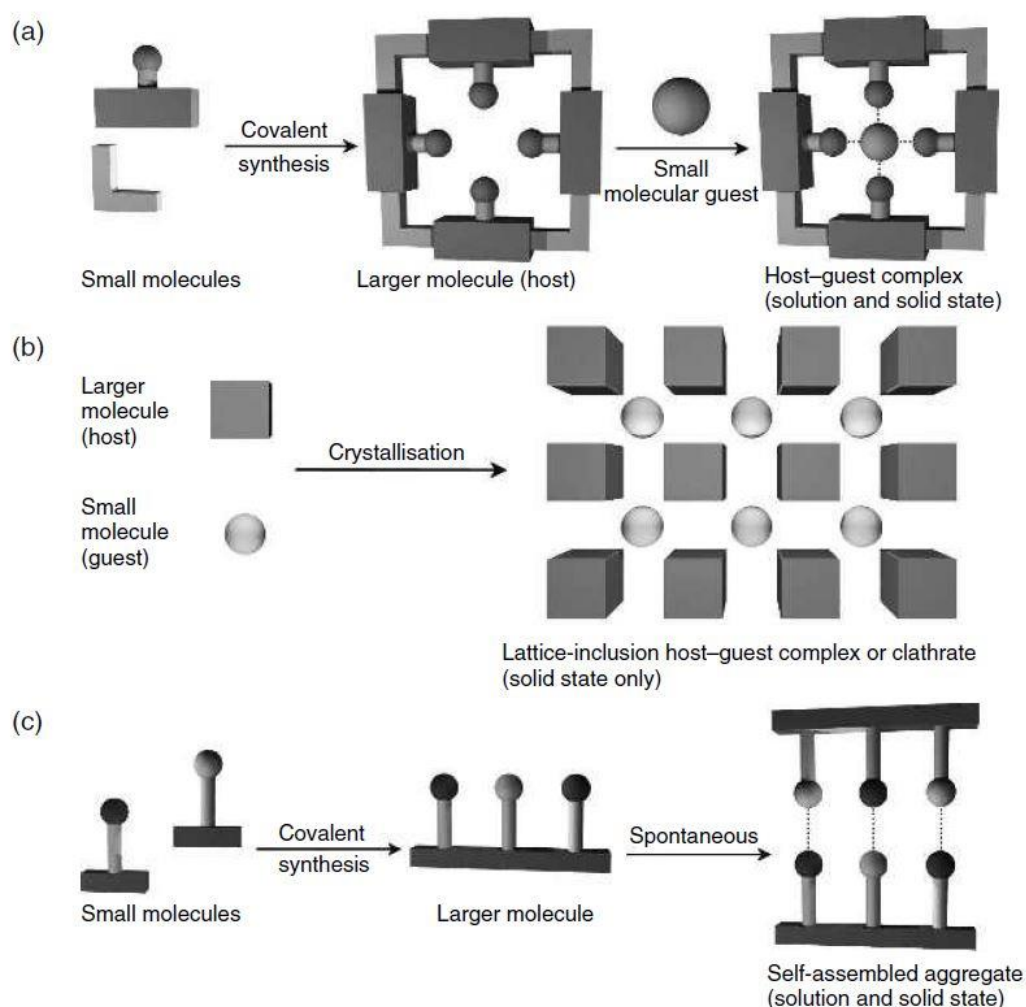


Figure 2.2. Rough classification of supramolecular structures. **(a)** Cavitands having an intrinsic host-guest binding property, **(b)** clathrands with extramolecular cavities in crystalline lattice and **(c)** supramolecular self-assembly aggregates. *With permission of Copyright © 2007, American Chemical Society.*⁶

Depending on the molecular structure, cavitands can be further divided into podands, coronands, cryptands, and spherands. Acyclic podands contain donor atoms (D) connected by the chain segment. These can also form more complex assemblies, where several podands are interconnected via the anchor group (Figure 2.3). Coronands can be described as cyclic versions of podands that appear as macrocyclic structures. Like podands, these can form multimers, where several coronands are connected through an anchor atom.^{4,7}

Cryptands are cage-like compounds, where chain segments and donors are interconnected by bridgehead atoms (B), which are typically carbon, nitrogen, sulfur or phosphorus. These molecule types are more rigid than coronands, showing less conformational flexibility and hence more binding specificity. However, the most rigid conformations are found from spherands. In these macrocycles binding sites are fixed in the space relative to each other, making the spherand well preorganized, which enhances the complexation strength.⁸ Preorganization and other complex stability related factors are discussed in the following chapters.

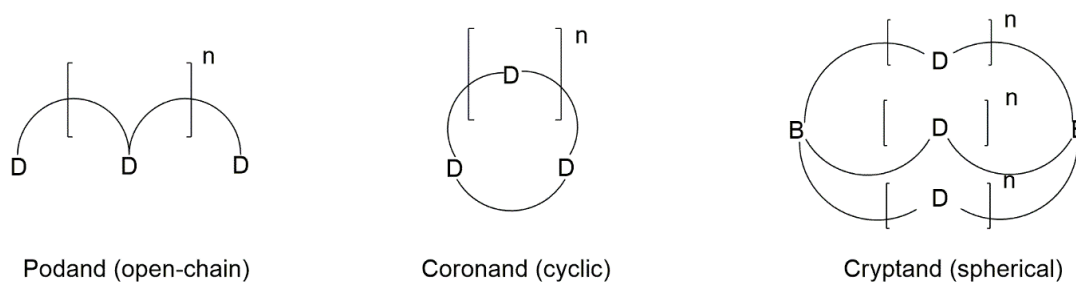


Figure 2.3. Subcategories of cavitands.⁷

2.3 Macroyclic effect and preorganization

Generally, macrocycles are defined as cyclic structures bearing at least one ring of a minimum of 12 atoms. The structures tend to have molecular weights in the 500 – 900 Da range and a vast number of donors/acceptors for intermolecular interactions. Macroyclic structures are widely abundant in nature as fundamental operational units in various biochemical processes.

Before the development of macrocycle synthesis methodologies, they were mainly extracted from natural products and peptides.⁹ According to current estimation, 20% of natural products appear as macrocyclic structures, from which over 50% obtain rings in the 13 – 19 atom range.¹⁰

Figure 2.4 shows that the most common occurrences appear to be 14, 16 and 18 sized rings. Cyclic structures provide extra rigidity and conformational restriction, which are the most important features of macrocycle functionality.

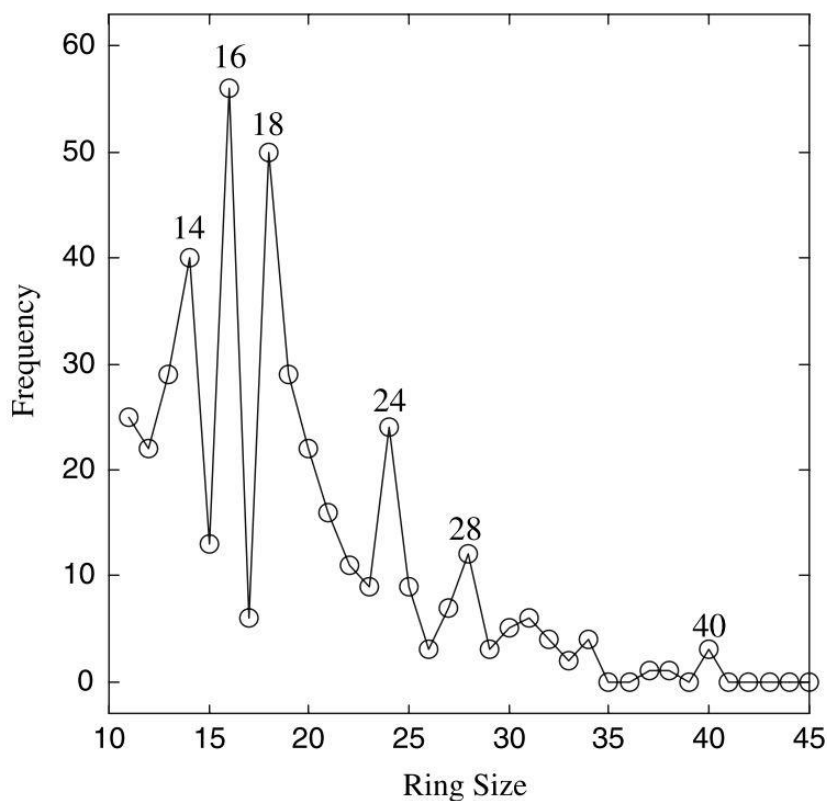


Figure 2.4. Macrocycle abundance frequency as a function of ring size. *With permission of Copyright © 2007, Springer Nature.*¹⁰

The stability of macrocyclic complexes can be partially explained by a macrocyclic effect, which relates to the chelation effect and preorganization. Chelation is observed among coronands, cryptands, and spherands, which all typically contain several donor/acceptor sites in their binding cavities. When multiple donors/acceptors contribute to the same binding site, the complexation is strengthened, leading to a higher binding affinity.¹¹ In addition, the preorganization of the macrocycle plays an essential role in the stability of a complex. Cram and colleagues¹² notated this aspect already during the early stages of supramolecular research. The studies showed that organization factor was proportional to the host-guest binding constant (K_a).¹³ This dependence is illustrated in Figure 2.5, where Na^+ ion complexation is carried with variously preorganized compounds and possessing similar acceptors at their binding sites.

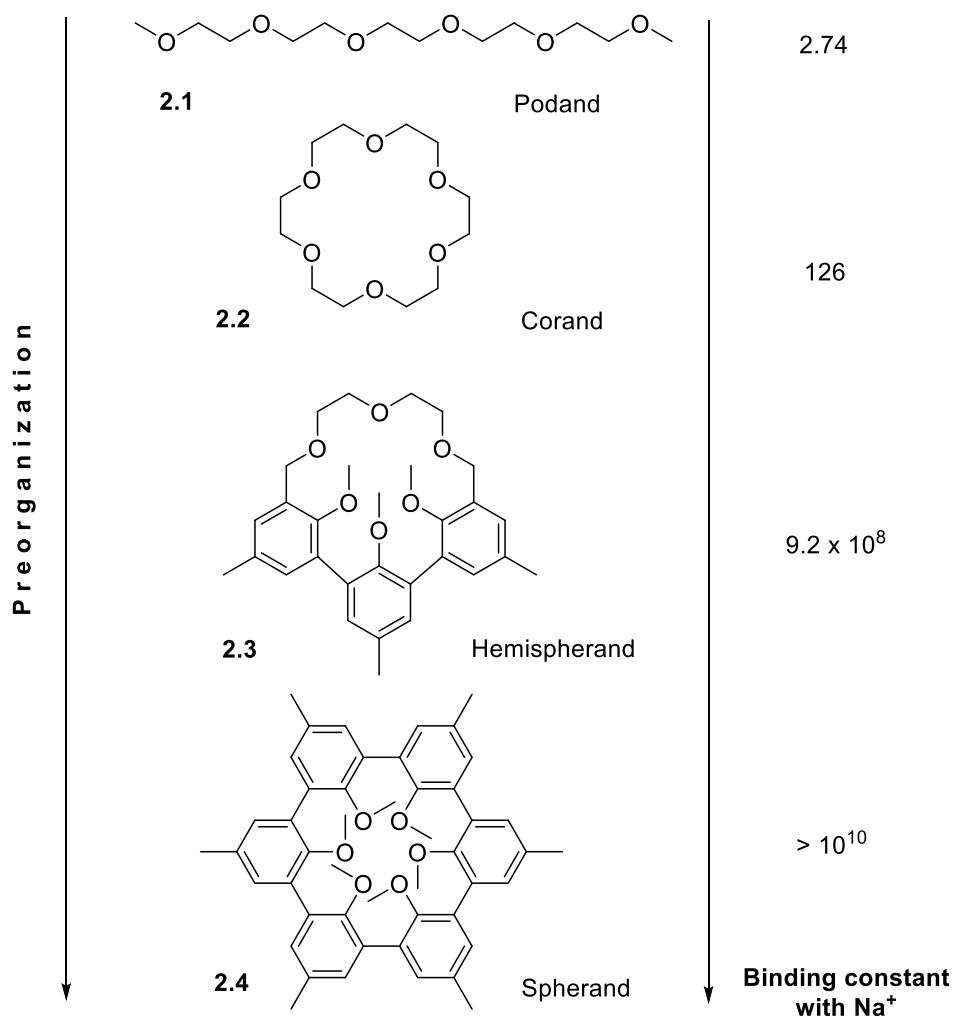


Figure 2.5. Comparison of Na⁺ binding constants in differently preorganized structures containing six oxygen donors.¹⁴

From the thermodynamic perspective, the host-guest binding process can be divided into two parts – energy required for interaction and energy of host rearrangement during complexation. According to equation (1), the sum of these terms represents the total complexation energy, where the change in free energy ΔG is derived from the Gibbs equation (2). Hence, the more negative $\Delta G_{\text{complexation}}$ is, the larger is the effect of preorganization.

$$\Delta G_{\text{complexation}} = \Delta G_{\text{interaction}} - \Delta G_{\text{rearrangement}} \quad (1)$$

$$\Delta G = -RT \cdot \ln K_{\text{association}} \quad (2)$$

In the case of well-preorganized hosts, the energy cost of rearrangement is already paid during the synthetic procedure, which leads to higher binding specificity and larger association constant. Achieving maximum preorganization is one of the main goals of macrocyclic molecular design in modern supramolecular chemistry.¹⁴

2.4 Supramolecular interactions

Supramolecular interactions occur between molecules through electromagnetic forces as attractive or repulsive interactions. In contrast to covalent bonding, intermolecular forces do not involve electron sharing, but rather occur due to polarizability and charge imbalance/transfer. They are also 10 – 100 times weaker than covalent interactions, ranging from 5 kJ/mol to 150 kJ/mol.¹⁵ Intermolecular interactions tend to determine essential chemical and physical properties of solid-, liquid- and gas state systems. Through self-assembly and organization control, intermolecular forces can sustain proper macromolecular shapes, retaining their functionality and hence being a crucial phenomenon in biological and supramolecular systems.^{4,16}

There is a vast amount of noncovalent bonding types, from which the most relevant are ion-ion, ion-dipole, dipole-dipole, hydrogen bonding (HB), halogen bonding (XB), van der Waals and various interactions involving π -systems.⁴ The hydrogen bonding is undoubtedly the most common and widely studied in supramolecular chemistry and macrostructural self-assembly. In addition to other weak interactions occurring in biological systems, HB plays a significant role in the functionality of DNA, peptide folding and molecular recognition, which allows communication on a biochemical level.¹⁷

Recently, also understanding and investigation of XB systems have brought new insight into the possibilities of utilizing noncovalent interactions in supramolecular applications. Main advantages of XB result from its bond directionality and binding specificity. These characteristics can be utilized *e.g.* in pharmaceuticals or functional material design.¹⁸ This chapter will briefly discuss only HB and XB interactions since they are the most relevant noncovalent forces related to the project.

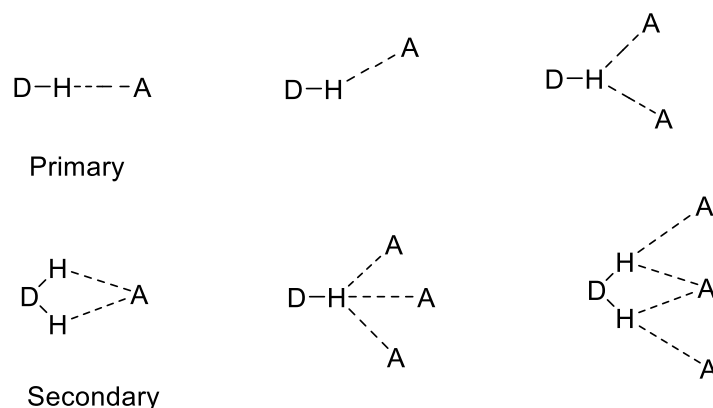
2.4.1 Hydrogen bonding

According to the IUPAC definition, HB occurs as an attractive interaction between Y-H, where Y is more electronegative than H, and an atom or a group of atoms located on the same or a different molecule. The system consists of acceptor (A) that possesses electron rich region (A = O, N, F, S) and a donor (D), which is electron deficient hydrogen.¹⁹ In addition to electrostatic bonding, strongest HBs has a partial orbital overlap and hence some covalent characteristics. This could be rationalized by a shorter van der Waals radii of hydrogen bonded assembly.¹⁷ Depending on the strength, HB interactions can be roughly divided into three groups, which properties are presented in [Table 2.1](#).

Table 2.1. Properties of HB interactions.⁴

	Strong	Moderate	Weak
Y – H ... A interaction	Mainly covalent	Mainly electrostatic	Electrostatic
Bond energy (kJ mol⁻¹)	60 – 120	16 – 60	<12
Y ... A (Å)	1.2 – 1.5	1.5 – 2.2	2.2 – 3.2
Y ... A (Å)	2.2 – 2.5	2.5 – 3.2	3.2 – 4.0
Bond angles (°)	175 – 180	130 – 180	90 – 150

Several HB geometries occur depending on environmental factors. Usually stronger HBs tend to have higher directionality achieving geometries close to 180°. Weaker interactions have less covalent character and more conformational freedom, occurring even at 90° angles. Interaction is called primary HB if it is a direct connection between a donor and an acceptor. Secondary hydrogen bonds bind to the neighboring HB systems, which are already primarily bonded (Figure 2.6). These types of interactions are typical in large self-assembly structures, *e.g.* DNA.⁴

Figure 2.6. Primary and secondary hydrogen bonding patterns.⁴

The presence of HB can be observed with various spectroscopic methods like FT-IR, NMR, and Raman. Infrared spectroscopy is particularly sensitive towards HB, causing the vibrational shift and band broadening. The stronger the HB, the more increased is the vibrational frequency of the bond, causing a larger band downshift.²⁰ Characteristic signatures are recognized in NMR due to the deshielding of D-H proton, which can be mostly observed with spin-spin couplings and nuclear Overhauser enhancement.¹⁹

HB formation and its strength are affected by several factors, which depend on the acceptor/donor molecular structure and environmental conditions. Herschlag and Pinney¹⁷ have simplified hydrogen bonding characteristics down to the five essential approximations that help to describe the overall nature of HB.

1. The length of HB stays constant regardless of the environment, which allows its consideration as a covalent species.
2. HB becomes shorter when ΔpK_a between donor and acceptor decreases resembling the supramolecular principle of complementarity. However, some deviations may be observed due to HB coupling and steric interactions.
3. HB complex formation free energy-wise (ΔG_f^{HB}) is more favorable in nonpolar environments since there are fewer competing donors and acceptors.
4. In contrast to previous, HB complexes are less stable in nonpolar environments due to the high free energy transfer from dipolar complex to nonpolar environments.
5. The free energy of HB complex formation (ΔG_f^{HB}) is more favorable with decreasing ΔpK_a . The phenomenon is observed in all solvents but is stronger in nonpolar environments.

2.4.2 Halogen bonding

The halogen bond occurs between the electrophilic region at the halogen atom and the nucleophilic region of another atom or an atom group. A halogen atom (X) is acting as an XB donor to acceptors, which are mostly atoms that possess high electron density and free electron pairs (Figure 2.7). Most commonly these are light pnictogens and chalcogens *e.g.* nitrogen, oxygen, sulfur, and selenium. Donors that form XB contain iodine, bromine, or chlorine as a halogen atom. In exceptional circumstances, also fluorine is known to take part in halogen bonding. Like hydrogen bonding, XB can have an intra- or intermolecular nature.^{18,21}

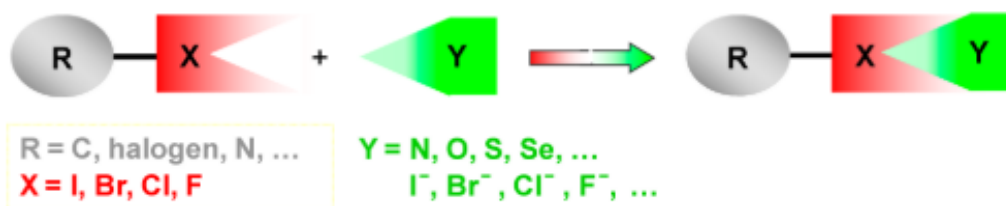


Figure 2.7. Schematic representation of halogen bond. *With permission of Copyright © 2016, American Chemical Society.*¹⁸

The emergence of XB interaction is described with a σ -hole occurring at the outermost part of X as a positive electrostatic potential. This arises mainly from the electronic properties of binding group R. Due to the electronegativity strength of R; three unshared electron pairs of halogen atom are attracted to R forming a negative electrostatic potential around the central region of X. The positive potential, a σ -hole, left at the outer shell of X can act as a supramolecular binding site for the electron-rich compounds.²² The bond is formed when electron-rich Lewis basic site of Y donates electron density to the Lewis acidic site of X. The strength and characteristics of formed XB depends highly on the individual interacting species and are affected by electrostatic effects, like polarization, charge transfer and dispersion forces.²³

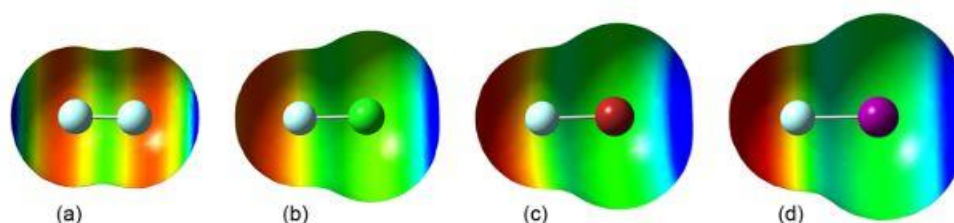


Figure 2.8. Surface electrostatic potential of XF compounds, where X=F, Cl, Br and I. The respective magnitudes of σ -hole are 56.7, 169.3, 205.9 and 258.3 kJ/mol. Results calculated by Wang *et al.* With permission of Copyright © 2016, American Chemical Society.²³

One of the interesting XB features is its high tunability. Since the anisotropic distribution of electron density is mainly caused by the binding group, changes in R and its substituents can have a large effect on the σ -hole size. This phenomenon is illustrated in Figure 2.8, where electrostatic surface potentials were calculated for different XF compounds by Wang and colleagues.²³ With growing electronegativity difference between X and F, the size of positive potential (σ -hole) significantly increases.¹⁸

σ -hole magnitude increases proportionally with the diameter of a halogen donor atom (X), defining the XB strength order to Cl < Br < I. Larger size comes together with higher polarizability and lower electronegativity, which are both important factors for σ -hole formation. For instance, fluorine as the smallest halogen is known to form really weak XB interactions only in some special conditions, *e.g.* fluorine molecule (F₂).^{24,25}

Recently, there has been a vast amount of studies conducted on XB interactions. It has become a promising tool in the fields of molecular recognition and functional material design. There are few interesting properties of XB which have attracted bigger attention of the academic society.²⁶

1. Forming σ -hole on the outermost surface of the X is strictly confined to the R-X covalent bond axis, which makes XB highly directional forming bond angle close to 180° .²⁵
2. The strength of a σ -hole is easily adjustable by changing the halogen atom or/and altering the electron-withdrawing properties of XB moiety.²⁴ A comparison could be made to H-bonding, where adjusting the strength requires major changes in the molecular structure.
3. R-X moieties are relatively nonpolar, which increases the hydrophobicity of a molecule. Hence halogen-bonded compounds are less affected by a polar environment, *e.g.* compared to hydrogen bonding, where solvent molecules are constantly competing for HBs.²⁷
4. Large van der Waals radii of the donor (halogen) atom can be utilized in more specific binding and modification of the compound's optoelectronic properties. Parker *et al.* were able to reach high specificity in binding DNA base pairs with bromine.²⁸

2.5 Crystal engineering

The main objective of crystal engineering is to investigate crystal packing principles through deeper understanding and utilization of intermolecular interactions. To obtain novel structures and functional materials, crystal design relies heavily on the observations and structural analysis of previous results. In contrast to classic molecular synthesis, where accurate synthetic schemes have an essential role in molecular design, synthetic protocols for crystal structures remain less predictable. Therefore crystal science requires consideration of multiple energetical, structural and synthetic factors, which incorporates theoretical and experimental approaches in multidisciplinary research context.²⁹

Supramolecular valence, which is governed by geometry and chemistry of intermolecular interactions, is the key concept in the design of crystal structures. The building blocks of crystals (tectons) consist of regular supramolecular motifs (synthons) that are employed in the engineering of crystalline materials. Some of the common supramolecular synthons are presented in [Figure 2.9](#). The design of tecton's geometry and topology aims to develop patterns, which define a material's functionality in terms of useful physical properties.³⁰ However, modern crystal engineering not only aims to develop crystals with purpose, but also defines new purposes for crystal design.³¹

Since intermolecular interactions are strongly defined by the enclosing environment, the solid-state has relevance in crystal design. It is also important to notice that same supramolecular synthons can emerge in various crystal structures, possessing different functionalities. Therefore, the minimum interference between single supramolecular synthons is a desirable goal. The synthesis of crystal structures is anything but straightforward and requires distinctive synthetic approaches. The most common methodologies include solution-phase methods, *e.g.* diffusion, evaporation, and slow cooling. More exotic approaches include crystal growth at low temperatures and elevated pressure, together with other solvent-free methods.³¹

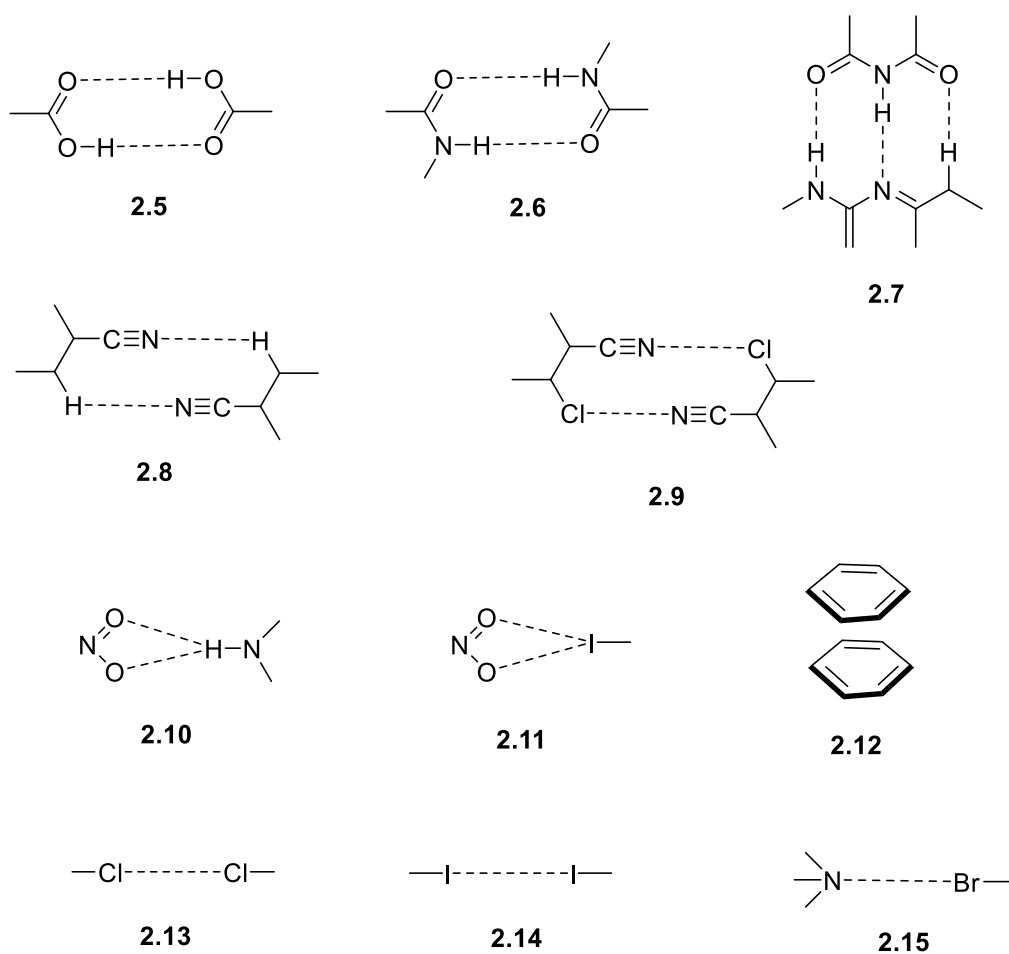


Figure 2.9. Examples of common supramolecular synthons.³⁰

3 Thioamide macrocycles

3.1 Thiocarbonyl structures

Electrophilic and nucleophilic nature of sulfur, together with its ability to form hypervalent compounds makes it a versatile tool in organic synthesis. Located below the oxygen in the periodic table, sulfur possesses d-orbitals, which allows it to appear at oxidation states of 2, 4 or 6 and have coordination numbers from 0 to 7. It has also lower electronegativity of 2.58 compared to oxygen's 3.44, which is observed as less polarized bonds with carbon atoms.

Due to the low electronegativity difference and a poor overlap of carbon's $2sp^2$ orbital with $3sp^2$ orbital of sulfur, thiocarbonyl (C=S) compounds are less stable than its carbonyl (C=O) analogues. Therefore, molecules containing C=S group must be stabilized through extra conjugation with adjacent, relatively electronegative substituents *e.g.* oxygen or nitrogen. This stabilization factor is well present in thioamide and thiourea compounds and will be discussed in the following chapters, together with other chemical aspects related to macrocycles bearing thiocarbonyl backbone.³

3.2 Thioamide and amide comparison

Description of thioamide's electronic properties can be explained by a comparison between its amide analogue. As mentioned above, C=S orbital overlap is poorer than in corresponding C=O, which also places C=S molecular orbital (MO) to a higher energy level.³² The energy gap is mostly reduced through the delocalization of C=S MO to adjacent bonds. This factor is strongly present in thioamide compounds, which appear as resonance structures presented in [Figure 3.1 a](#). Several studies have confirmed that due delocalization rotational barrier of thioamide derivatives is significantly larger than in amides.^{33,34,35,36} This results in reduced conformational flexibility and hence increases the preorganization of supramolecular synthon, which can be utilized in the design of selective ligands.

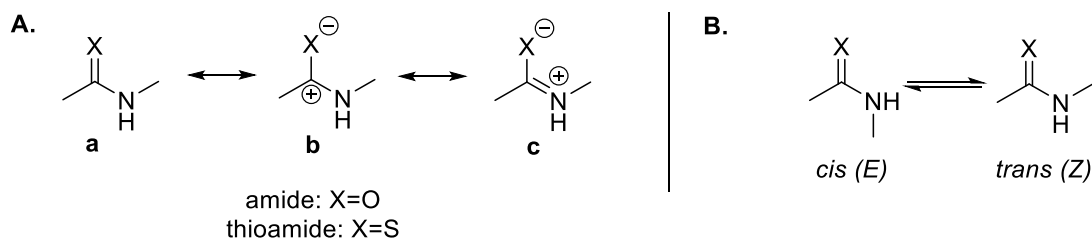


Figure 3.1. **(a)** Resonance structures of peptide-bond isosteres **(b)** Equilibrium of *cis-trans* conformations in peptide bond.³⁴

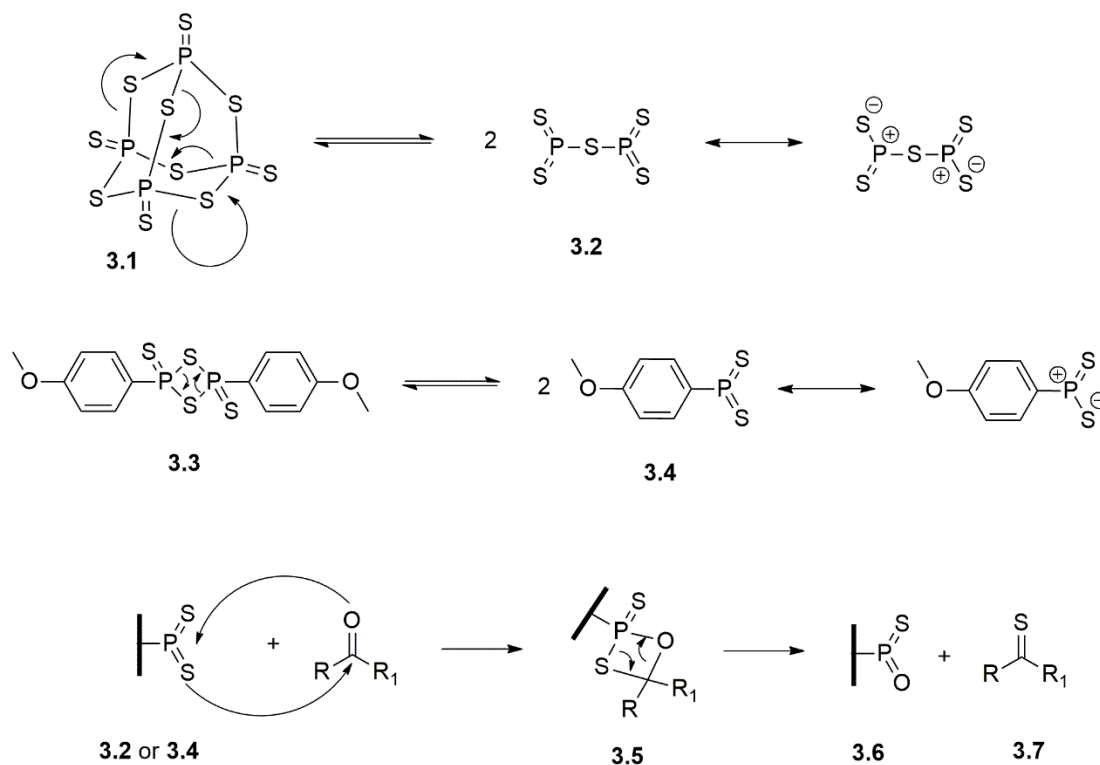
Planar conformation of peptide bond mostly emerges from conformation **c** (Figure 3.1), where nitrogen's lone pair n is delocalized into C=O(S) antibonding orbital π^* . Delocalization in thioamides is increased due to sulfur's greater affinity for the lone electron pair of nitrogen.³⁶ According to computational studies, the thioamide C=S bond appears to be longer (1.65 Å) than the corresponding C=O bond (1.23 Å) in amides. Besides, the delocalization of nitrogen lone pair slightly reduces the C-N bond length (1.35 Å), whereas C-N bond in amide is 1.37 Å.³⁴

Regarding the noncovalent interactions, thioamides are relatively good hydrogen bond donors. Hydrogen bonding in O=C-NH \cdots S=C is approximately 6.7 kJ/mol weaker than O=C-NH \cdots O=C, but S=C-NH \cdots O=C hydrogen bonding appears stronger by 8.4 kJ/mol.³⁴ This is mostly a result of increased NH acidity in thioamides and sulfur's ability to stabilize S=C-NH \bar{c} anions, compared to their amide analogues.³⁷ Hydrogen bonding lengths are generally longer and less directional in thiocarbonyls. This feature, together with thioamide's ability for more efficient conformational stabilization through $n \rightarrow \pi^*$ interactions, could offer more possibilities in structural supramolecular design.

3.3 Synthetic methodologies of thioamide macrocycles

Most of the endeavors in synthetic of thioamide macrocycles have been carried through carbonyl transformation by Lawesson's reagent (LR) **3.3** or phosphorus pentasulfide (P₄S₁₀) **3.1** (Scheme 3.1). These reagents have remained as the most important tools in thionation chemistry and have been especially applied in reactions on the amide group. Due to amide's high reactivity thionation remains selective even with the presence of ester, ketone and lactone groups. According to Scheme 3.1, the process is initiated by refluxing LR or P₄S₁₀ in toluene, benzene or xylene, giving the dissociation intermediates of **3.2** and **3.4**. The reaction with carbonyl continues via ring containing intermediate **3.5**, which decomposes to the thiocarbonyl structure **3.7**.³⁸

Invariably all synthetic methods for macrocyclic thioamide structures involve utilization of LR and P₄S₁₀. In contrast, the synthetic procedures for acyclic amides appear to be much more diverse. The most common methods include thioacylation of cyanate precursors with Na₂S \cdot 9H₂O in the presence of [DBUH][OAc]³⁹ and condensation of aldehydes with amines and elemental sulfur.⁴⁰



Scheme 3.1. Decomposition route of P_4S_{10} **3.1**, Lawesson's reagent **3.3** and thionation mechanism with amides.³⁸

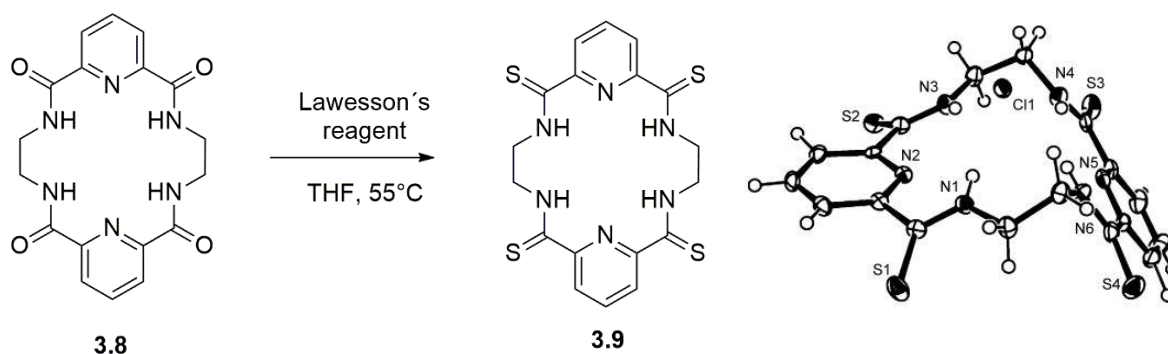
3.4 Conformational studies

Past studies on thioamide macrocycles have been mostly conducted from a biophysical perspective on several cyclic peptide backbones. Various studies have shown changes in conformational properties of macrocycles occurred due to thionation of amide. Verma and colleagues⁴¹ noted that thioamide substitution to macrocyclic peptides reduced their flexibility and, in some cases, strengthened binding affinity through increased preorganization factor.

Internally oriented thioamides caused major conformational changes to macrocycles, which is the result of $\text{C}=\text{S}$ poor hydrogen bond acceptor ability. It was also realized that a larger radius of sulfur atom alters intramolecular van der Waals interactions, reflecting on macrocycle conformations. Although thioamides have been extensively applied in various branches of synthetic organic chemistry, their prospects as macrocyclic ligands have not been studied systematically.⁴¹

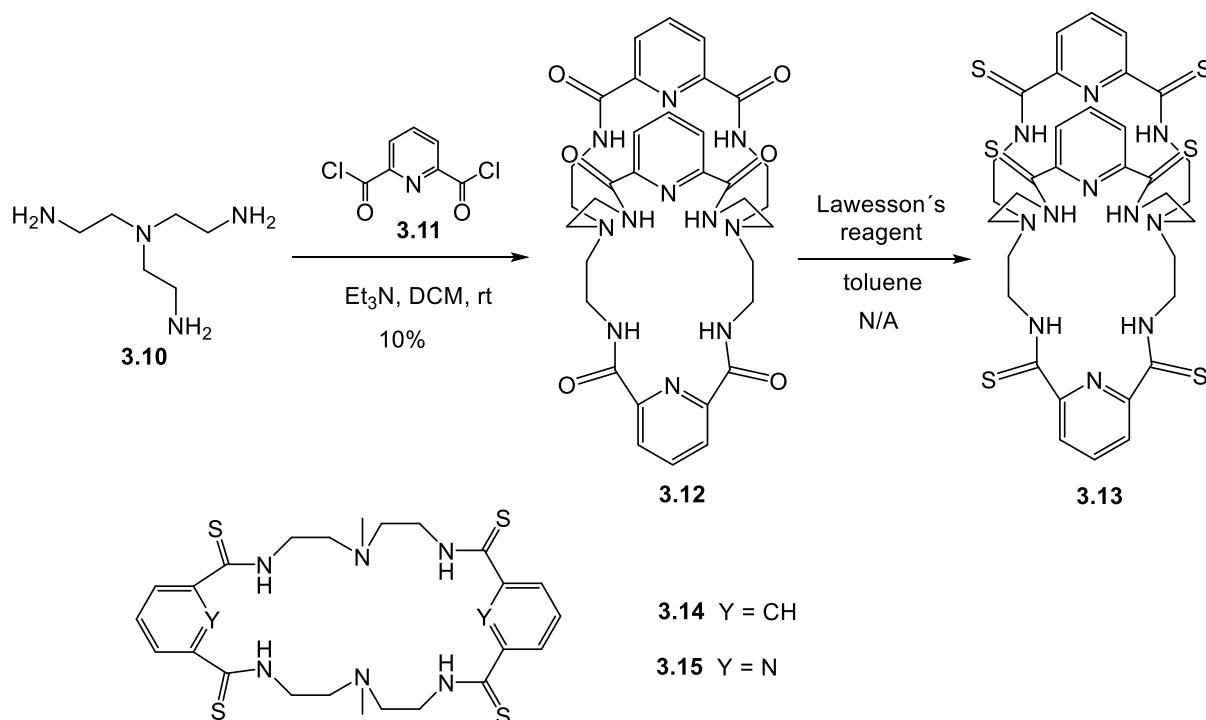
3.5 Anion-binding receptors

Increased acidity of thioamide NH-group has been mostly exploited in the design of anion-binding receptors. High binding affinity is rationalized by strong HB interaction that forms between the amide and an anion. The affinity of the host is usually increased through the chelation effect by designing receptors with several thioamide groups. An example of typical anion receptor design can be demonstrated with macrocyclic polythiolactam receptor **3.9** designed by Inoue and colleagues.⁴² Compound **3.9** was synthesized with LR, obtaining a 56% yield (Scheme 3.2). Compared to its precursor **3.8**, the thionated receptor expressed good solubility in organic solvents (DMSO, THF) and showed NMR downfield shifts upon addition of tetrabutylammonium salts. The downfield occurs due to increased acidity of the NH in thioamide, which enhances the binding to anionic species via HB interaction.



Scheme 3.2. (left) Thionation of macrocyclic thiolactam and its (right) crystal structure of 1:1 complex with chloride ion obtained from DMSO. *With permission of Copyright © 2003 Elsevier Science Ltd.*⁴²

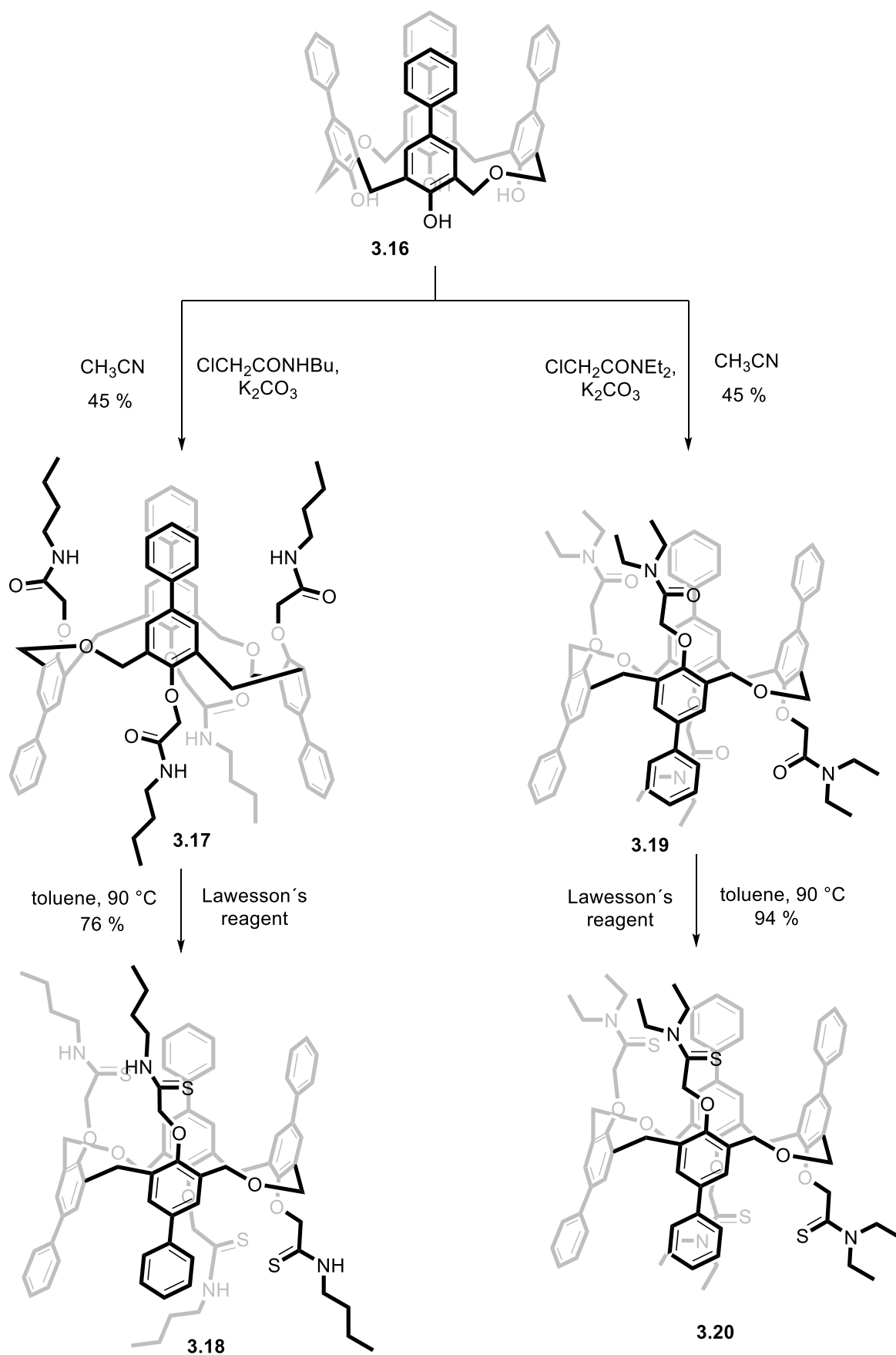
Hossain *et al.*⁴³ designed cryptand-type bicyclic polythioamide receptors with capabilities towards anion-binding (Scheme 3.3). It was observed that monocyclic systems **3.14** and **3.15** expressed higher affinities towards H_2PO_4^- , HSO_4^- , NO_3^- , ClO_3^- , F^- , Cl^- , Br^- , and I^- than corresponding amide precursors. This was claimed by NMR downfield shifts in all liquid-phase studies. However, the phenomenon was opposite between bicyclic receptors **3.12** and **3.13**. Here the affinities towards studied anions were higher for amide derivative **3.12**. According to Hossain's hypothesis, this might be a result of altered intramolecular hydrogen bonding patterns, when C=O groups are changed to C=S moieties.



Scheme 3.3. Synthesis route of polythioamide bicyclic cryptand **3.13** and its corresponding monocyclic derivatives **3.14** and **3.15** by Hossain and colleagues.⁴³

3.6 Cation-binding receptors

By studying tetrahomodioxacalix[4]arene tetraamide receptors No *et al.*⁴⁴ noticed that cation binding affinity was increased with thionated derivatives. C=S being a soft base thioderivatives expressed high selectivity towards Ag⁺-ion. Receptors were obtained with Lawesson's reagent with a 94.5% yield for **3.20** and 76.2% for **3.18** (Scheme 3.4). NMR studies revealed the importance of intramolecular hydrogen bonding for compound **3.17** in conformational stability. Due to stronger hydrogen bonding of C=O, **3.17** remained predominantly in 1,3-alternate conformation. In contrast, compound **3.18** appeared in a major 1,2-alternate conformer.



Scheme 3.4 Synthesis route of tetrahomodioxacalix[4]arene tetraamide receptors and preferred conformations of 1,2-altered for **3.18** – **3.20** and 1,3-altered for **3.17**.⁴⁴

4 Thiourea macrocycles

4.1 Thiourea structures

Most of the urea containing supramolecular structures have been currently applied in the design of anion receptors, due to their strong hydrogen bonding ability of NH-groups. Like in thioamides, increased HB strength of thiourea is predominantly a result of well-stabilized anionic structure $S=CNH^-$. Extra stabilization by sulfur makes protons of nitrogen more acidic with a pK_a value of 21.1 compared to corresponding urea with a pK_a of 26.9 (both measured in DMSO).⁴⁵ Hence it can be claimed that HB forming ability strongly correlates with the acidity of the NH-groups. Besides sulfur's stabilization of thiourea anion, adjacent substituents have a significant role on strength of intermolecular interactions.

Interesting feature of thiourea is that due to nitrogen lone pair (n) interaction to sulfur antibonding orbital (π^*), the conformation of the thiourea group becomes planar. Kim *et al.*³⁶ calculated dihedral angles for S-C-N-H(*cis, trans*) to be 1.88 and 174.14 at the ground state. For urea, corresponding angles are 11.8 and 151.6. As with thioamides, lone pair delocalization in thiourea increases conformational rigidity and rotational barrier. These factors affect hydrogen bonding patterns of thiourea aggregates. The planar nature of thiourea favors ribbon-type interactions over the chains, which are most common in urea structures (Figure 4.1). However, both interaction types remain weaker for thiourea than in urea analogues.⁴⁶

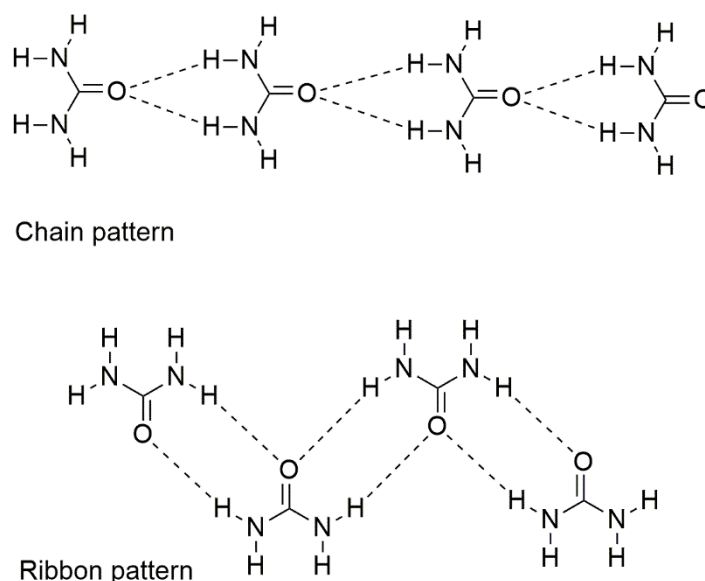


Figure 4.1. Chain and ribbon hydrogen bonding patterns of (thio)urea.⁴⁶

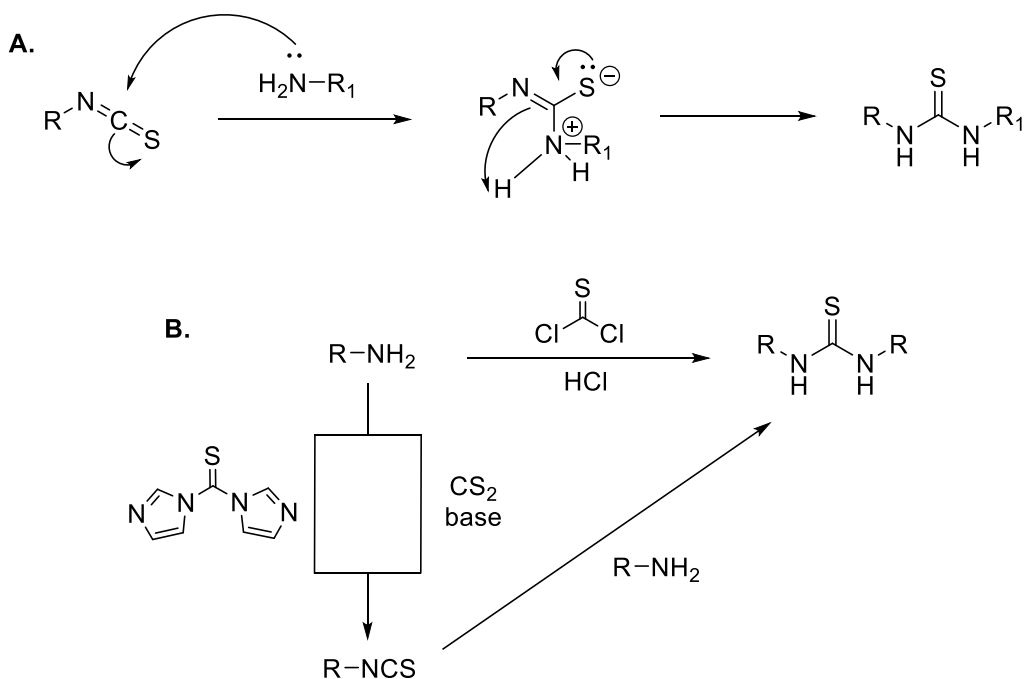
In this context, it is essential to emphasize the importance of adjacent thiourea substituents. Regarding the previous study, hydrogen-bonding interactions between thioureas were weaker than in amides. These interactions can be tuned by altering the NH-group acidity with proper side-chain structure. According to several studies, adjacent anion-form stabilizing substituents effectively lower the pK_a value of thiourea. Phenyl has been the most common tool for this purpose, leading to a higher hydrogen bonding affinity. Scheerder *et al.*⁴⁷ noticed that adjacent phenyls can enhance thiourea acidity so well, that NH hydrogen bond acceptor ability dominates sulfur's weaker hydrogen bond accepting ability over hydrogen, forming more stable thiourea than urea dimers.

Recently, there has been an ongoing discussion regarding thiourea's ability to act as a sulfur-based halogen bond acceptor. Being a relatively soft and large acceptor, sulfur tends to form less directional XB interactions, compared to corresponding elements in the second period. By conducting a computational study on S \cdots I interactions, Arman and colleagues⁴⁸ noted that halogen bonds were roughly orthogonal to the ribbon plane in crystals, where I \cdots S-C-N dihedral angles varied from 66.6° to 97.7°. The bonding nature is quite different considering nitrogen \cdots halogen XBs, where interaction is more directional. It has been claimed that lack of this directionality in sulfur acceptors is beneficial for structural adaptability in various supramolecular assemblies.

4.2 Synthetic methodologies of thiourea macrocycles

According to the recent literature the most common methodology for thiourea synthesis is carried through amine addition to isothiocyanate (Scheme 4.1 a). The reaction is sensitive to moisture, requiring dry synthesis conditions. The reaction solvent is usually chosen based on the applied amine and isothiocyanate backbones. There are several methods to prepare isothiocyanate precursors. Most common from these are amine to isothiocyanate conversion with carbon disulfide or 1,1-thiocarbonylimidazole. Thiourea can be also directly obtained from amines through coupling with thiophosgene in an acidic environment (Scheme 4.1 b).

In the synthesis of macrocyclic structures, several important aspects must be considered. These consider mostly the challenge in optimizing ring/chain equilibrium to avoid polymer formation. The widely applied methodology includes slow-addition and high dilution techniques, which drive the reaction equilibrium towards ring formation. Besides, low reaction temperature and macrocyclization catalysts may be applied.⁴⁹ Applied synthetic methodologies for various thiourea macrocycles together with their utilization are covered in the following chapters.

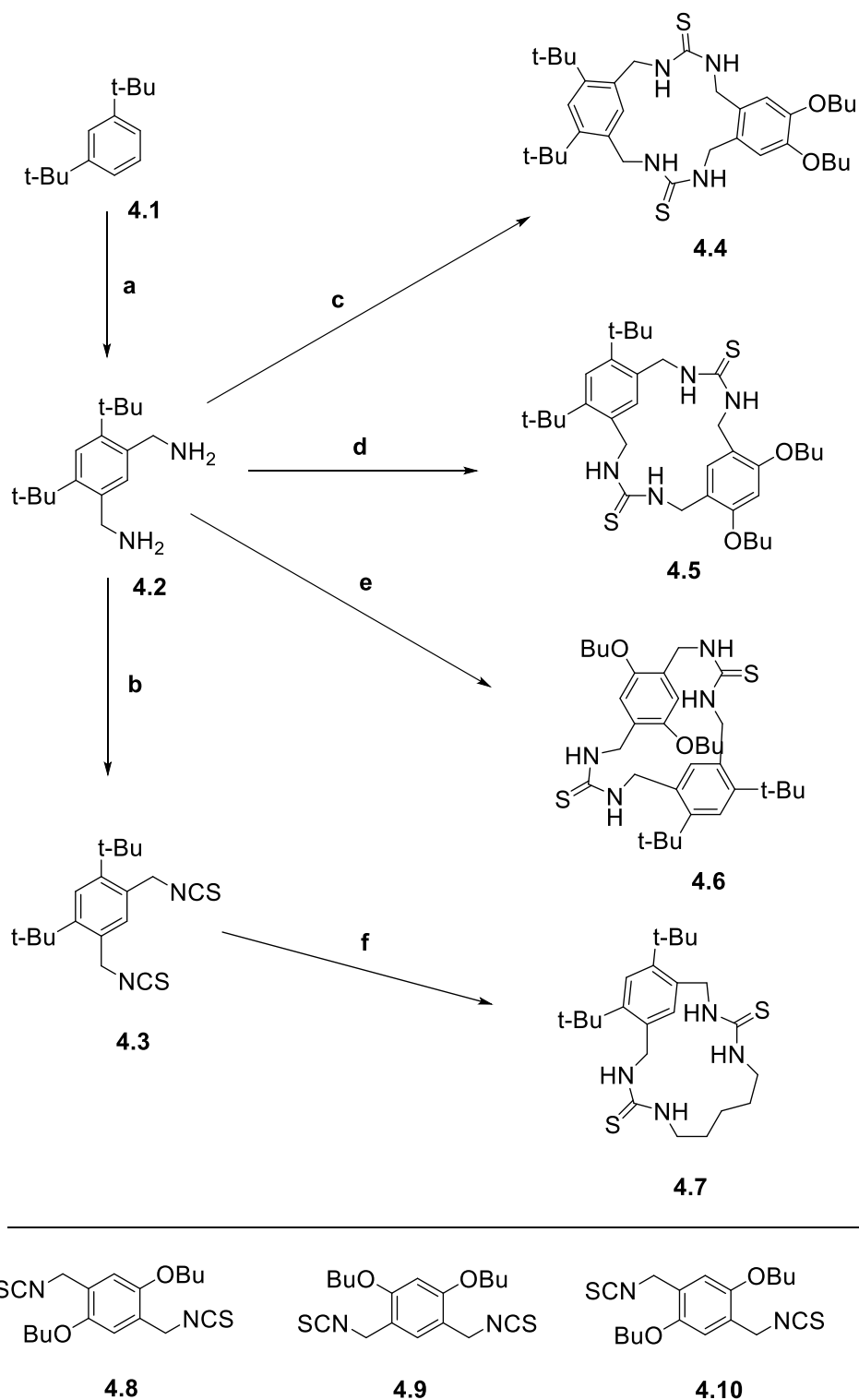


Scheme 4.1 **(a)**. General mechanism for thiourea synthesis. **(b)**. Most common isothiocyanate and thiourea synthetic pathways.

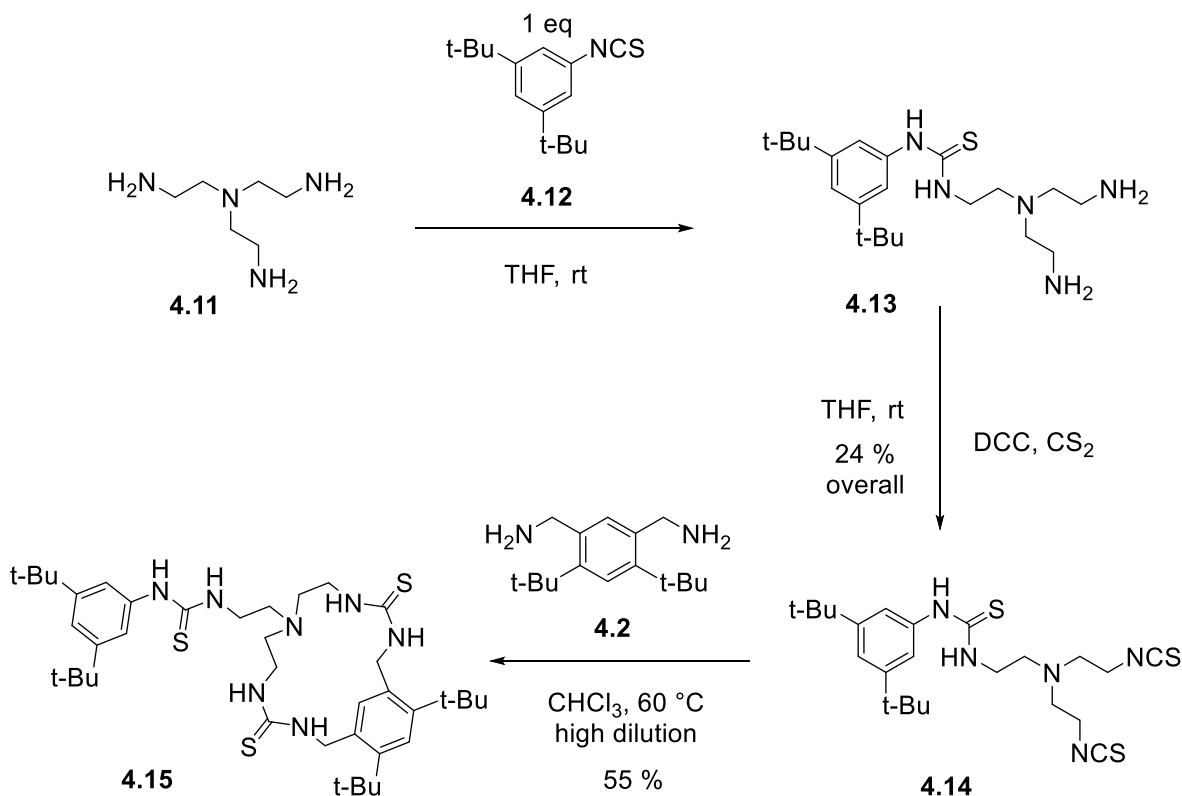
4.3 Anion-binding structures

Compared to thioamide receptors, synthesized macrocyclic thioureas appear to have higher structural diversity and utilization possibilities. This is mostly a result of wider synthetic opportunities of thiourea and the presence of two NH-groups. The increased acidity of NH moieties has been widely exploited in the complexation of anionic species, focusing the research of macrocyclic thioureas to the development of anion and anion pair receptors.

Sasaki *et al.*⁵⁰ examined the role of conformation and macrocyclic flexibility by conducting Anion-binding comparison studies among various cyclophane structures. The group synthesized five macrocyclic thiourea cyclophane derivatives **4.4** – **4.7** (Scheme 4.2) and **4.15** (Scheme 4.3). The study showed that all the structures possess similar selectivity to anions, respectively $\text{H}_2\text{PO}_4^- > \text{CH}_3\text{COO}^- > \text{Cl}^- > \text{HSO}_4^- > \text{Br}^-$. However, the results showed that cyclic hosts **4.4**, **4.5**, **4.7** and **4.15** possessed a relatively larger Anion-binding affinity. Since the basicity order of applied anions is $\text{CH}_3\text{COO}^- > \text{H}_2\text{PO}_4^- > \text{HSO}_4^- > \text{Cl}^- > \text{Br}^-$, it could be claimed that all examined hosts are most selective to the H_2PO_4^- anion. Sasaki and colleagues also noticed that **3** totally lacked Anion-binding ability, which most likely occurred due to the *trans-cis* binding geometry and thiourea groups facing outside of the cyclophane.



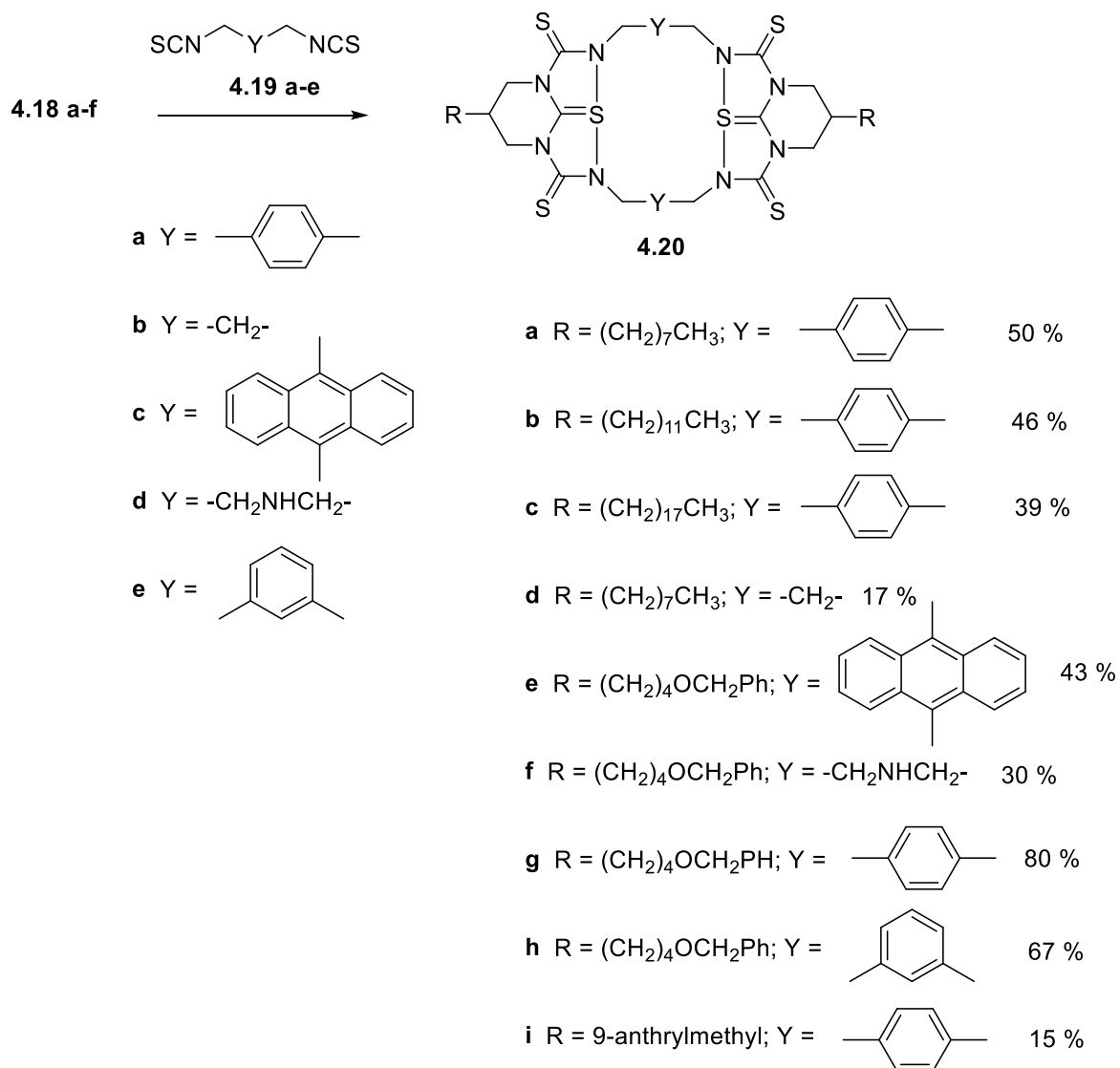
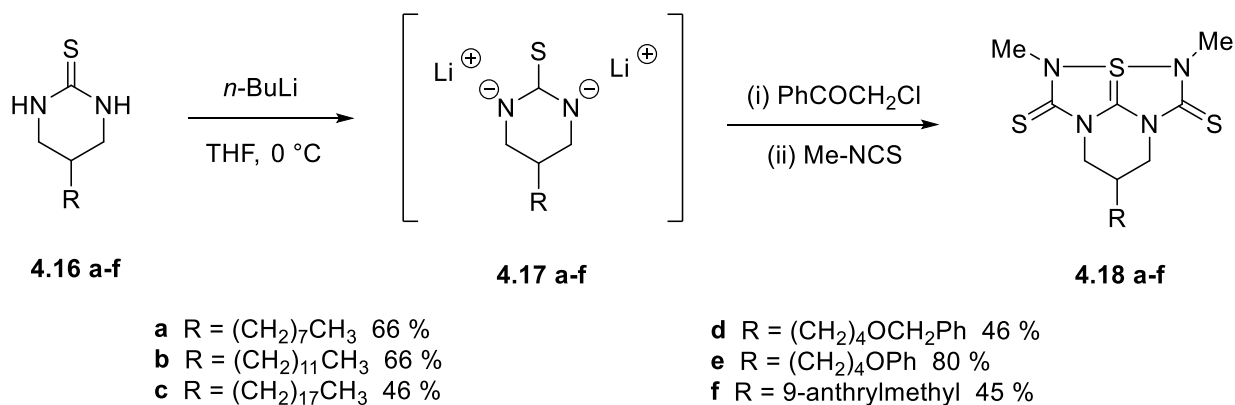
Scheme 4.2. Synthesis routes of cyclic receptors by Sasaki *et al.*⁵⁰ Reagents and conditions: (a) (i) $\text{ClCH}_2\text{OCH}_3$, ZnCl_2 , 60°C , (ii) potassium phthalimide, DMF, 100°C , (iii) H_2NNH_2 , H_2O , EtOH, reflux, 4%; (b) DCC, CS_2 , THF, room temperature, 93%; (c) **4.8**, CHCl_3 , high dilution, 60°C , 79%; (d) **4.9**, CHCl_3 , high dilution, 60°C , 70%; (e) **4.10**, CHCl_3 , high dilution, 60°C , 31%; (f) 1,5-diaminopentane, CHCl_3 , high dilution, 60°C , 75%.



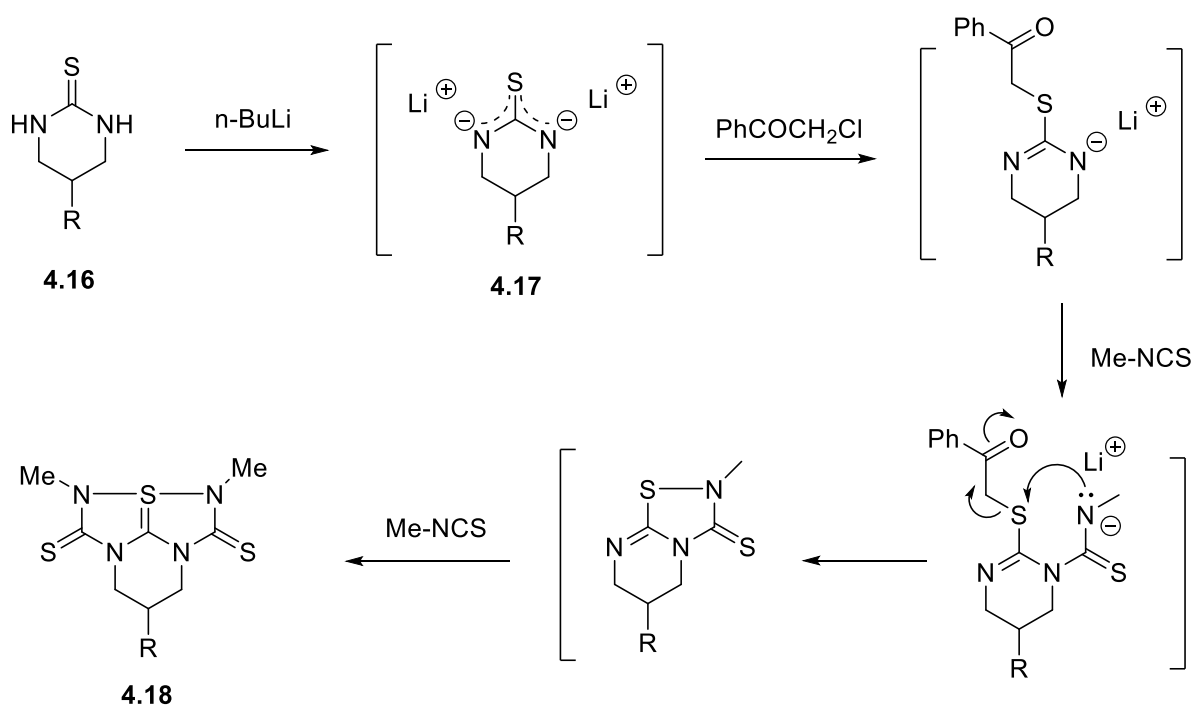
Scheme 4.3. Synthesis route for Lariat-type thiourea receptor **4.15** by Sasaki *et al.*⁵⁰

Matsumura and colleagues applied a slightly different approach by synthesizing hypervalent sulfur macrocycles through the reaction of 10-S-3 tetraazathiapentalene derivatives with various diisothiocyanates. [Scheme 4.4 \(a\)](#) shows the first steps of the synthetic procedure, where deprotonation of 10-S-3 tetraazathiapentalene follows by the reaction with PhCOCH₂Cl and addition of methyl isothiocyanate, producing precursors **4.18 a-f** for further macrocycle synthesis. Similar synthesis route has been applied by Matsumura *et al.*⁵¹ in the previous studies. More comprehensive reaction path is presented in [Scheme 4.4 \(b\)](#).

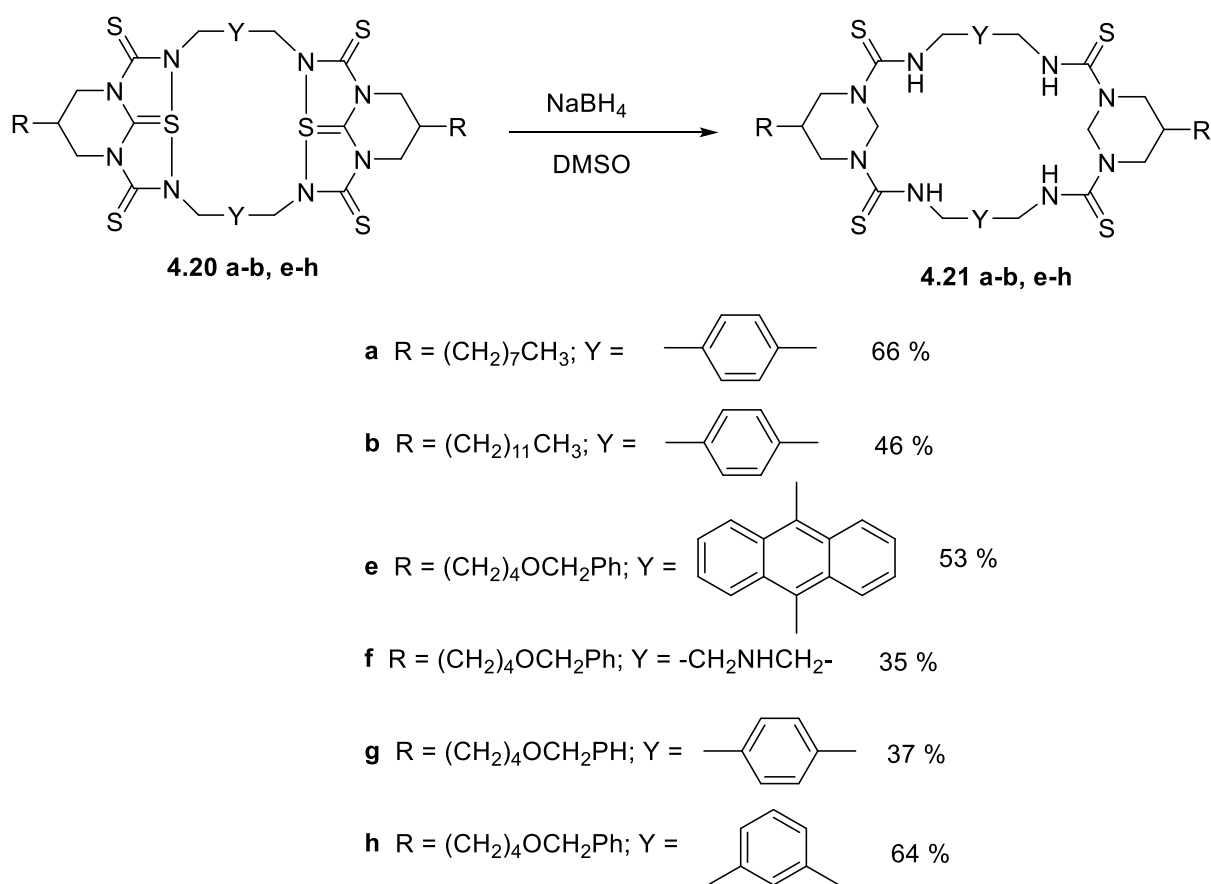
Compounds **4.18 a-f** were converted to macrocyclic products **4.20 a-i** through treatment with diisothiocyanate derivatives **4.19 a-e** by refluxing the reaction mixtures for 24 h in dry conditions and the room temperature in benzene, toluene or DMSO depending on the reagent solubility. Generally, the product yield appeared to be highest in macrocyclic compounds **4.20 a-c**. Further procedures carried a subsequent reduction with NaBH₄ afforded thiourea macrocycles **4.21 a-b, e-h** with moderate 35-66% yields ([Scheme 4.5](#)). Obtained macrocycles were not studied for coordination, but according to Matsumura should be well applicable as anion receptors.⁵²



Scheme 4.4 (a). Synthesis of hypervalent sulfur macrocycle precursors **4.18 a-f** and obtained macrocyclic structures **4.20 a-i** through addition of isothiocyanate derivatives **4.19 a-e** by Matsumura *et al.*⁵²



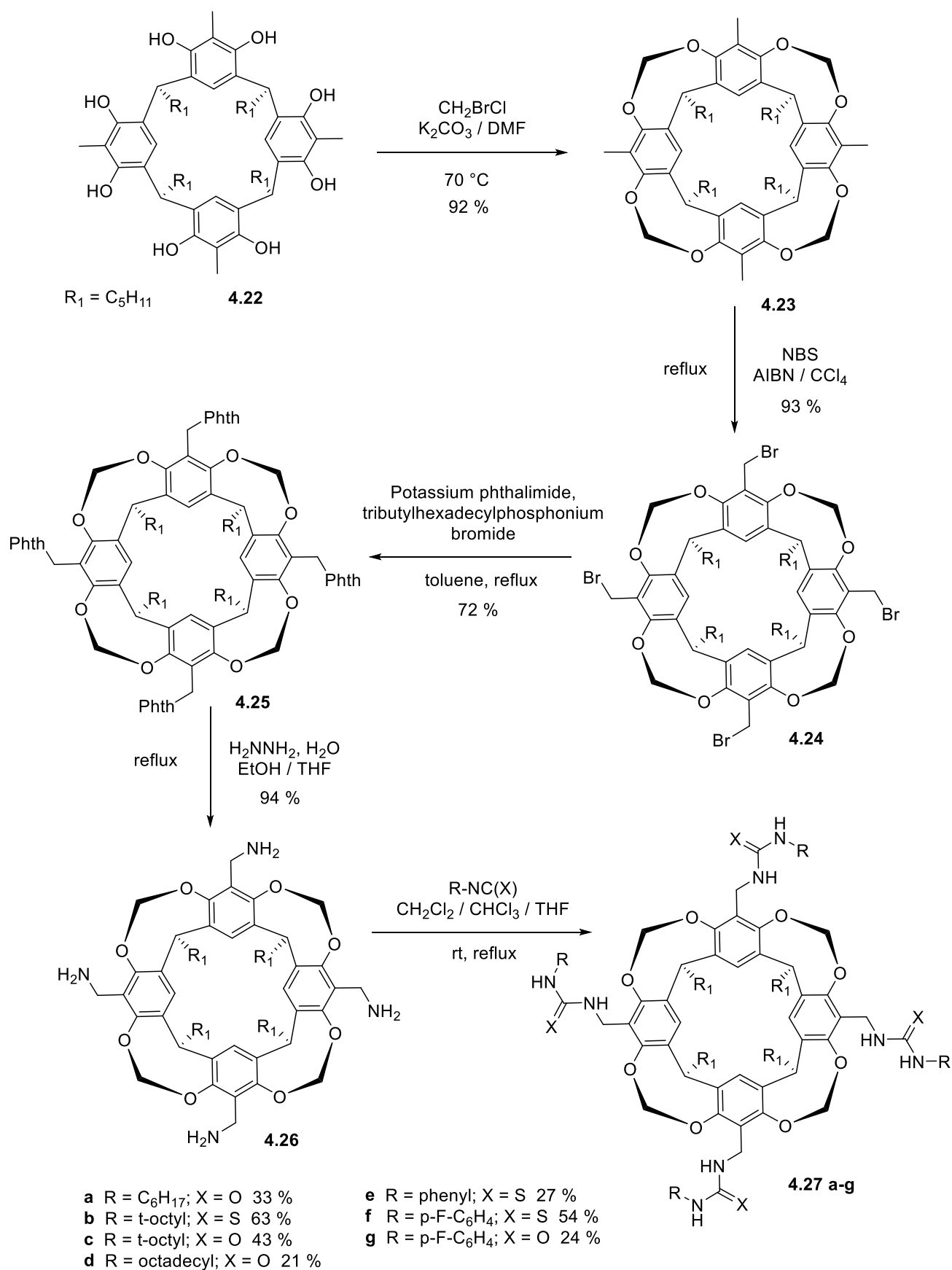
Scheme 4.4 (b) Reaction mechanism for the formation of tetraazapentalenes **4.18 a-f** by Matsumura *et al.*⁵¹



Scheme 4.5. Reduction of hypervalent sulfur macrocycles.⁵²

With the aim of synthesizing rigid cavitand derivatives, Boerrigter *et al.*⁵³ conducted the study on urea and thiourea resorcinarene macrocycles. Compounds **4.27 a-g** were obtained through the reaction of aminomethylcavitand **4.26** with various isocyanates and isothiocyanates. The preparation of aminomethylcavitand **4.26** was conducted via a four-step synthesis from resorcinarene **4.22**, reported by the previous study by Boerrigter (Scheme 4.6).⁵⁴

The reaction of **4.24** with potassium phthalimide in toluene gave compound **4.25** and the subsequent treatment with hydrazine hydrate in ethanol/THF compound **4.26** with an overall yield of 67%. According to Boerrigter and colleagues, following reactions of **4.26** with iso(thio)cyanate derivatives proceeded slowly, most likely due to moderate solubility of reagents in DCM. The solubility was increased by applying isothiocyanates with longer aliphatic chains. Synthesized receptors **4.27 a-g** expressed high affinity via hydrogen bonding towards halide anions. Higher affinity was rationalized with the absence of cavitand's intramolecular hydrogen bonding, due to the presence of sulfur.⁵³

Scheme 4.6. Synthesis of resorcinarene thiourea derivatives by Boerrigter *et al.*⁵³

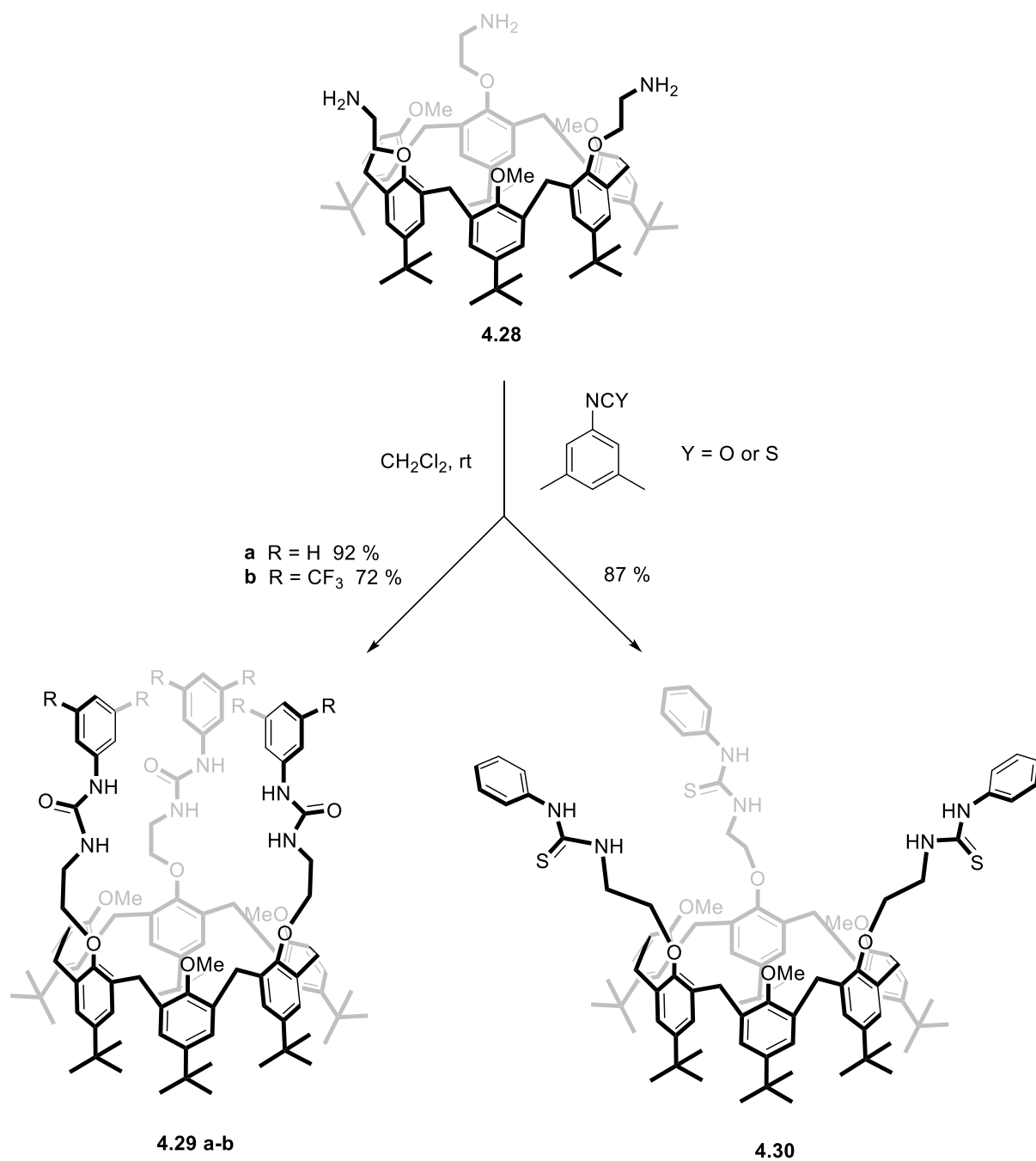
4.4 Anion pair receptors

Successive attempts have been reported in derivatizing calixarene structures containing thiourea moieties. Hamon *et al.*⁵⁵ were able to produce cooperative ion pair receptor bearing higher conformational flexibility and strong coordinating groups. Reaction of calix[6]trisamine with phenylthiocyanate gave calix[6]tristhiourea **4.30** up to 92% yields (Scheme 4.7). Calix[6]trisamine **4.28** was originally prepared by Le Gac *et al.*⁵⁶ by per-alkylation of $X_6H_3Me_3$ with ethyl bromoacetate with a strong base (NaH), reaction with NH_3 in MeOH and amide group reduction with BH_3/THF , obtaining 79% yield.

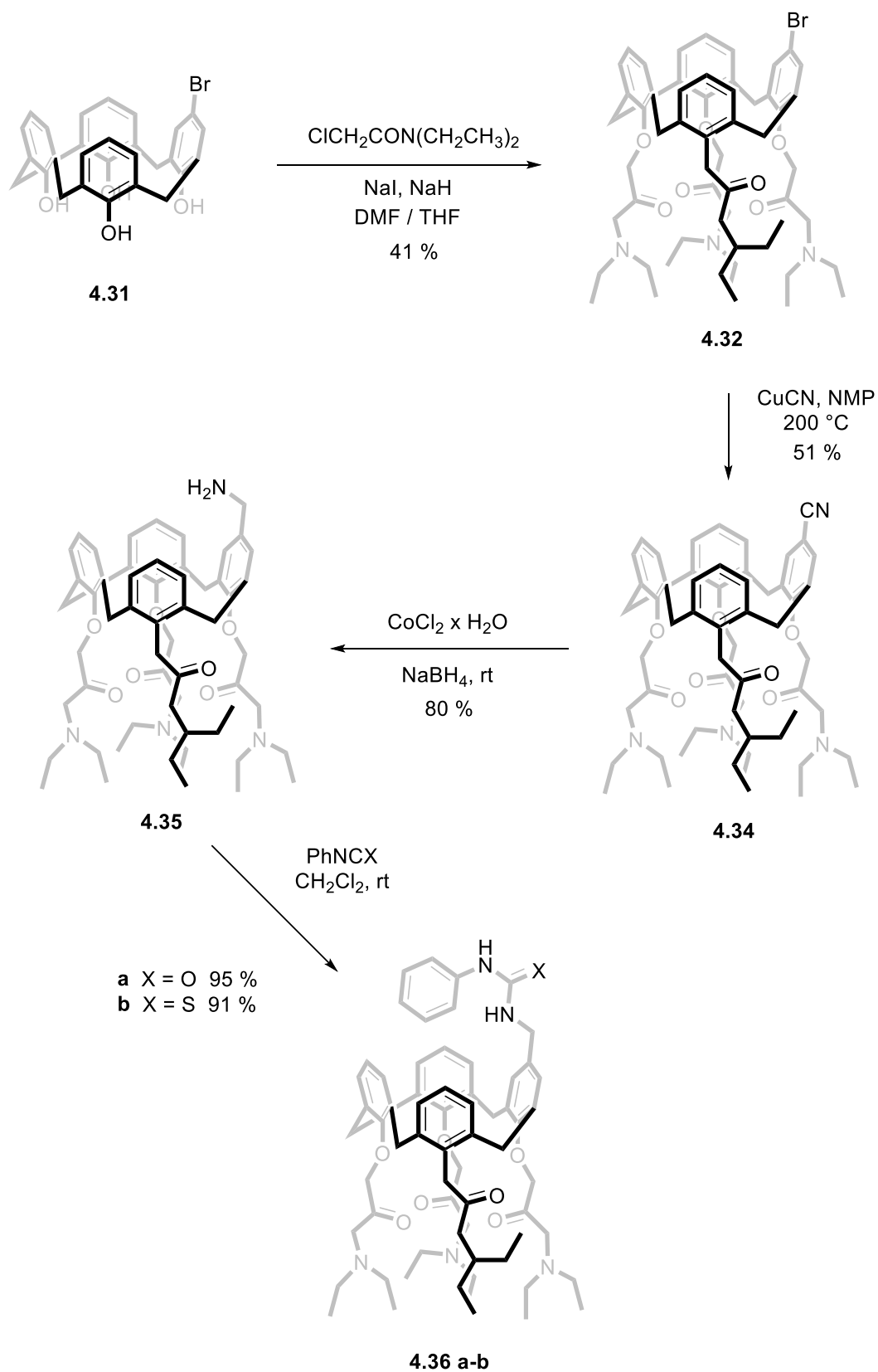
Calix[6]tristhiourea **4.30** expressed complexation abilities towards various X^- anions (*i.e.*, Cl^- , I^- , Br^- , AcO^- , HSO_4^- , ClO_4^- and PF_6^-), which were added as tetra-*n*-butylammonium salts (TBA^+X^-). Hamon and colleagues also synthesized analogical calix[6]trisurea macrocycles **4.29 a-b**, which were compared with corresponding thiourea structures. Studies showed that urea moieties form a stronger intramolecular hydrogen bonding network in nonpolar solvents, whereas thiourea orientates outside the cavity, most probably due to sulfur's weaker HB acceptor ability. Despite these facts, compound **4.30** showed weaker Anion-binding affinities than the trisurea **4.29** derivative.⁵⁵

A relatively similar approach was carried out by Pelizzi and colleagues, who synthesized mono(thio)urea derivatized ditopic receptors from calix[4]arene backbones. The synthesis route is presented in Scheme 4.8, where starting reagent **4.31** was obtained by calix[4]arene bromination.⁵⁷ Further reaction with α -chloro-*N,N*-diethylacetamide/NaH in THF/DMF resulted in compound **4.32**. Compound **4.33** was obtained by Br/CN exchange, carried with CuCN at 200 °C in *N*-methylpyrrolidone (NMP). This was further reduced to **4.34** with $NaBH_4$ in the presence of $CoCl_2$. Final products **4.35 a-b** were attained, analogically to Scheme 4.6, with phenyliso(thio)cyanate ($PhNCX$).⁵⁸

The studies confirmed that Anion-binding affinity of **4.35 a** receptor roughly followed the basicity order of a guest. It was assumed that the size of the nonpolar cavity was reduced due to electrostatic repulsion of multiple amide groups, making **4.35 a** unideal for aromatic guests. Straight thiourea linkage to aromatic sidechain in both, **4.30** and **4.35 a**, increase the hydrogen bonding ability of NH.³⁷ Reduced cavity size and increased NH-acidity seemed to have a positive impact on acetate anion selectivity.⁵⁸



Scheme 4.7. Synthesis route and recognition properties of calix[6]tris(urea and -thiourea Hamon *et al.*⁵⁵

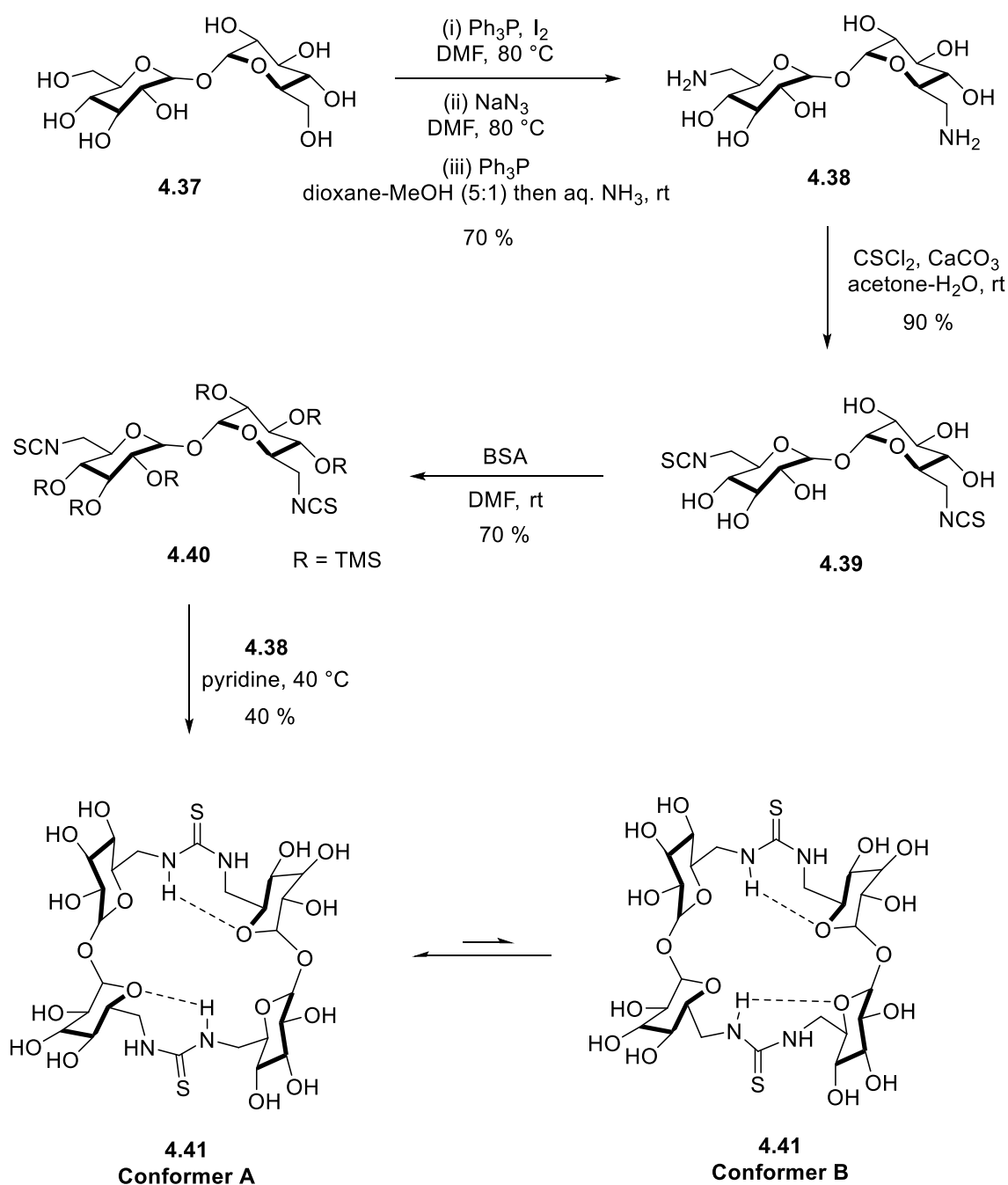


Scheme 4.8. Synthesis route of calix[4]arene tetramide mono(thio)urea derivative by Pelizzi

*et al.*⁵⁸

4.5 Cation binding thioureas

Fernandez and colleagues⁵⁹ conducted a conformational study on macrocyclic poly(thiourea)oligosaccharides by synthesizing sugar-thiourea coronand **4.41** (Scheme 4.9). Due to the failure to condense **4.38** directly with **4.39** into a macrocyclic structure, TMS protection of OH-groups was performed to isothiocyanate precursor **4.39**. It was noticed that seven-membered intramolecular NH...O hydrogen bonds were the main factor in the conformational behavior, placing the macrocycle predominantly as the conformer **A**.



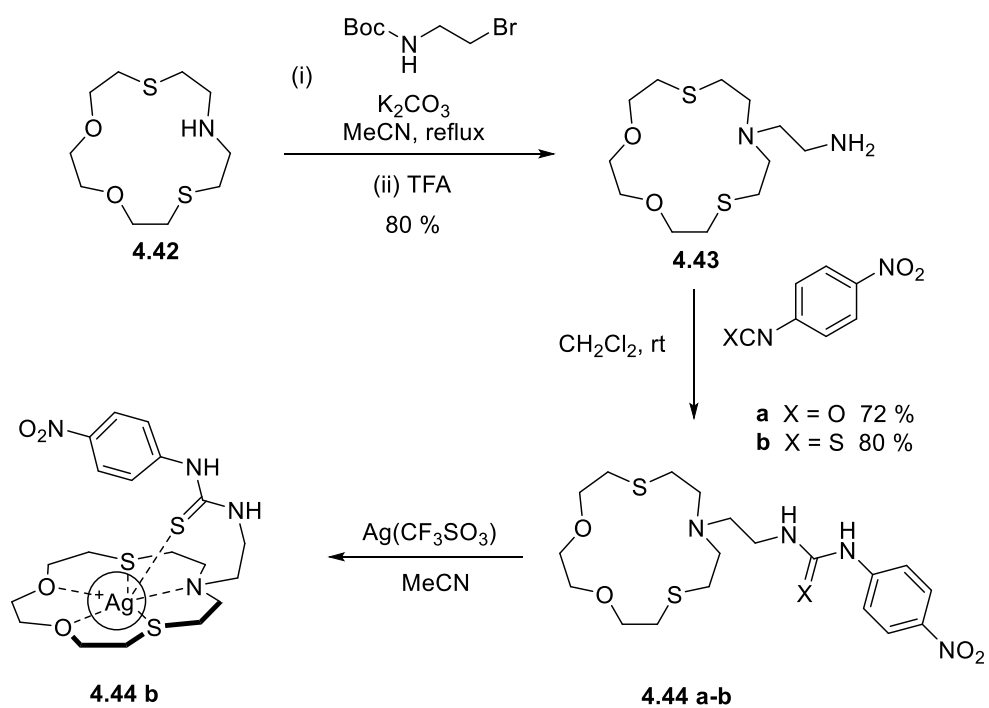
Scheme 4.9. Poly(thioureylene)oligosaccharide synthesis and its conformations by Fernandez *et al.*⁵⁹

HBs are strongly affected by the solvent polarity, which also causes variations in the rotational barrier of thiourea *Z/E* conformations. According to the cation-binding studies, the water-soluble derivative **4.41** displayed preferential Cs⁺ binding affinity (Cs⁺ > K⁺ > Na⁺). Additional tests with divalent cations showed the formation of the strong Cu²⁺ complex among Zn²⁺, Ba²⁺, and Ca²⁺.⁵⁹

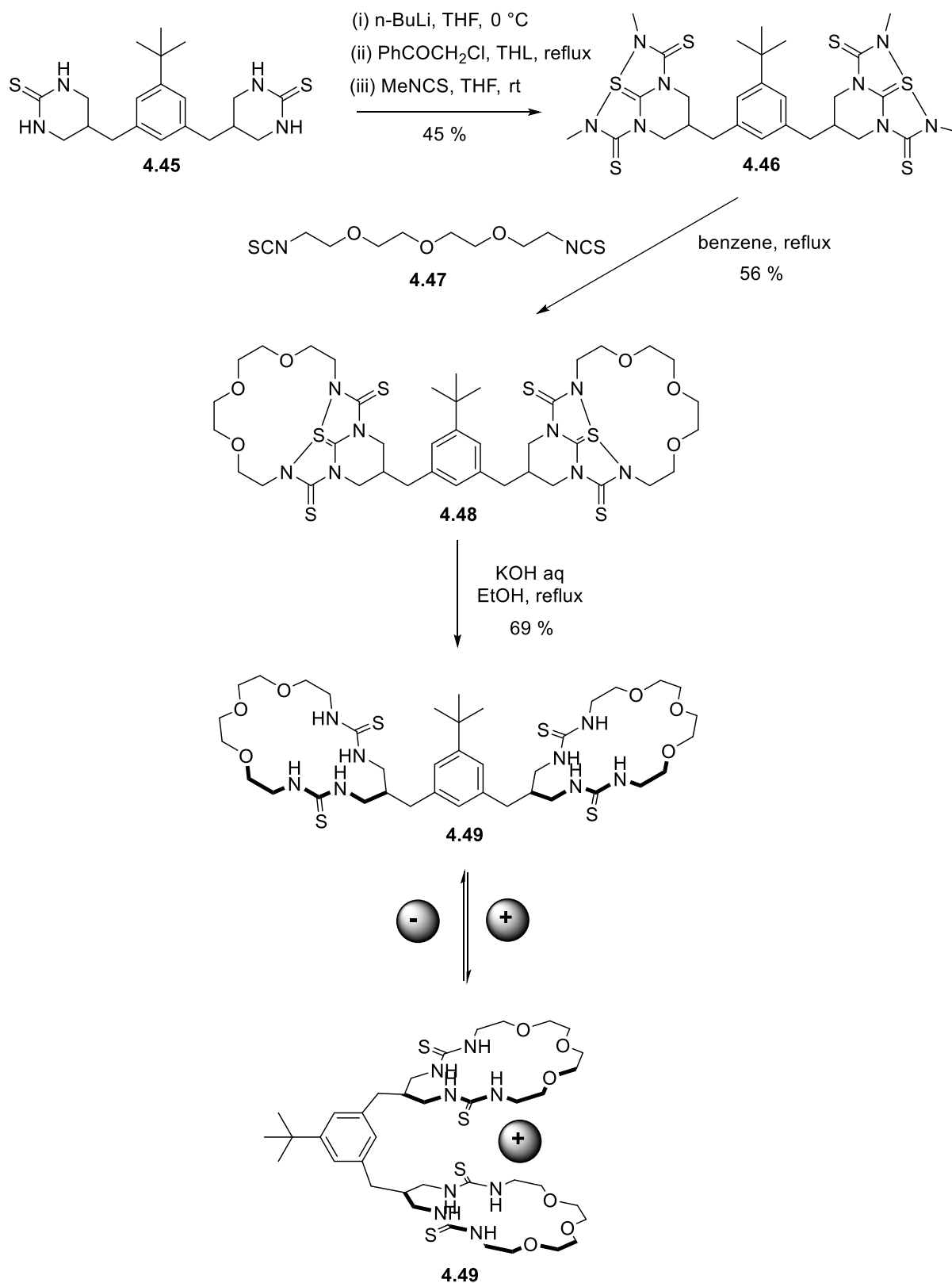
4.6 Ditopic thiourea receptors

A significant increase in coordination ability for silver(1)salts was observed in ditopic receptor **4.44 b**, designed by Amendola *et al.*⁶⁰ The synthesis strategy of **4.44** involved linkage of Boc-protected amine to 15-membered NO₂S₂ crown with the subsequent addition of 4-nitrophenyl iso(thio)cyanate (Scheme 4.10). In general, these kinds of sulfur-containing crowns have potential in the complexation of d¹⁰ cations, which prefer soft acid-base interactions. Amendola observed that the complexation of metal cation to the C=S group resulted in a 10³ – 10⁶-fold increase of anion association constant at the NH groups. Titration experiments also showed that N-H deprotonation, carried by F⁻ anion, strengthened C=O(S)···Ag interaction. This was most likely the result of oxygen's electron pair delocalization to the C-N bond, which changes (thio)carbonyl's sp² hybridization to sp³.

A similar approach of derivatizing crown structures with thiourea was conducted by Okumura *et al.*⁶¹ Synthesized macrocyclic compound **4.49** (Scheme 4.11) expressed binding affinity towards dihydrogen phosphate and Li⁺, Na⁺, K⁺, NH₄⁺ cations. ¹H NMR studies showed that the addition of tetrabutylammonium dihydrogen phosphate caused a downfield shift of NH-groups, indicating the hydrogen bond formation. NMR titration results suggested 1:2 complex stoichiometry with the binding constant of 3.94 · 10⁵. The receptor **4.49** showed also strong color change from transparent to the dark red upon the cation addition.



Scheme 4.10. Synthesis route of ditopic silver(1) receptors **4.44 a-b** and representation of Ag^+ coordination with receptor **4.44 a**.⁶⁰

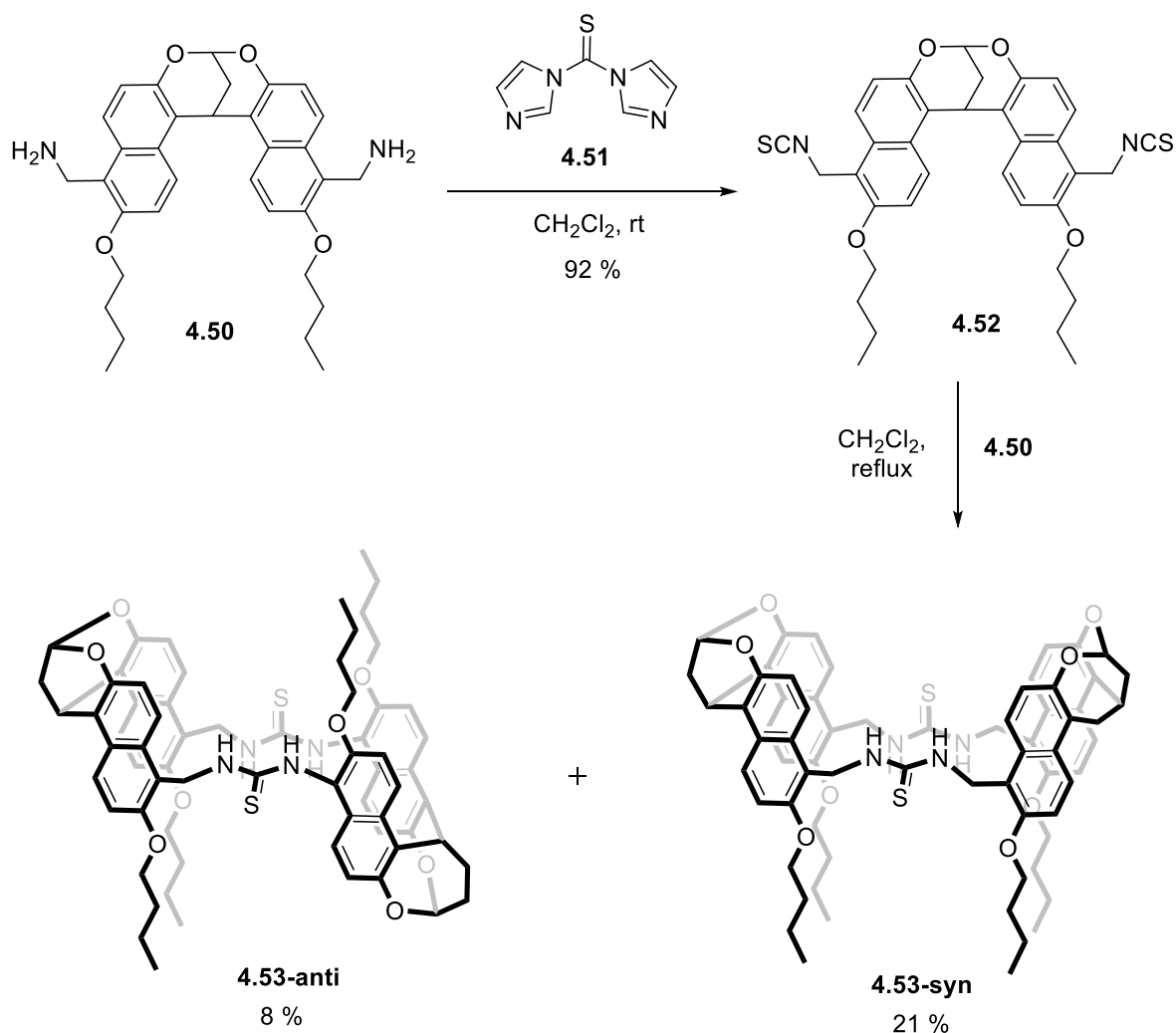


Scheme 4.11. Synthesis route for dimacrocylic thiourea receptor and its conformational changes upon cation/anion additions by Okumura *et al.*⁶¹

4.7 Thioureas as neutral hosts

Huang *et al.*⁶² reported the evidence for thiourea's ability to act as *endo*-functionalized hosts for neutral nucleophilic molecules. Urea and thiourea derivatized molecular tubes were synthesized by coupling diamino bis-naphthalene with iso(thio)cyanate, giving the products **4.53** and its urea derivative in *syn*- and *anti*-conformations (Scheme 4.12).

The NMR titration experiments with structures **1-9** (Figure 4.2) in non-polar media showed higher binding constants for thiourea derivatives with compounds **1-4** and **6-8**. As in anionic receptors, higher binding affinity is mostly rationalized by increased acidity of thiourea's NH groups. In addition, increased hydrogen bonding ability with thiourea groups contributed with C-H \cdots π interactions to aromatic rings of hosts, which was observed as an exceptionally strong binding between guest **4** and **4.53-anti** structure.⁶²



Scheme 4.12. Synthesis of *endo*-functionalized molecular tube **4.53**, its conformations by Huang *et al.*⁶²

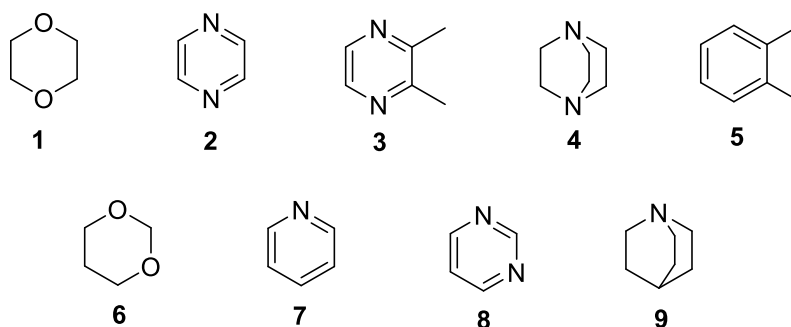
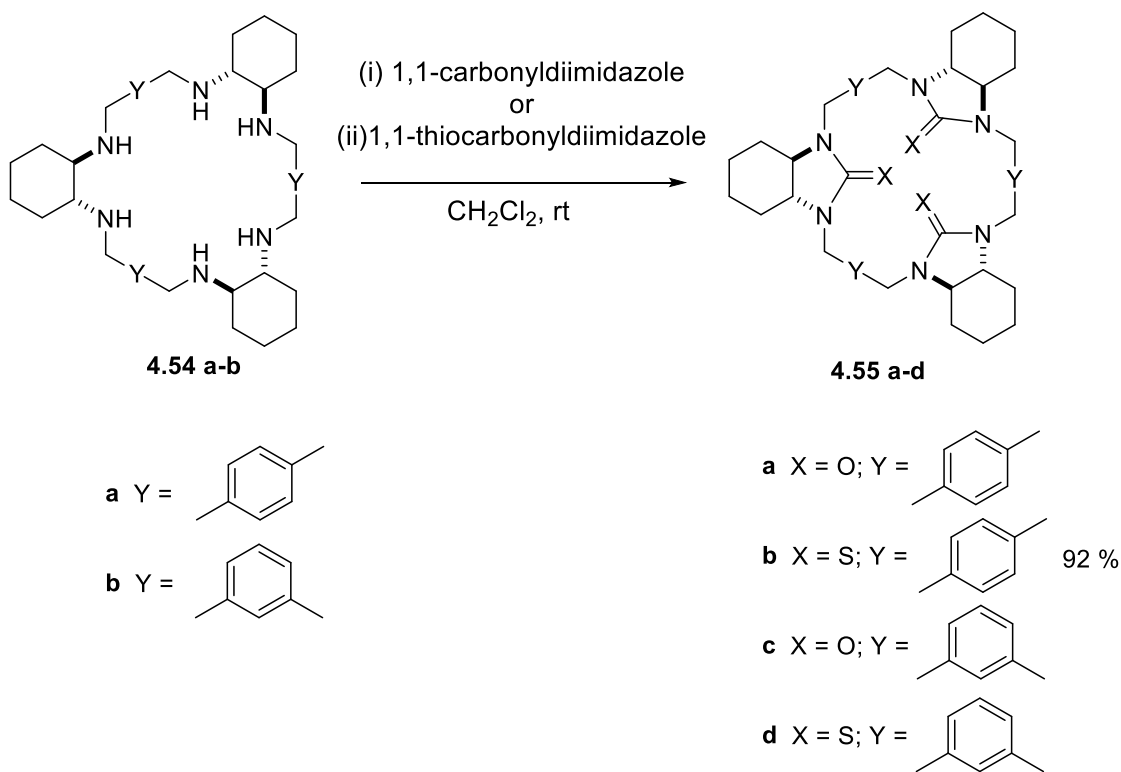


Figure 4.2. Synthesis of *endo*-functionalized molecular tube **4.53**, its conformations and neutral guests **1-9** applied in complexation studies by Huang *et al.*⁶²

4.8 Thioureas in gelation

Recently some of the macrocyclic thiourea structures have been applied in the development of metallogel properties. Prusinowska *et al.*⁶³ obtained an enantiomeric urea and thiourea derivatives **4.55 a-d** of trianglamine (Scheme 4.13), which formed symmetrical bilayer motifs and metallogels with Cu (I), Ag (I) and Cu (II) salts. Figure 4.3 shows the crystal structure of thiourea trianglamine molecule **4.55 b** together with its lattice structure. Independent molecules in *N,N*-dimethylformamide (DMF) formed bilayers that were arranged in a zipper shaped motif.

Studies showed that chirality and enantiomeric purity had a significant effect on metal ion gelation. This was especially observed with compound **4.55 b** upon the formation of supramolecular metallogel with Ag. Gelation was totally prevented with samples below $ee = 50\%$. Formation of a semigel started at $ee = 50\%$, whereas full gelation with metals was observed with ee over 70% .⁶³



Scheme 4.13. Synthesis of thiourea trianglamine derivatives **4.55 a-d** by Prusinowska *et al.*⁶³

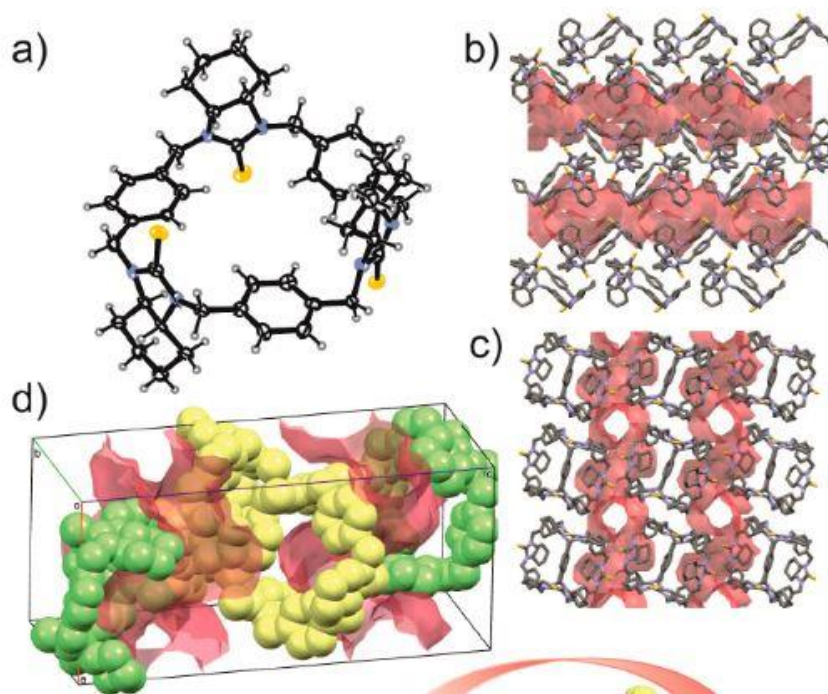


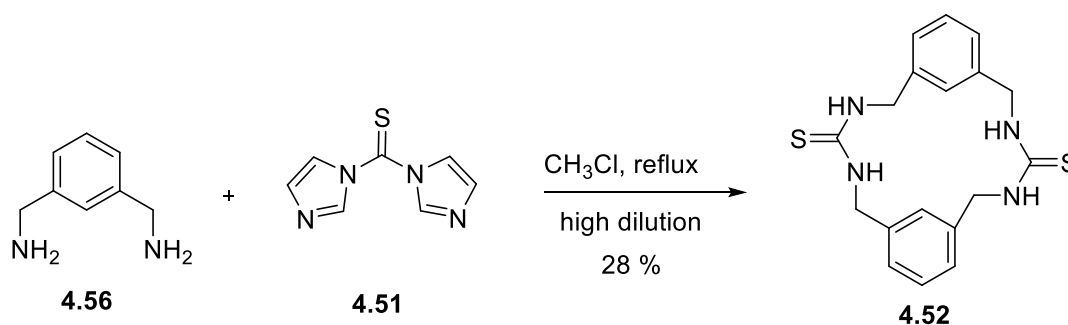
Figure 4.3. **(a)** Crystal structure of thiourea trianglamine **4.55 b**. Representations of crystal packing along **(b)** and in lattice direction **(c)**, where intermolecular channels are filled with the solvent molecules. *With permission of Copyright © 2018, American Chemical Society.*⁶³

4.9 Thiourea crystalline frameworks

In contrast to urea-based frameworks, research on thiourea crystal structures has been less explored. Urea moieties tend to form stable one-dimensional chains, bound by hydrogen bonding network between NH protons and C=O. These groups adopt three centered assembly motifs, where urea groups exist primarily in *trans-trans* conformation.⁶⁴ As described at the beginning of the chapter, macromolecular thiourea structures express more conformational flexibility, appearing mostly in *trans-trans* and *trans-cis* forms. Due to this thioureas appear as zig-zag chains and dimers (Figure 4.1) in the solid-state.²⁹

Sindt and colleagues⁶⁴ investigated the effect of macrocyclization on the assembly directing ability and conformations in crystalline solids. By invoking the lack of thiourea macrocycle reports in the crystalline phase, Sindt *et al.* incorporated thiourea groups into the *m*-xylene macrocycle (Scheme 4.14). The synthetic strategy of *bis*-thiourea *m*-xylene **4.52** was similar to Sasaki *et al.*⁵⁰ by the addition of 1,1'-thiocarbonyldiimidazole to *m*-xylylenediamine. The procedure required the simultaneous addition of both precursors in high dilution under the reflux condenser.

Crystallization of compound **4.52** was carried in DMF showed that thiourea groups possessed *trans-trans* conformation and were perpendicular ($\sim 87^\circ$) to *m*-xylylene rings (Figure 4.4 left). Sulphur hydrogen bonds were formed from two different adjacent molecules, which is atypical for thiourea *trans-trans* binding behavior. The **4.52** crystals with $\text{NH}_2\text{CH}_2\text{CH}_2\text{NH}_2$ (Figure 4.4 right) were found to appear in both, *cis-trans* and *trans-trans* conformations, most likely *trans-trans* being the major conformer.⁶⁴



Scheme 4.14. *Bis*-thiourea *m*-xylylene macrocycle **4.52** synthesis by Sindt *et al.*⁶⁴ For product purification recrystallization using vapor diffusion of water into DMF was required.

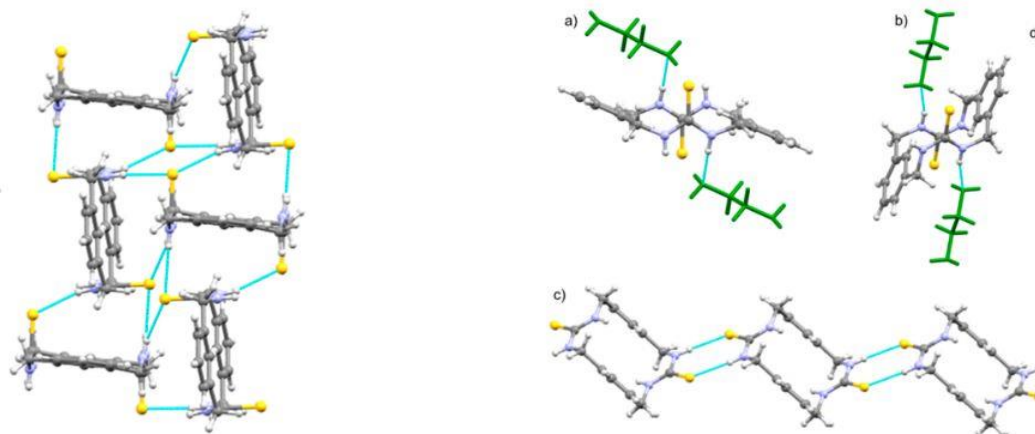


Figure 4.4. (left) Hydrogen bonding in crystal structure of *bis*-thiourea macrocycle **4.52** of *trans-trans* conformation. (right) **(a)** **4.52** · NH₂CH₂CH₂NH₂ *trans-trans* conformer **(b)** *cis-trans* conformer of **4.52** · NH₂CH₂CH₂NH₂ **(c)** *cis-trans* macrocycle chains. With permission of Copyright © 2018, American Chemical Society.⁶⁴

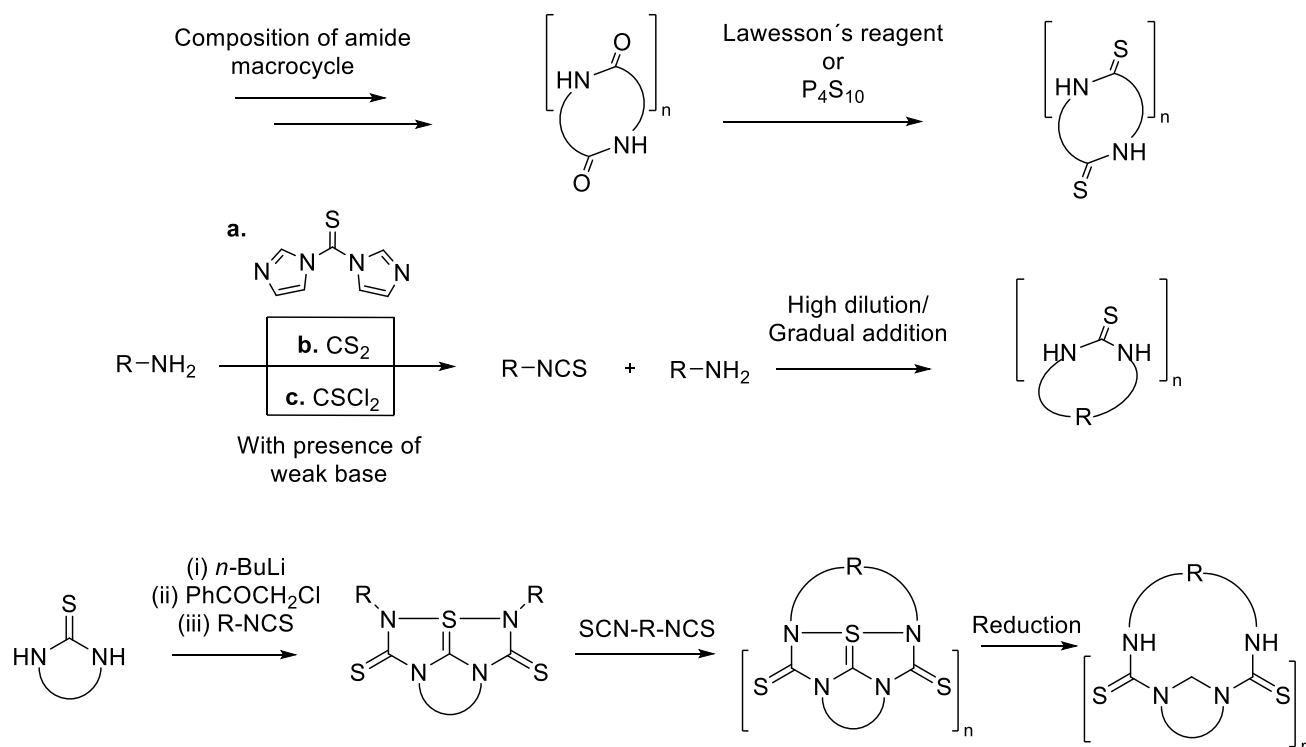
5 Conclusion

Thioamide and thiourea macrocyclic structures offer new possibilities for supramolecular chemistry research. Sulfur's larger size and higher polarizability result in higher acidity of adjacent NH-groups, which strengthens the hydrogen bonding properties. According to recent literature, this aspect is utilized in the design of anion receptors. The binding site at thiocarbonyl sulfur is known to complexate well soft Lewis acid metal cations, from which Ag⁺ is the most studied.

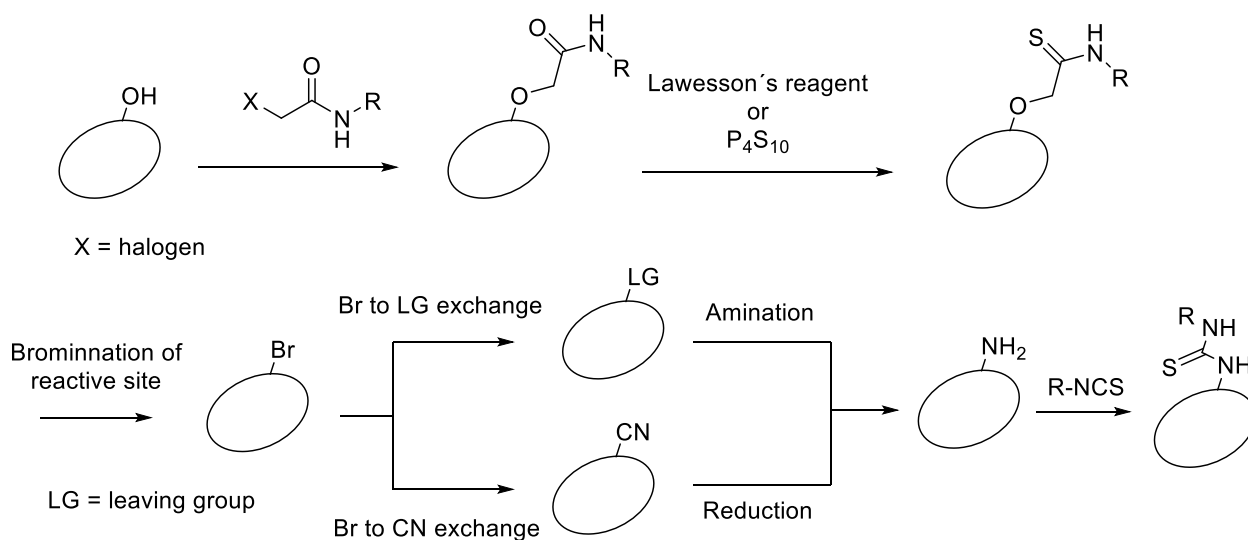
The main challenge in macrocycle synthesis is to reach a favorable equilibrium between ring- and chain formations, which requires high dilution and gradual addition techniques. Synthesis of thioamide receptors is carried from corresponding amide derivatives via a one-step reaction with Lawesson's reagent. Thiourea receptor synthesis is mostly done through amine to isothiocyanate addition, but the reduction of hypervalent sulfur compounds and straight amine to thiourea conversion with thiophosgene is also applied (Scheme 5.1).

In comparison to acyclic thiocarbonyl structures, macrocyclic receptors containing sulfur are less studied. Research on thioamide receptors has been mostly carried from a biophysical perspective by converting previously known amide receptors to corresponding thioamide derivatives. Insertion of sulfur is observed as conformational changes in receptors, which alters the binding properties. Due to more versatile synthetic possibilities of thiourea macrocycles their research has been more diverse, focusing not just on the NH-binding site, but also on the utilization of thiocarbonyl's sulfur.

A. Thioamide and thiourea enclosed in the cyclic structure



B. Thioamide and thiourea outside of the cyclic structure



Scheme 5.1. Summary of thioamide and thiourea macrocyclic receptor synthetic pathways covered in the theoretical part.

Experimental section

6 Objectives

The experimental part was conducted as a part of the project on “Robust S⋯I⁺⋯S halogen-bonded supramolecular assemblies”. Having a nature of fundamental research, the primary goal was to synthesize thiourea receptors, which might serve as potential halogen bonding acceptors. Guidelines for the synthesis were mostly gathered based on previous experimental studies, with some attempts to synthesize new compounds. To obtain information about XB complexation properties, successfully produced receptors were tried for crystallization with iodine-containing halogen bond donors ([Figure 6.1](#)) and as pure compounds.

To avoid toxic reagents (carbon disulfide, thiophosgene) commonly applied in the synthesis of thiourea; commercially available isothiocyanate derivatives were mostly used. Some of the multisubstituted isothiocyanates were tried to derivatize from corresponding bromine- and amine structures. Amines were further coupled with isothiocyanates through addition-reaction to form thiourea- receptors. Due to poor solubility of thiourea in common organic solvents, final products were mostly obtained through precipitation from the reaction mixture.

Some of the successfully synthesized receptors were tested for complexation by preparing crystallization samples with **A**, **B** and **C** guests ([Figure 6.1](#)). Besides, there were several endeavors to crystallize pure receptors to obtain their solid-state structures. For crystallizations, several strategies were applied including crystallization from pure solvents, solvent mixtures and diffusion enhanced crystallizations. The large size and poor solubility of receptors make the crystallization process relatively challenging.

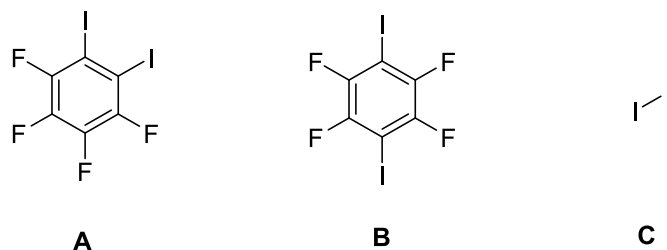
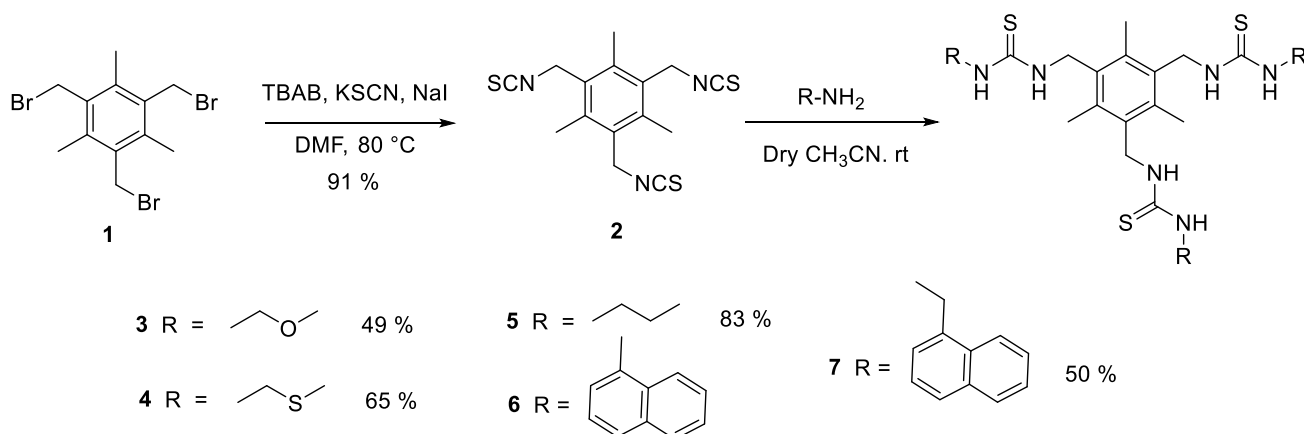


Figure 6.1. Guests applied in crystallization tests.

7 Synthesis of thiourea receptors

This chapter is categorized into four synthesis projects on thiourea receptors. The synthesis part contains the theoretical and overall experimental approach of thiourea ligand synthesis. Detailed synthetic methods and characterization of obtained structures are presented in the [10 Experimental procedures – section](#). All collected NMR- and MS spectra are found in the [appendix](#). For clarity, the numbering of compounds is reset to start from 1.

7.1 Receptors based on 1,3,5-tris(bromomethyl)-2,4,6-trimethylbenzene backbone



Scheme 7.1. Synthesis route for 1,3,5-tris(bromomethyl)-2,4,6-trimethylbenzene based tripodal thiourea ligands.

Compounds **3**, **4**, **5** and **7** were synthesized based on procedure reported by Akhtar *et al.*⁶⁵ The first step consisted of compound **1** bromine substitution to isothiocyanate group with the presence of tetrabutylammonium bromide (TBAB), potassium isothiocyanate (KSCN) and sodium iodide in dimethylformamide ([Scheme 7.1](#)). Sodium iodide was acting as a catalyst, enabling Br to I substitution based on the NaBr precipitation according to the Finkelstein reaction principle.^{66,67} Solubility of sodium thiocyanate to organic phase was enhanced via the addition of TBAB. Product **2** was extracted with ethyl acetate producing pale yellow powder after solvent evaporation.

Successful attempts in the synthesis of **2** produced desired compounds in relatively good yields. The most challenging part appeared to be the extraction and purification of **2**. Due to the vast amount of TBAB, the strong emulsion was formed between organic and inorganic phases. To solve this issue amount and proportion of TBAB and KSCN was altered ([Table 7.1](#)). It is observed that the most successful result was obtained in synthesis **C** with a larger proportion of

KSCN and higher concentration for all reagents. However, based on such scarce data set it is impossible to derive any specific correlations to optimize the reaction.

Due to the formed emulsion, purified product **2** contained a large amount of TBAB. The purification process was performed by diluting crude **2** into chloroform and filtrating mixture several times through a thin silica layer, which successfully trapped charged TBAB molecules. Synthesis proceeded to thiourea derivatives **3 – 7** through amine addition to isothiocyanate **2** in dry acetonitrile under the argon atmosphere. Final products were obtained as a precipitate from the reaction mixture and purified by washing with the reaction solvent. Reactivity of applied amines seemed to follow the electronegativity of sidechains. [Table 7.2](#) shows how yields increase within the decrease of sidechain polarity, affecting the nucleophilicity of the amine tail. This might have been the reason for failure in the synthesis of compound **6**, where adjacent electron-withdrawing naphthyl-group prevented amine addition to isothiocyanate **2**.

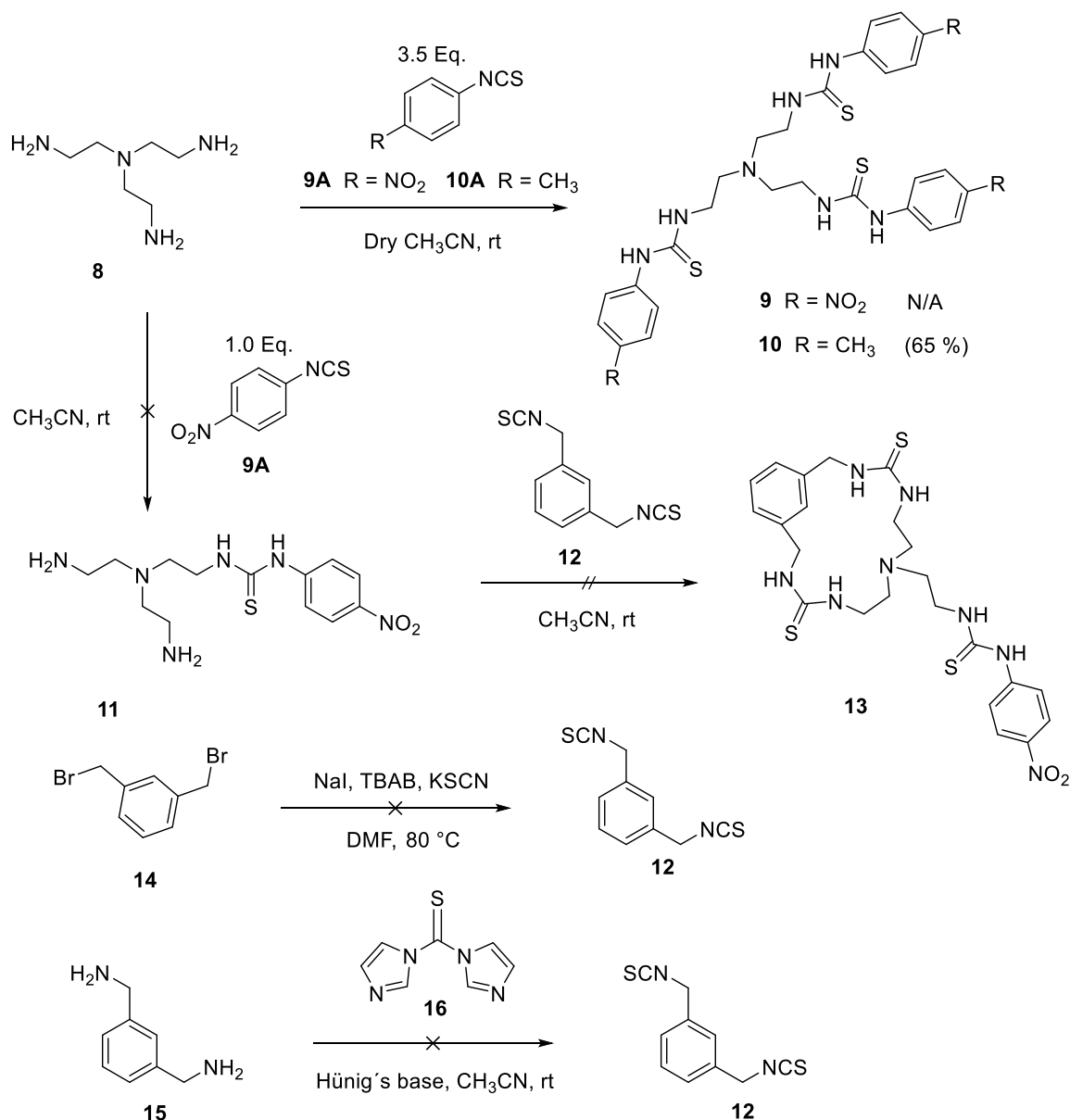
Table 7.1. Performed synthesis for compound **2**

	A.	B.	C.
1	1.02 g, 2.5 mmol	0.22 g, 0.54 mmol	1.47 g, 3.7 mmol
TBAB	3.19 g, 9.9 mmol, 4 eq	0.53 g, 1.6 mmol, 3 eq	4.41 g, 13.7 mmol, 3.7 eq
KSCN	1.59 g, 16.4 mmol, 6.7 eq	0.34 g, 3.5 mmol, 6.5 eq	2.69 g, 27.7 mmol, 7.5 eq
NaI	0.32 g, 2.1 mmol, 0.9 eq	0.07 g, 0.43 mmol, 0.8 eq	0.48 g, 3.2 mmol, 0.9 eq
2	0.17 g, 0.5 mmol	0.12 g, 0.35 mmol	1.12 g, 3.36 mmol
Yield	17 %	65 %	91 %
Solvent	DMF, 80 ml	DMF, 50 ml	DMF, 60 ml

Table 7.2. Yield comparison for products **3 – 7**

Compound	3	4	5	6	7
Yield (%)	49	64	83	no product	50

7.2 Receptors based on tris(2-aminoethyl) amine backbone



Scheme 7.2. Applied synthesis route for tris(2-aminoethyl) amine-based ligands.

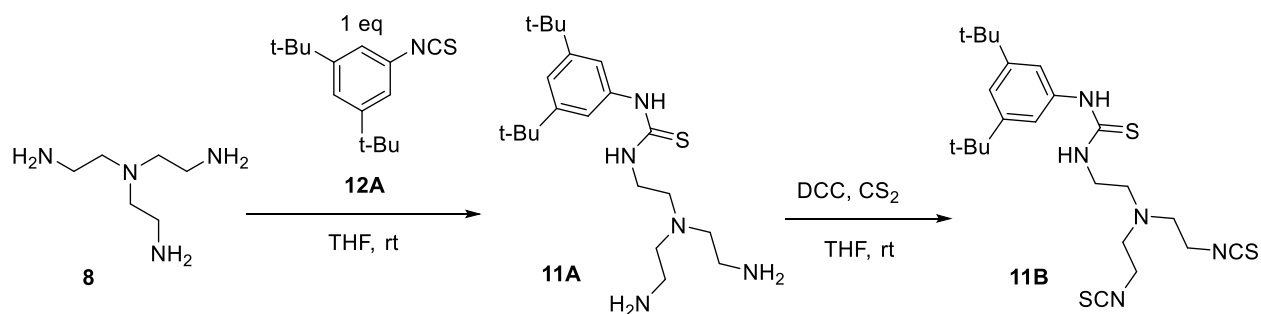
One approach was to build tripodal ligands on the trisamine **8** backbone with various thiourea sidechains attached. The synthesis protocol for compounds **9** and **10** involved similar procedures as in the preparation of ligands **3-7** (Scheme 7.2). Products were obtained through stirring tris(2-aminoethyl) amine **8** with 3.5 eq. of isothiocyanate reagents (**9A**, **10A**) at the room temperature in acetonitrile under argon. 4-Nitrophenyl isothiocyanate **9A** generally produced larger yields and expressed higher reactivity than *p*-tolyl isothiocyanate **10A**. However, based on the made observations, this phenomenon cannot be explained unambiguously.

Synthesis plan for Lariat type ligand **13** was designed based on the work of Sasaki *et al.*⁵⁰ To avoid the use of *N,N'*-dicyclohexylcarbodiimide (DCC) and carbon disulfide applied by Sasaki in amine to isothiocyanate conversion, two different strategies were tested for the synthesis of the compound **12**. The conversion of 1,3-bis(bromomethyl)benzene **14** to isothiocyanate derivative **12** was carried out according to procedure based on Akhtar *et al.*⁶⁵ Another approach was to perform addition of 1,1-thiocarbonylimidazole **16** to 3-(aminomethyl)benzylamine **15** based on the study of Huang *et al.*⁶²

All endeavors to synthesize **12** from **14** by applying Finkelstein reaction principle⁶⁶ with NaI, TBAB and KSCN resulted in the strong emulsion during the extraction phase. To reduce emulsion, the synthesis procedure was tested without the addition of TBAB and NaI. However, the lack of these reagents prevented the progression of reaction and the desired product was not obtained. Improvement wise other solvents could have been applied or various techniques for trapping excess cations from the reaction mixture (*e.g.* coordination to the crown ether) to reduce the presence of ionic species in the solution. Due to the lack of time, these ideas were left to the next project.

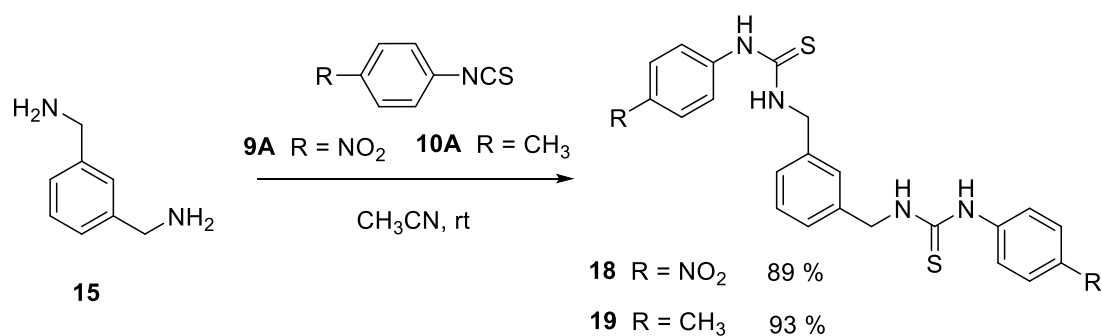
There are several literature reports of bisamine conversions to isothiocyanates with 1,1-thiocarbonylimidazole **16**.^{62,68} Based on these, trials for the conversion of **15** to corresponding isothiocyanate **12** were conducted with the presence of a weak base (Hünig's). Reactions were carried out in the room temperature under argon atmosphere. Even after column purification, NMR results showed the presence of different components, possibly indicating to polymer formation. NMR spectra also showed the presence of thiourea protons around 9 – 10 ppm, which is most probably the result of the reaction between remained reagent **15** and product **12**. According to the literature, the amine addition was performed in one-pot, but gradual addition should be considered.

For the synthesis of Lariat type receptor **13**, Sasaki *et al.*⁵⁰ applied trisamine **8** to isothiocyanate addition followed by treatment with DCC and CS₂ in the same pot (Scheme 7.3). Straight conversion of amines to isothiocyanates eliminates complications caused by amines during the purification process. This problem was observed while attempting to purify crude **11** with silica column chromatography. Obtained fractions contained a mixture of mono- and disubstituted products. For this purpose, alternative purification methods (*e.g.* reverse phase- and ion-exchange chromatography) suitable for highly polar and basic compounds could have been applied.



Scheme 7.3. Synthesis route for precursor of Lariat type receptor **13** by Sasaki *et al.*⁵⁰

7.3 Dipodal based on 3-(aminomethyl) benzylamine backbone

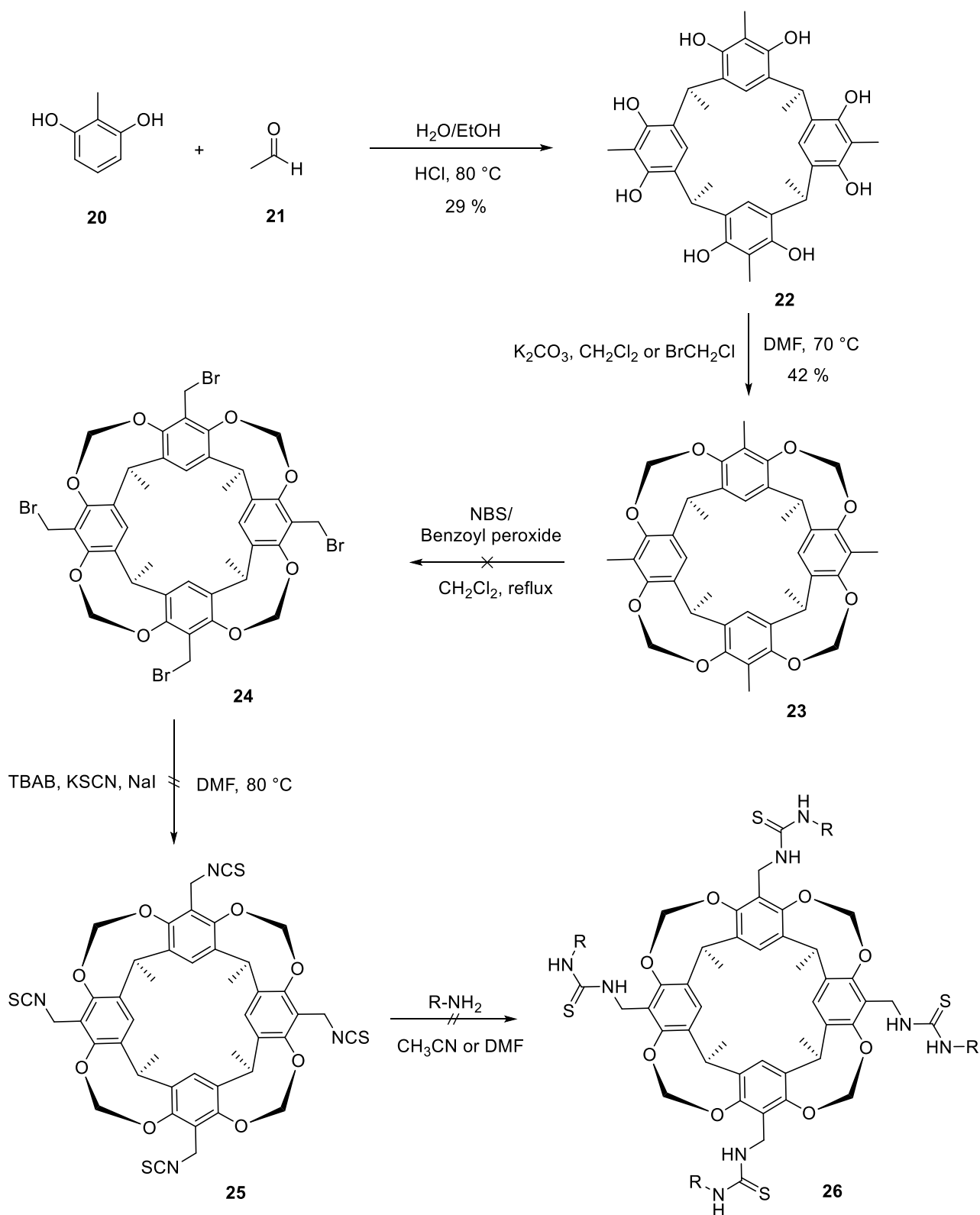


Scheme 7.4. Synthesis procedure for 3-(aminomethyl) benzylamine based dipodal ligands.⁶⁹

Various bis-thiourea derivatives were observed to act as antimalarial and antimicrobial agents due to weak interactions to amino acids.⁶⁹ Many of these examples exploited hydrogen bonding to sulfur, which could also be a potential site for the formation of halogen bond. Two different dipodal thiourea ligands (**18**, **19**) were synthesized through 3-(aminomethyl) benzylamine **15** addition to aromatic isothiocyanates **9A** and **10A** (Scheme 7.4).

All reactions were performed in dry conditions under argon with acetonitrile as a solvent. Products were obtained as a precipitate from the reaction mixture with relatively high yields of 80 – 90%. Due to the fine structure of formed precipitate, product purification by filtration was unsuccessful. As an alternative method, purification was performed by decantation multiple times in cold acetonitrile. In comparison to previous studies by Pingaew *et al.*^{69,70} change of reaction solvent from dichloromethane to acetonitrile produced higher yields for **18** and **19**.

7.4 Tetramethylcalix-[4]-resorcinarene based cavitands

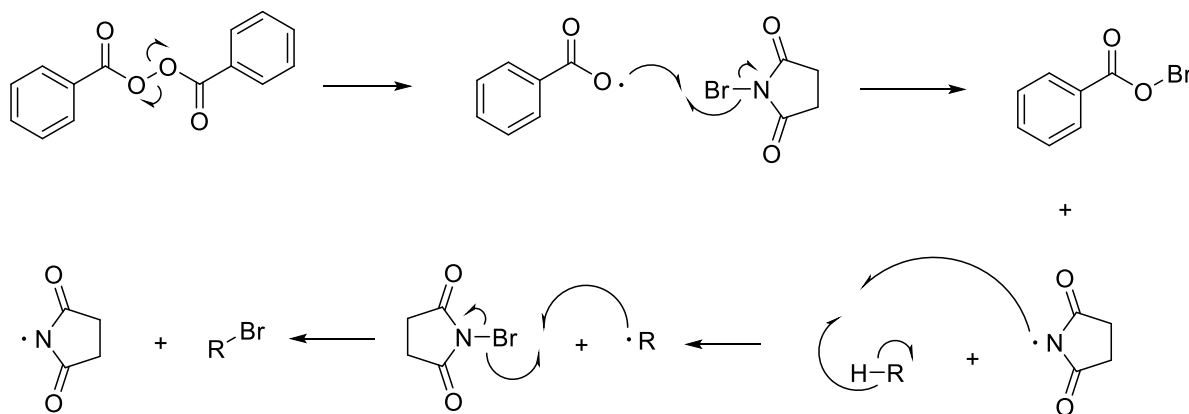


Scheme 7.5. Synthesis route for tetramethylcalix-[4]-resorcinarene based thiourea cavitands.

Calixarenes are well known from their cone-shaped three-dimensional structure and ability to act as a host for smaller molecules. Their good availability and functionalization possibilities offer broad applications for host-guest chemistry.⁷¹ Based on these reasons calix-[4]-resorcinarene structure was chosen for the backbone of thiourea receptor **26**. With the methylation of hydroxyl groups, cavitand would remain more rigid, directing thiourea sidechains on one side of the cavitand. Idea was that this feature could offer an interesting foundation for molecular cage architecture.

The primary goal was to synthesize resorcinarene-based cavitand **25**, which could be further converted to thiourea derivative through the addition of amine tail (Scheme 7.5). Synthesis route to cavitand **24** was conducted based on previous studies of Moussaoui *et al.*⁷² and Hu *et al.*⁷³ Procedure started with a classical resorcinarene synthesis methodology by coupling 2-methylresorcinol **20** with acetaldehyde **21** in acidic H₂O/EtOH solution to obtain cavitand **22**. For the synthesis of **23**, methyl addition between OH-groups was performed with CH₂Cl₂ or BrCH₂Cl in the presence of K₂CO₃ in dimethylformamide. The use of BrCH₂Cl gave slightly better yields due to its higher reactivity. However, with the marginal difference in yields (35% vs. 42%), CH₂Cl₂ could be preferred because of its eco-friendlier nature.

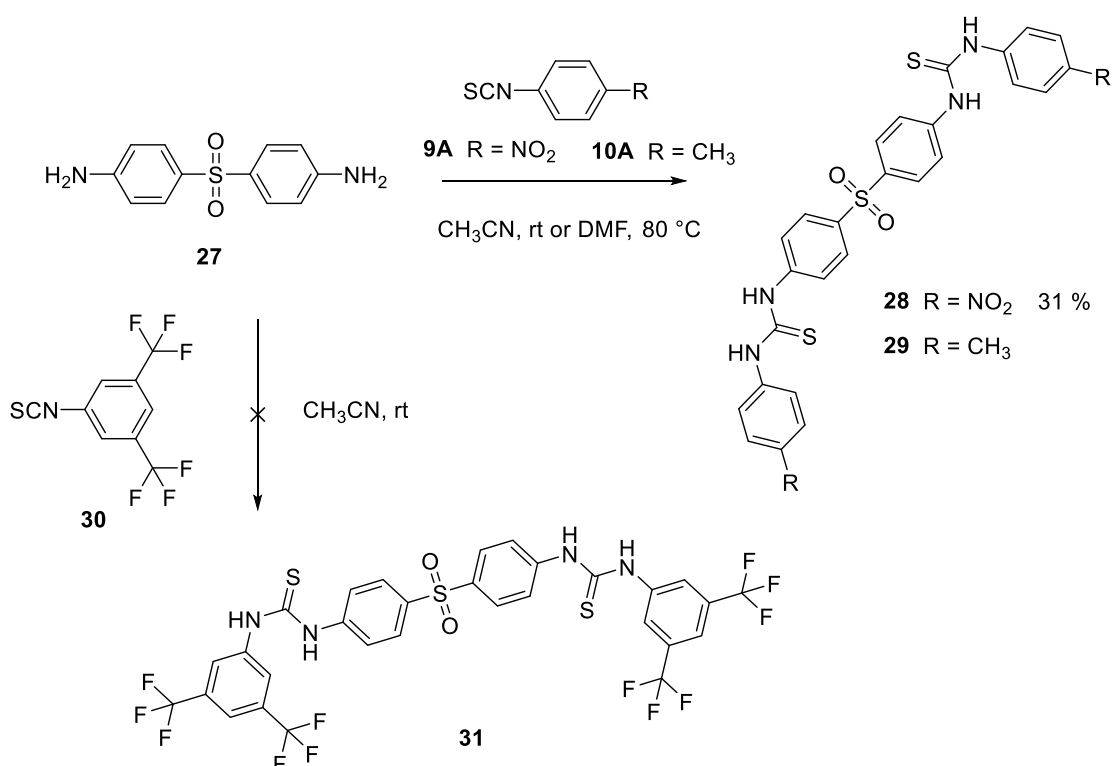
Many Wohl–Ziegler bromination⁷⁴ attempts were performed on aromatic methyl tails of **23**. Benzoyl peroxide was applied as an initiator through radical reaction with *N*-bromosuccinimide (NBS) (Scheme 7.6). There are several reasons for failure while performing this type of bromination on four methyl groups. In addition to the reaction's high sensitivity towards moisture, there are competing mechanisms. Most probable of these is bromination of CH-junctions between aromatic rings. Here product forms through tertiary radical intermediate. According to the mass spectra, bromination occurred only on one methyl group of **23**.



Scheme 7.6. Proposed reaction mechanism of Wohl–Ziegler bromination with benzoyl peroxide initiator.

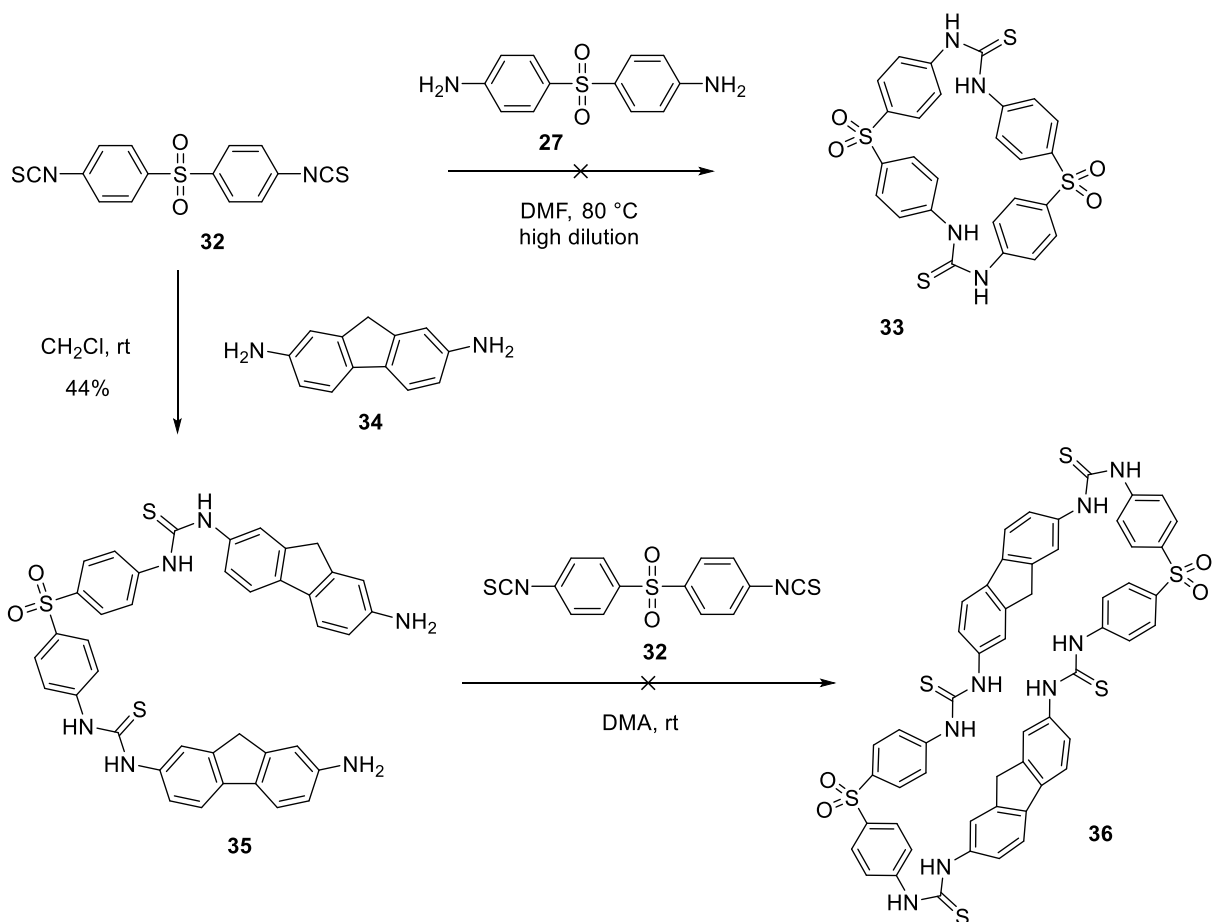
7.5 Phenyl sulfone and phenyl ether based thiourea receptors

Syntheses attempts of three dipodal thiourea derivatives **28**, **29** and **31** were performed (Scheme 7.7). Only compound **28** was obtained with a maximum yield of 31%. Compound **28** has been synthesized before by Ghorab *et al.*⁷⁵ with yields close to 80%. In contrast to our procedures, Ghorab applied dioxane as a solvent. Previous experience based on the synthesis of compounds **3** – **7** shows that the occurrence of electron-withdrawing groups (EWG) close to the amine site, lower the nucleophilicity and hence reactivity. On the NCS-site the situation is opposite. In the synthesis of **28**, the nitro group at the para-position increases the reactivity of **10A** through extra stabilization of the transition phase after the amine attack.

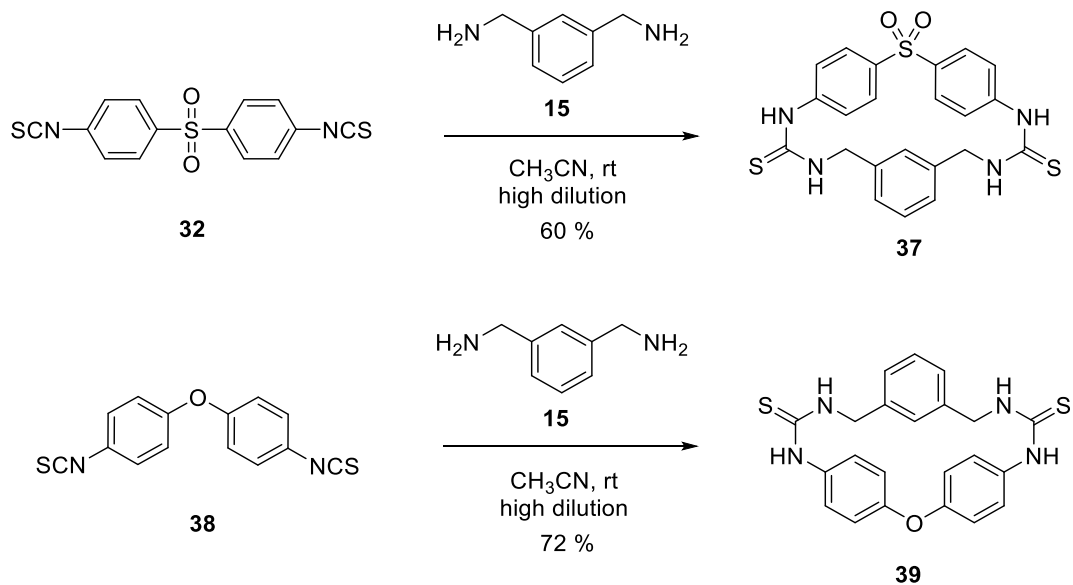


Scheme 7.7. Synthesis route for bis(4-aminophenyl)sulfone based acyclic thiourea ligands.⁷⁵

Macrocyclic thiourea derivatives **33** and **36** were attempted to synthesize as new structures (Scheme 7.8). To minimize the formation of side products, syntheses were performed in high dilution with the gradual addition of both components. Compound **27** expressed low solubility in common organic solvents, which was most likely due to the intermolecular hydrogen bonding network between amine and sulfone. Since reactions were performed in DMF, the probability of reaction mixture containing water was relatively high. This together with high torsional tension of product **33** might have been the reason for failure in synthesis. The extremely low solubility of compound **36** prevented its characterization.



Scheme 7.8. Synthesis route for macrocyclic thiourea ligands with phenylsulfone backbone



Scheme 7.9. Synthesis route for macrocyclic thiourea ligands with 3-(aminomethyl)benzylamine backbone.

Previous studies on sulfone and phenyl ether-based thiourea structures exploited only acyclic dipodal ligands. Examples of these were Ghohab *et al.*⁷⁵ investigating thiourea's abilities in antimicrobial activity and Yang *et al.*⁷⁶ applying dipodal thioureas as the selective catalyst for Michael additions. According to Scheme 7.9 two macrocyclic thiourea structures, **37** and **39** were synthesized with relatively high yields. Despite the high dilution method, final products contained small proportions of cyclization products **40** and **41** (Figure 7.1).

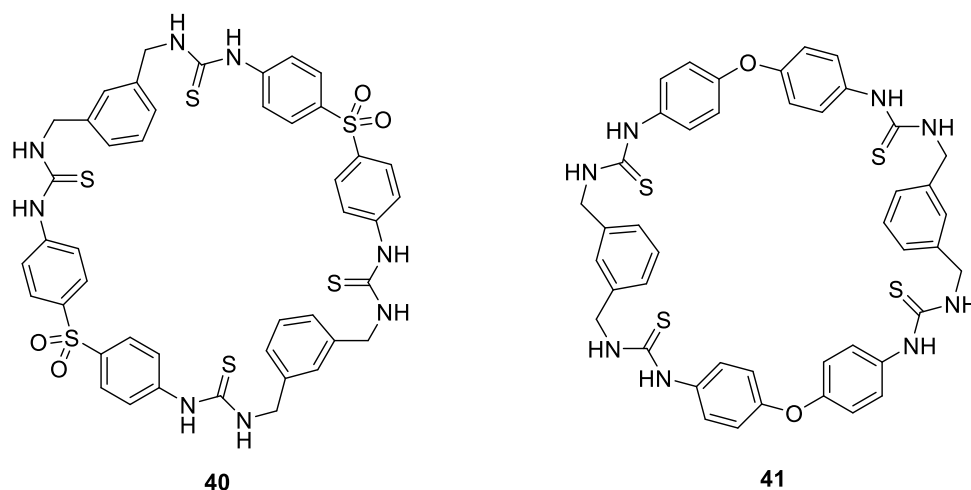


Figure 7.1. Cyclization products from synthesis of **37** and **39**.

8 Complexation studies and crystal structures

Most of the previously obtained halogen-bonded crystal structures were based on nitrogen or oxygen acting as an XB acceptor. A typical example of the acceptor is pyridine containing structures that have been proven to bind relatively well to Br⁺, I⁺ and XB donors on aromatic backbone (Figure 8.1).^{77,78} Sulfur is less explored in this field and only a few crystal structures with halonium ion (I⁺) have been successfully crystallized. These have been mostly thiourea or heterocycles bearing the thione-group.^{79,80,81}

Upon the addition of I₂, its effect and product formation are highly solvent dependent. According to the studies of Tamilselvi and Mugesh⁸¹ treatment of **MDT** structure with I₂ in water produced (**MDTox-H**) I₅⁻ complex with disulfide bond as the main product. Similar treatments in dichloromethane resulted in the formation of halogen-bonded structure (**MDT.I.MDT**) I₅⁻ (Figure 8.2).

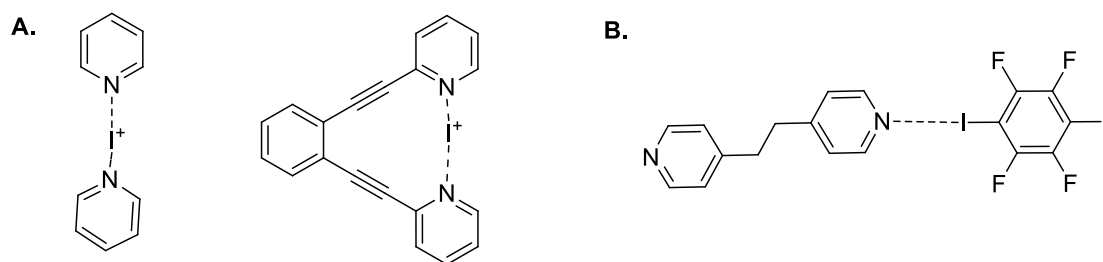


Figure 8.1. Typical pyridine containing XB assemblies **(a)** Structures of [bis(pyridine)iodine]⁺ and [bis(pyridinylethynyl)benzene iodine]⁺ **(b)** Pyridinyl ethane coordinated with 1,4-diodotetrafluoro benzene.⁷⁸

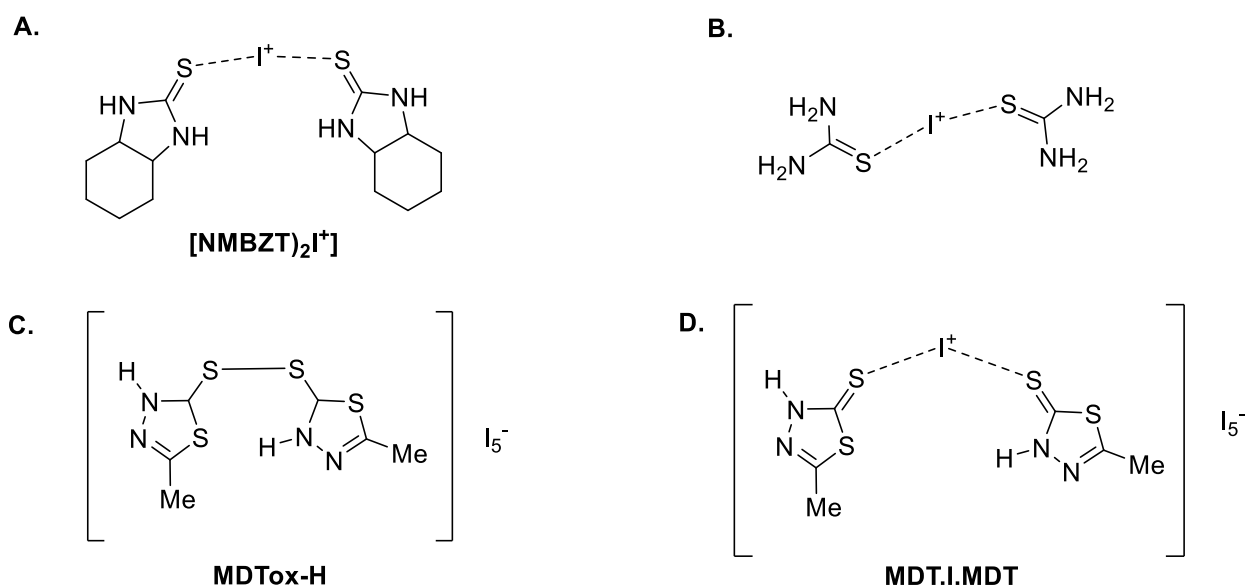


Figure 8.2. Examples of previously obtained thiocarbonyl-halonium ion structures. Iodonium complexes with **(a)** Benzimidazole-2-thione⁷⁹ **(b)** Thiourea⁸⁰ and **(c)** Methyl thiadiazole thione.⁸¹

8.1 Performed crystallizations

Crystallization attempts were performed to compounds **2** – **5**, **7** and **9**. For crystallization, DMF and DMSO solvents were applied. To fasten the crystallization process additional diffusion-enhanced samples were also prepared with dichloromethane as antisolvent. Pure iodine was added to the vials in 1:1, 1:2, 1:3, 1:4 and proportions. With classical halogen bond donors, **A** and **B** (Figure 6.1), 2:3 proportion was applied.

Samples with pure iodine added were analyzed for coordination with NMR. In each attempt, iodine seemed to express chemical reactivity towards thiourea moieties. This can be observed from the ^1H -NMR spectra presented in Figure 8.3. The broadening of the peaks indicates the occurrence of an ongoing dynamic process resulting in the decomposition of ligands. This was also supported by the formation of pure sulfur (S_8) in several crystallization samples.

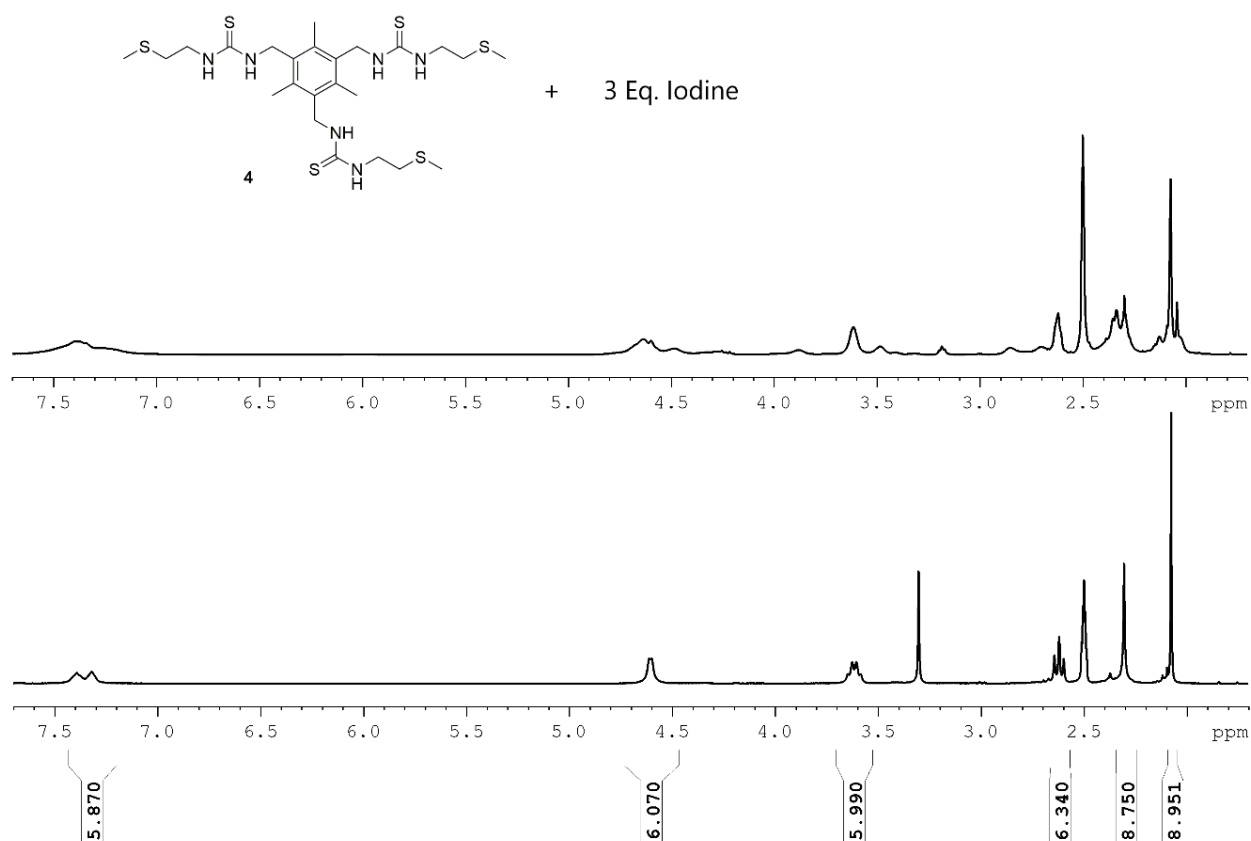
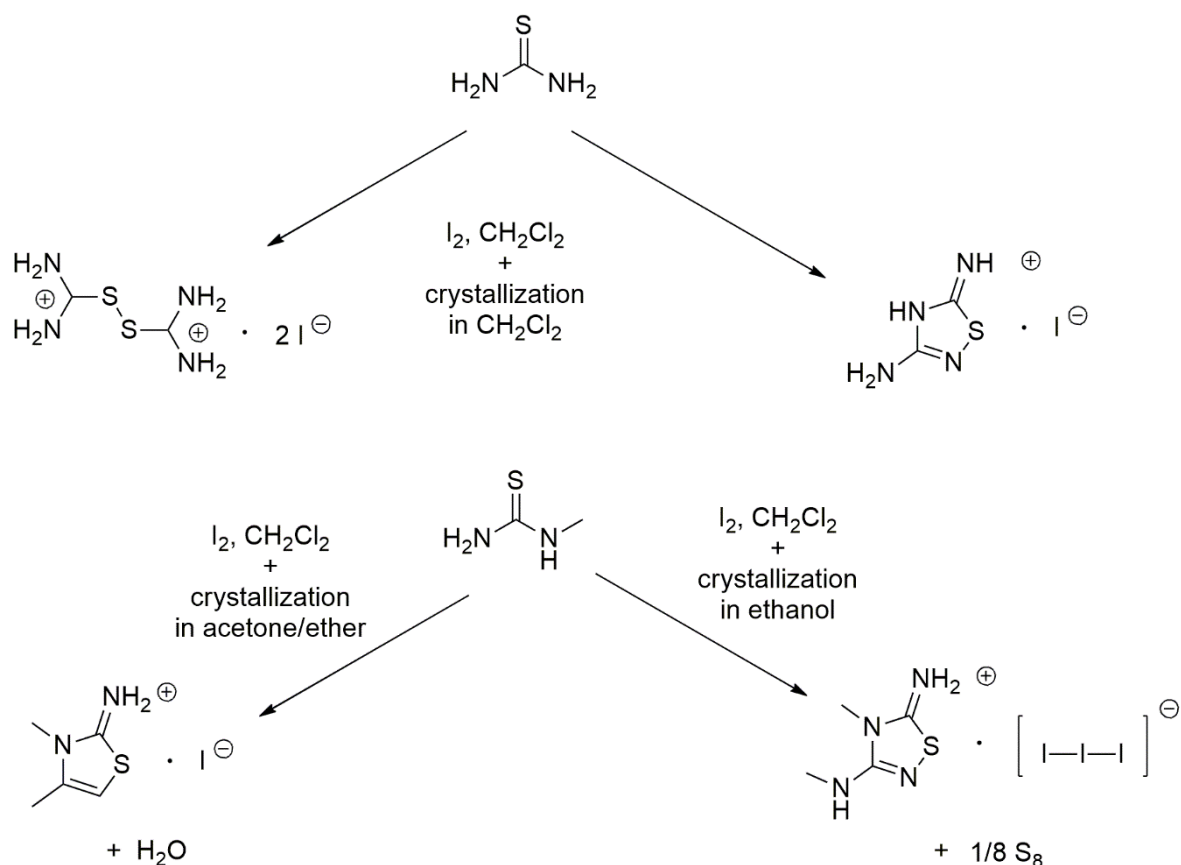


Figure 8.3. ^1H -NMR spectra of pure ligand **4** (below) and with 3 eq. of iodine added (above).

Being a relatively strong oxidizer, iodine can react in various ways with investigated thiourea receptors. There is no clear mechanistic insight into the reaction pathways that may occur during the ligand decomposition. Most likely, the reaction starts via iodine addition to thiocarbonyl, which transfers the double-bond electron pair towards NH-group. Experimental studies of Biesiada *et al.*⁸² on thiourea and methylthiourea have proved the formation of aminothiazoles and aminothiadiazaoles with the presence of iodine (Scheme 8.1).



Scheme 8.1. Evidence of thiourea and methylthiourea decomposition in the presence of excess iodine by Biesiada *et al.*⁸²

From the tripodal receptors, compounds **3** and **5** showed decent halogen bonds to classical donors **A** and **B** (Figure 8.4 and 8.5). The lengths of XBs varied between 3.3 – 3.6 Å depending on the structure. XB angles lined up close to the direction of the C-I bond, ranging between 170 – 180°, which is a typical behavior considering the high directionality of the halogen bond. Acceptor angles $\text{C}=\text{S}\cdots\text{I}$ had a large variety of 90 – 130°, which is a common phenomenon due to the large size and soft nature of the sulfur atom. All tripodal receptors seemed to stack on top of each other via the hydrogen bonding network between thiocarbonyl and NH-groups. This behavior was observed in crystal structures with both classical donors **A** and **B**. ORTEP representations of all obtained crystal structures are found in the [appendix](#).

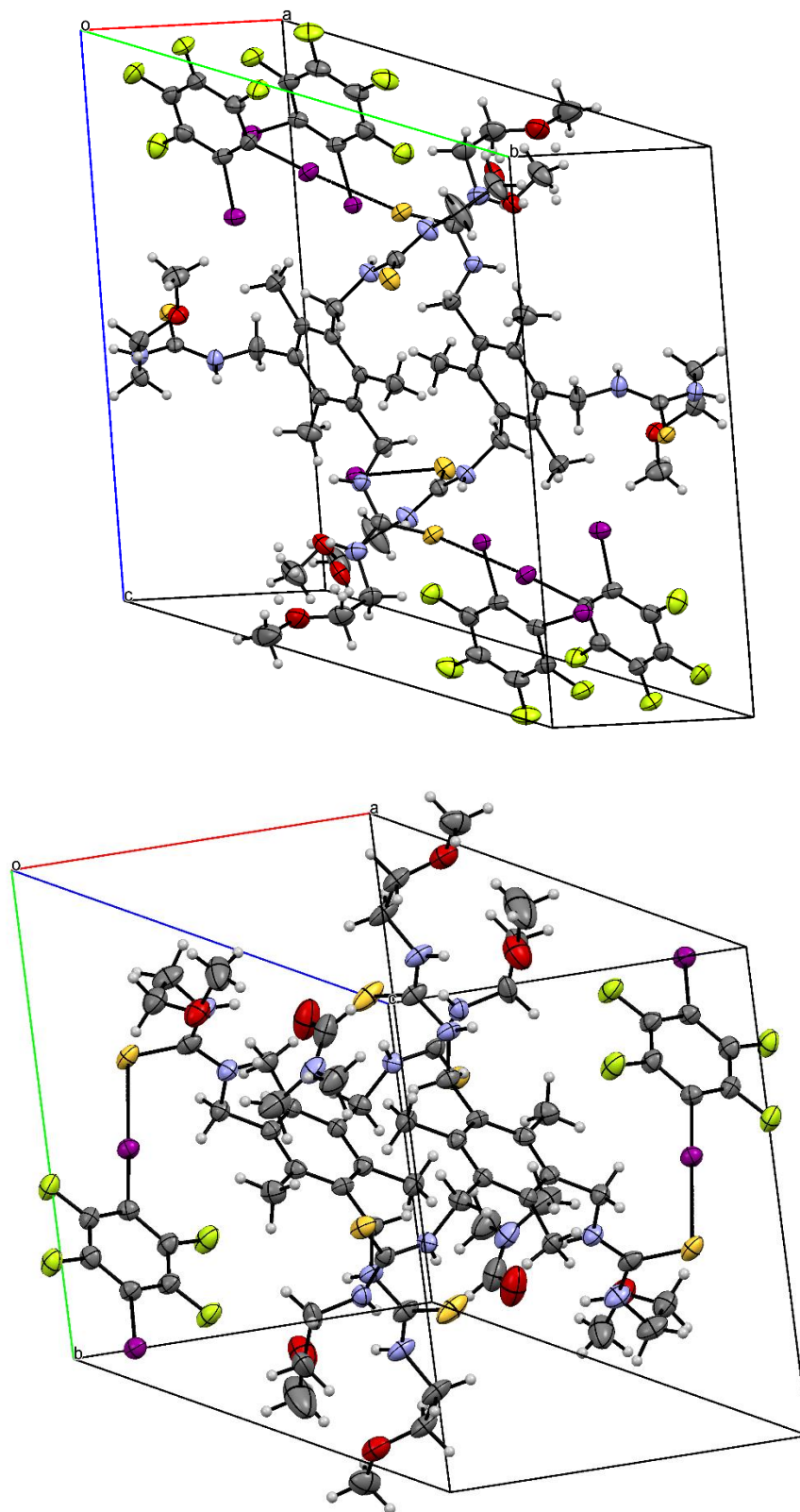


Figure 8.4. Packing structure of receptor **3** with (upper) 1,2-diodotetrafluorobenzene and (lower) 1,4-diodotetrafluorobenzene.

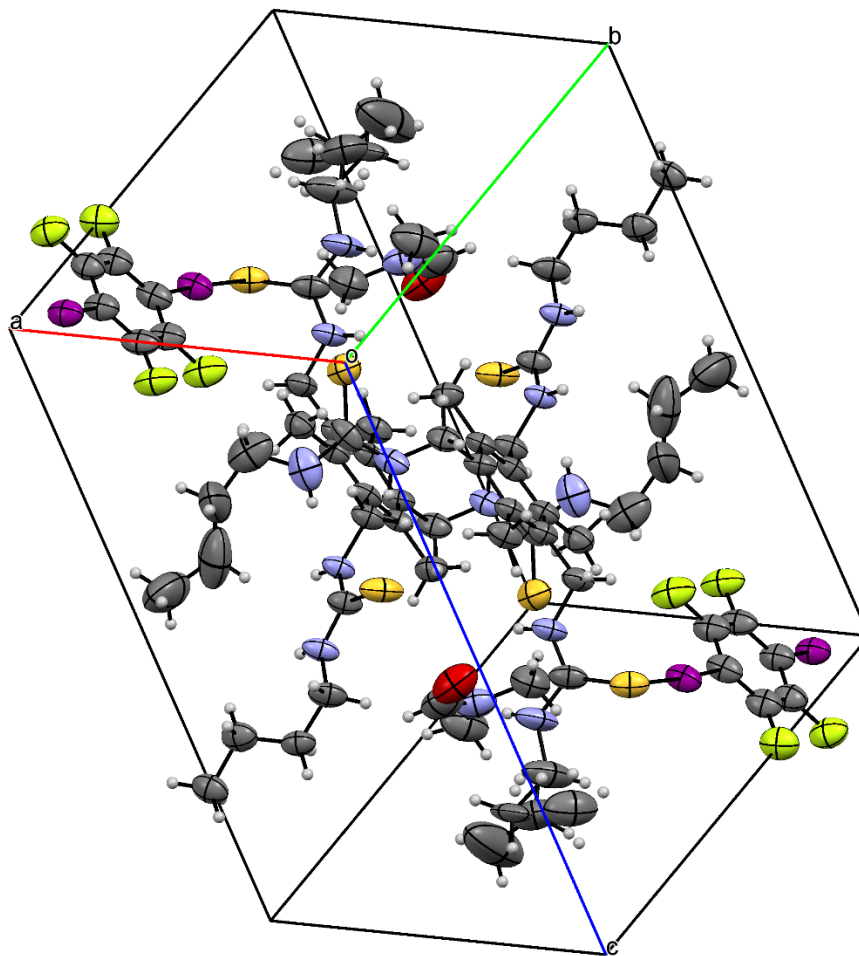


Figure 8.5. Packing structure of receptor 5 with 1,4-diodotetrafluorobenzene.

9 Conclusion

Synthesis of thiourea receptors is relatively straightforward, occurring via addition-reaction between amine and isothiocyanate. Since the transition phase is highly moisture sensitive, reactions should be performed with dry solvents and glassware under the atmosphere of inert gas. To synthesize more versatile receptors containing several thiourea-moieties, various methodologies to produce isothiocyanate-precursors can be applied. Most commonly, these are carried as NH_2 to NCS conversion with 1,1-thiocarbonylimidazole or carbon disulfide with the presence of a weak base.

The biggest challenge in the synthesis of receptors with several thiourea-groups is the possibility of by-product formation and crude purification. Due to the extensive hydrogen bonding network between thiourea moieties, the solubility of receptors in common organic solvents is remarkably decreased. This limits the use of chromatographical purification methods. In addition, the presence of compounds with several NCS- and NH_2 - groups in the reaction mixture can easily afford the polymer formation.

Based on the complexation studies of tripodal thiourea receptors, the chemical reaction between the ligand and I_2 in DMSO or DMF solution occurs in each case. This was backed up by the broadening of NMR peaks and the formation of S_8 in the crystal samples. However, some of the tripodal receptors successfully formed halogen bonds with 1,2-diiidotetrafluorobenzene and 1,4-diiidotetrafluorobenzene.

In general, the low solubility of produced receptors makes them rather unpractical, regarding the characterization, crystallization and potential applications. The low volatility of DMSO and DMF makes the crystallization process extremely slow and most likely affects the outcome of the reaction. The solubility of receptors might be increased through side-chain modifications or with the presence of anionic species, which loosen the hydrogen bonding network between thiourea moieties.

10 Experimental procedures

10.1 Overall procedures

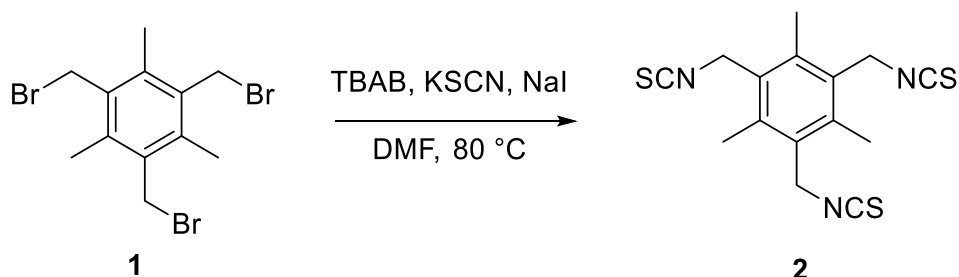
All syntheses were performed in dry conditions under argon atmosphere, if not mentioned otherwise. Acetonitrile and dichloromethane were dried with MBraun SPS-800-solvent drying apparatus. Other applied solvents were HPLC grade. TLC tests were performed with Merck TLC Silica gel 60 F254 disks. Chromatographic purifications were done with silica column Merck Silica gel 60 (230-400 mesh). Products were characterized with NMR (Bruker Avance III HD 300 MHz and Bruker Avance III 500 MHz) and mass spectrometry (MicroMass LCT Premier). Melting points were measured with Stuart Scientific Melting Point Apparatus SMP3. Crystal structures were analyzed with Rigaku OD SuperNova single crystal diffractometer. Applied commercially available reagents are presented in [Table 10.1](#).

Table 10.1. Reagents utilized in syntheses.

Compound	Purity (%)	Supplier
Potassium isothiocyanate	> 99.0	Merck Chemicals
Tetrabutylammonium bromide	> 99.0	Fluka Chemika
1,3,5-Tris(bromomethyl)-2,4,6-trimethylbenzene	> 98.0	TCI
Sodium iodide	99.5	Alfa Aesar
2-Methoxyethylamine	> 98.0	TCI
2-(Methylthio)ethylamine	97.0	Sigma-Aldrich
1-Naphthylmethylamine	97.0	Aldrich Chemistry
Butylamine	> 99	Merck Schuchardt
Tris(2-aminoethyl) amine	96.0	Acros Organics
4-Nitrophenyl isothiocyanate	98.0	Aldrich Chemistry
Naphthyl-(1)-amine	> 99.0	Merck Chemicals
1,3-Bis(bromomethyl)benzene	> 97.0	Apollo Scientific
3-(Aminomethyl)-benzylamine	99.0	Aldrich Chemistry
1,1-Thiocarbonylimidazole	> 95.0	TCI
<i>p</i> -Tolyl isothiocyanate	97.0	Aldrich Chemistry
2,6-Dihydroxytoluene	≈ 90	Fluka Chemika

Acetaldehyde	99.5	Riedel-de Haen
Potassium carbonate	99.8	VWR Chemicals
Benzyl peroxide	97.0	Merck Schuchardt
<i>N</i> -Bromosuccinimide	99.0	Sigma-Aldrich
Bromochloromethane	99.0	Sigma-Aldrich
Bis(4)-aminophenyl sulfone	> 98.0	TCI
Isothiocyanatophenyl sulfone	> 98.0	TCI
4-Isothiocyanatophenyl ether	98.0	Fluorochem
2,7-Fluorenediamine		TCI
3,5-Bis(trifluoromethyl)phenyl isothiocyanate	98.0	Fluorochem

10.2 1,3,5-Trimethyl-2-,4,6-tris(isothiocyanatomethyl) benzene



Scheme 10.2. Synthesis route for compound **2**.

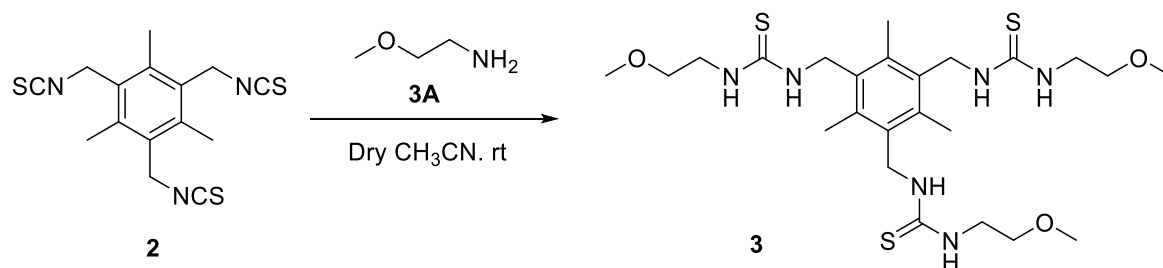
Compound **2** was synthesized from commercially available 1,3,5-tris(bromomethyl)-2,4,6-trimethylbenzene **1**. To the stirring solution of compound **1** (1.47 g, 3.69 mmol, 1 eq.) were added sodium iodide (0.481 g, 3.20 mmol, 0.9 eq.), potassium thiocyanate (2.69 g, 27.7 mmol, 7.5 eq.) and tetrabutylammonium bromide (4.41 g, 13.7 mmol, 3.7 eq.) (Scheme 10.2). The mixture was stirred at 80 °C for 4 hours. The formed precipitate was filtrated and remained solvent diluted with water (80 ml). The extraction of the organic phase was performed with ethyl acetate. The remaining TBAB was extracted by filtration through silica. After solvent evaporation, 1.22 g of pale-yellow product was obtained (91.1%).

$^1\text{H NMR}$ (500 MHz, CDCl_3) δ 4.72 (s, 6H), 2.48 (s, 9H).

$^{13}\text{C NMR}$ (125 MHz, CDCl_3) δ 137.4, 133.5, 131.25, 44.1, 16.4

$[\text{M}+\text{Na}]^+$ 356.0319 Mp. 125 – 128 °C

10.3 1,1',1''-((2,4,6-Trimethylbenzene-1,3,5-triyl) tris(methylene))tris(3-(2-methoxyethyl)thiourea)



Scheme 10.3. Synthesis route for compound **3**

To the stirring solution of 1,3,5-trimethyl-2,4,6-tris(isothiocyanatomethyl) benzene **2** (0.288 g, 0.86 mmol) a solution of 2-methoxy ethylamine **3A** (0.5 ml, 5.2 mmol, 6 eq.) in 6 ml of acetonitrile was added (Scheme 10.3). Progression of the reaction was followed with TLC Hex:EtOAc (20:80). The reaction was running for 2.5 d forming a white precipitate to the solution. The precipitation was filtered and washed with acetonitrile giving 0.238 g of white powder with 49.4% yield.

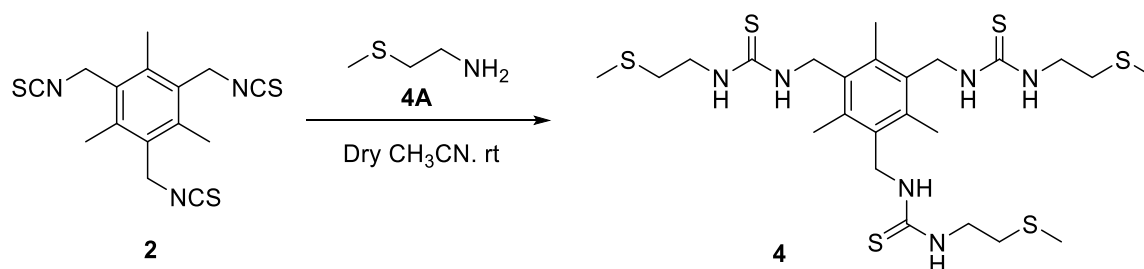
¹H NMR (500 MHz, DMF-d₇) δ 7.48, 7.38 (s, 6H, NH), 4.74 (d, 6H, 4.2 Hz), 3.50 (t, 6H, 5.4 Hz), 3.29 (s, 9H), 2.39 (s, 9H)

¹³CNMR (125 MHz, DMF-d₇) δ 184.2, 137.7, 134.1, 71.8, 58.8, 44.8, 16.6.

[M+Na]⁺ 581.2363

Mp. = 195 – 198 °C

10.4 1,1',1''-((2,4,6-Trimethylbenzene-1,3,5-triyl) tris(methylene))tris(3-(2-(methylthio)ethyl)thiourea)



Scheme 10.4. Synthesis procedure for compound **4**

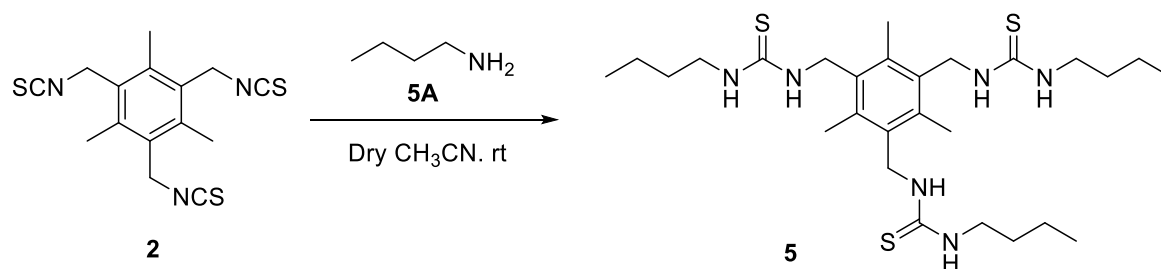
To the stirring solution of 1,3,5-trimethyl-2-,4,6-tris(isothiocyanatomethyl) benzene **2** (0.260 g, 0.78 mmol) a solution of 2-(methylthio) ethylamine **4A** (0.4 ml, 3.9 mmol, 5 eq.) was added (Scheme 10.4). Progression of the reaction was followed with TLC Hex:EtOAc (20:80). The reaction was running for 3.5 h forming a white precipitate to the solution. The precipitation was filtered and washed with ACN giving 0.309 g of white powder with 65.3% yield.

^1H NMR (500 MHz, **DMSO-d6**) δ 7.35, 7.28 (s, 6H, NH), 4.56 (d, 6H, 3.6 Hz), 3.57 (q, 6H, 6.4 Hz), 2.58 (t, 6H, 6.8 Hz), 2.27 (s, 9H), 2.04 (s, 9H)

^{13}C NMR (125 MHz, **DMSO-d6**) δ 182.3, 136.6, 132.8, 43.3, 42.7, 32.5, 16.0, 14.5.

$[\text{M}+\text{Na}]^+ 629.1672$, $[\text{M}+\text{H}]^+ 607.1853$, Mp. 219 – 221 °C

10.5 1,1',1''-((2,4,6-Trimethylbenzene-1,3,5-triyl) tris(methylene))tris(3-butylthiourea)



Scheme 10.5. Synthesis procedure for compound **5**

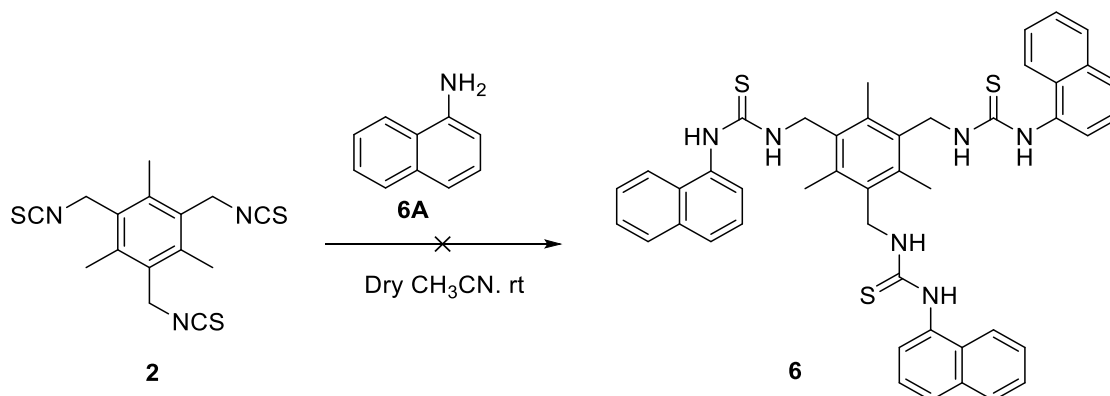
To the stirring solution of 1,3,5-trimethyl-2-,4,6-tris(isothiocyanatomethyl) benzene **2** (0.268 g, 0.78 mmol) butylamine **5A** (0.358 g, 4.82 mmol, 6.2 eq.) was added (Scheme 10.5). Progression of the reaction was followed with TLC Hex:EtOAc (40:60). The reaction was running for 3 h forming a white precipitate to the solution. The precipitation was filtered and washed mechanically with ACN giving 362 mg of white powder product with 83.2% yield.

^1H NMR (500 MHz, **DMF-d7**) δ 7.41 (s, 3H, NH), 7.15 (s, 3H, NH), 4.72 (d, 6H, CH_2 , 3.8 Hz), 3.54 (6H, CH_2 , overlap with H_2O) 2.38 (s, 9H, CH_3), 1.54 (p, 6H, 7.4 Hz), 1.34 (sx, 6H, CH_2 , 7.4 Hz), 0.9 (t, 9H, CH_3 , 7.4 Hz)

^{13}C NMR (125 MHz, **DMF-d7**) δ 184.0, 137.8, 134.1, 44.7, 34–36 (overlap with DMF), 32.2, 20.7, 16.6, 14.2.

$[\text{M}+\text{Na}]^+ 575.2977$ Mp. = 246 – 248 °C

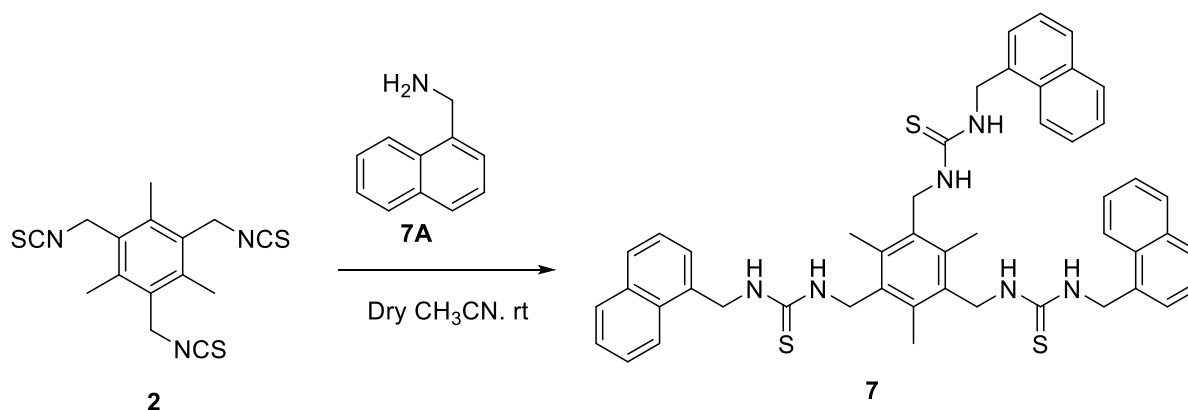
10.6 1,1',1''-((2,4,6-Trimethylbenzene-1,3,5-triyl)tris(methylene))tris(3-(naphthalen-1-yl)thiourea)



Scheme 10.6. Synthesis procedure for compound **6**.

1,3,5-Trimethyl-2-,4,6-tris(isothiocyanatomethyl) benzene **2** (0.164 g, 0.49 mmol) and naphthyl-(1)-amine **6A** (0.370 g, 2.58 mmol) were weighted in the reaction flask and dissolved in 15 ml dry acetonitrile (Scheme 10.6). The reaction was run at room temperature for one day. Progression of the reaction was followed with TLC Hex:EtOAc (1:1). The synthesis did not produce the desired product, reaction mixture containing only starting reagents.

10.7 1,1',1''-((2,4,6-Trimethylbenzene-1,3,5-triyl) tris(methylene))tris(3-(naphthalen-1-ylmethyl)thiourea)



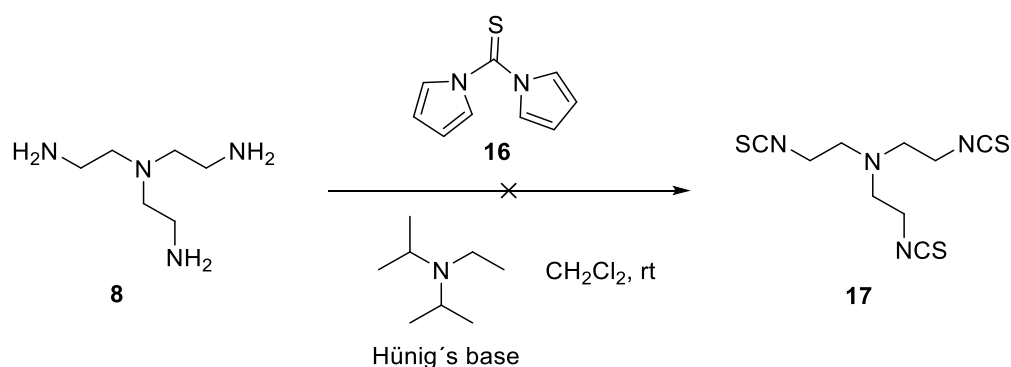
Scheme 10.7. Synthesis procedure for compound **7**

To the stirring solution of 1,3,5-trimethyl-2-,4,6-tris(isothiocyanatomethyl) benzene **2** (0.040 g, 0.12 mmol) in dry acetonitrile 1-naphthylmethylamine **7A** (0.075 g, 0.48 mmol, 0.071 ml, 4 eq.) was added (Scheme 10.7). The reaction was stirred overnight at the room temperature.

Formed white precipitate was filtrated and washed with acetonitrile. After drying, 0.048 g of white powder was obtained 49.5 %.

^1H NMR (500 MHz, **DMSO-d6**) δ 8.06, 7.95, 7.85 (d, 9H, Ar-H, 7.8 Hz), 7.63 (s, 3H, NH), 7.45-7.58 (12H, Ar-H), 7.23 (s, 3H, NH), 5.11 (s, 6H, CH₂), 4.65 (s, 6H, CH₂), 2.31 (s, 9H, CH₃)

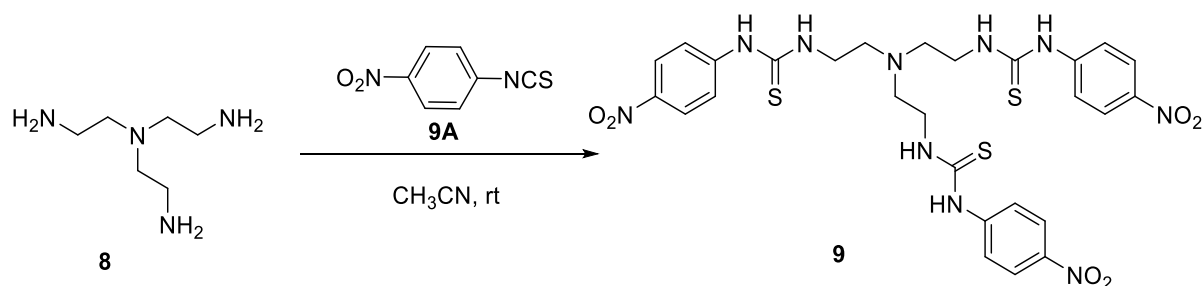
10.8 Tris(2-isothiocyanatoethyl) amine



Scheme 10.8. Synthesis procedure for compound **17**

1,1-Thiocarbonylimidazole **16** (2.032 g, 11.4 mmol, 4.2 eq.) was dissolved in dry dichloromethane. Hünig's base (1.06 g, 8.20 mmol, 3 eq.) and tris(2-aminoethyl)amine **8** (0.40 g, 2.74 mmol) in 40 ml dichloromethane were added during 30 min through the dropping funnel (Scheme 10.8). Reaction mixture was stirred for 3 h at the room temperature. The product was filtered through silica and washed with hexane:EtOAc (20:80). After solvent evaporation, 0.129 g of oily crude was obtained. Synthesis did not produce the desired product.

10.9 *N*1-(4-nitrophenyl)-*N*2, *N*2-bis(2-((4-nitrophenyl)amino)ethyl)ethane-1,2-diamine



Scheme 10.9. Synthesis procedure for compound **9**

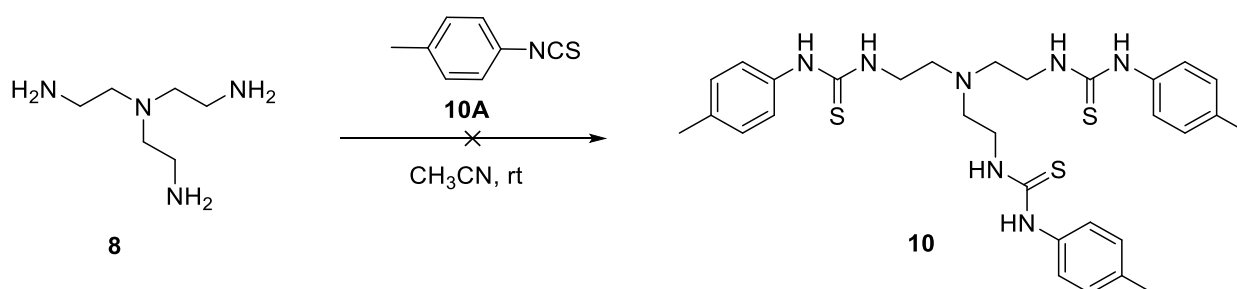
To the stirring solution of 4-nitrophenyl isothiocyanate **9A** (0.713 g, 3.96 mmol, 4 eq.) in 20 ml of dry acetonitrile tris(2-aminomethyl)amine **8** (0.147 g, 1.0 mmol) was added (Scheme 10.9). The reaction mixture was stirred for 2 hours in the room temperature under argon atmosphere. Progression of the reaction was followed by TLC hexane:EtOAc (20:80). The reaction produced bright yellow precipitate, which was filtrated and washed with acetonitrile 3 x 50 ml. After drying 0.782 g of a yellow solid product was obtained. Due to the measurement error of tris(2-aminomethyl)amine **7** yield is unknown.

^1H NMR (500 MHz, **THF-d8**) δ 9.48 (s, 3H, NH), 8.09 (d, Ar-H, 9.1 Hz), 7.71 (s, 3H, NH), 7.68 (d, Ar-H, 9.1 Hz), 3.79 (q, 6H, CH₂, 5.5 Hz), 2.89 (t, 6H, CH₂, 6.4 Hz)

^{13}C NMR (125 MHz, **THF-d8**) δ 182.1, 146.7, 144.2, 125.3, 122.0, 53.8, 43.8

$[\text{M}+\text{H}]^+$ 687.1609, $[\text{M}+\text{Na}]^+$ 709.1437, $[\text{M}+\text{K}]^+$ 725.1172, Mp. = 190 – 197 °C

10.10 *N1-(p-Tolyl)-N2,N2-bis(2-(p-tolylamino)ethyl)ethane-1,2-diamine*



Scheme 10.10. Synthesis procedure for compound **10**

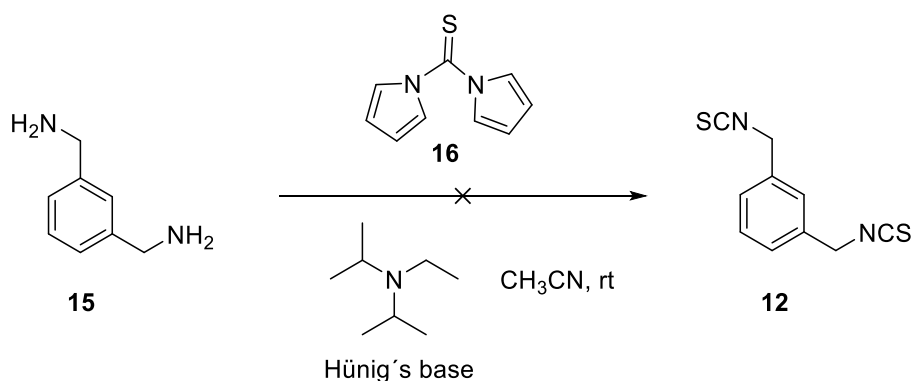
To the stirring solution of *p*-tolyl isothiocyanate **10A** (0.936 g, 6.27 mmol, 3.3 eq) in 15 ml of dry acetonitrile tris(2-aminoethyl)amine (0.293 g, 2.01 mmol, 300 μ l) was added (Scheme 10.10). The reaction mixture was stirred under argon at the room temperature for 3 hours. Progression was followed with hexane:EtOAc (20:80) TLC. Crude was purified with silica column hexane:EtOAc (20:80) giving a wet yellow oil. The desired product was not obtained. After vacuum drying, 0.770 g of product was obtained 64,5%. Despite purification, NMR analysis showed the remains of ethyl acetate and *p*-tolyl isothiocyanate in the product.

^1H NMR (500 MHz, **CDCl**₃) δ 8.20 (s, 3H, NH), 7.08 (s, 12H, Ar-H), 6.78 (s, 3H, NH), 3.68 (s, 6H, CH₂), 2.66 (s, 6H), 2.26 (s, 9H, CH₃)

^{13}C NMR (125 MHz, **CDCl**₃) δ 181.3, 136.8, 134.5, 130.4, 125.3, 53.4, 43.2, 21.2

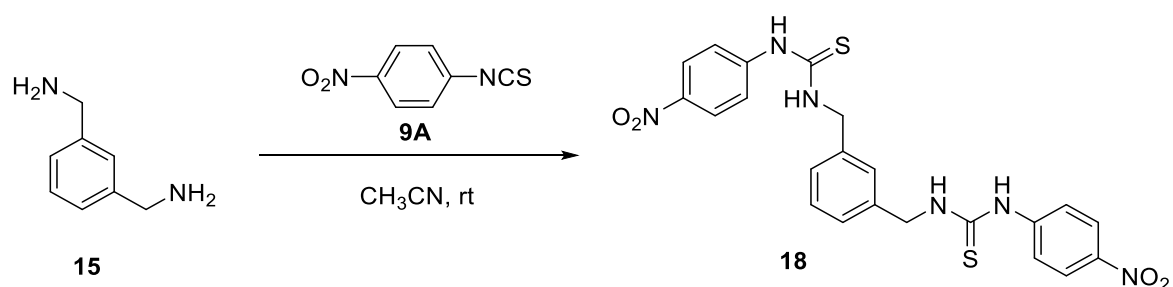
$[\text{M}+\text{H}]^+$ 594.2531, $[\text{M}+\text{Na}]^+$ 616.2309

10.13 1,3-Bis(isothiocyanatomethyl)benzene

Scheme 10.13. Alternative synthesis procedure for compound **12**

To the stirring solution of 1,1-thiocarbonylimidazole **16** (1.308 g, 7.3 mmol) in 15 ml of dry acetonitrile 3-(aminomethyl)benzylamine **15** (0.40 g, 2.9 mmol, 2.5 eq.) was added (Scheme 10.13). Hünig's base (0.750 g, 5.8 mmol, 0.8 eq.) was dissolved in 10 ml of acetonitrile and gradually added through the dropping funnel during 15 min. Shortly after addition yellow precipitate was formed. The reaction was stirred at the room temperature under argon for 2.5 h. Progression was followed with TLC hexane:EtOAc (20:80). The white precipitate was filtrated and remained solvent evaporated, producing brown oil. The oil was run through the column with MeOH:CHCl₃ (5:95) as an eluent. All components contained a mixture of different products. The desired product was not obtained.

10.14 1,1'-(1,3-Phenylenebis(methylene))bis(3-(4-nitrophenyl)thiourea)

Scheme 10.14. Synthesis procedure for compound **18**

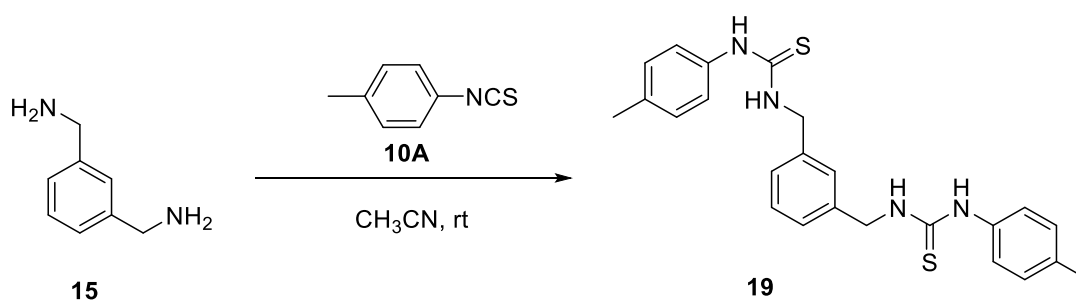
To the stirring solution of 4-nitrophenyl isothiocyanate **9A** (1.323 g, 7.34 mmol, 2.5 eq) in dry acetonitrile 3-(aminomethyl)benzylamine **15** (0.4 g, 2.9 mmol, 0.388 ml) was added (Scheme 10.14). The reaction mixture was stirred at the room temperature for 2 hours. The formed yellow precipitate was washed and decanted with cold acetonitrile. After solvent evaporation, 1.278 g of bright yellow powder was obtained 88.8%.

^1H NMR (500 MHz, CD_3COCD_3) δ 9.49 (s, 2H, NH), 8.17 (d, 4H, Ar-H, 9.2 Hz), 8.07 (s, 2H, NH), 7.92 (d, 4H, Ar-H, 9.2 Hz), 7.46 (s, 1H, Ar-H), 7.32 (s, 3H, Ar-H), 4.90 (d, 4H, CH_2 , 5.6 Hz)

^{13}C NMR (125 MHz, CD_3COCD_3) δ 182.7, 147.5, 144.5, 140.1, 130.0, 128.1, 125.7, 122.8, 49.2

$[\text{M}+\text{Na}]^+ 519.0874$, $[\text{2M}+\text{Na}]^+ 1015.1837$

10.15 1,1'-(1,3-Phenylenebis(methylene))bis(3-(*p*-tolyl)thiourea)



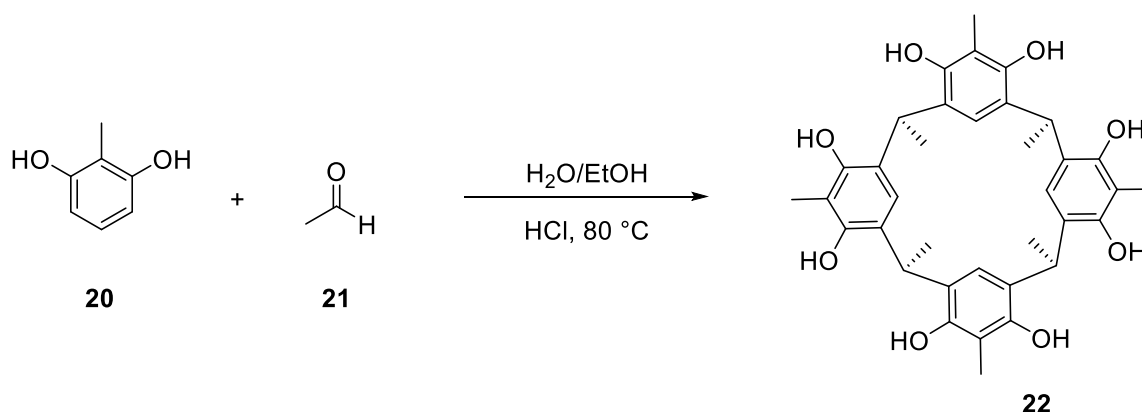
Scheme 10.15. Synthesis procedure for compound **19**

To the stirring solution of *p*-tolyl isothiocyanate **10A** (1.095 g, 7.35 mmol, 2.5 eq) in dry acetonitrile 3-(aminomethyl) benzylamine **15** (0.40 g, 2.9 mmol, 0.388 ml) was added (Scheme 10.15). The reaction mixture was stirred at the room temperature for 3 hours. The formed white precipitate was washed and decanted with cold acetonitrile. After solvent evaporation, 1.178 g of white powder was obtained 93.4%.

^1H NMR (500 MHz, DMSO-d_6) δ 9.50 (s, 2H, NH), 8.02 (s, 2H, NH), 8.07 (s, 2H, NH), 7.20-7.32 (3H, Ar-H, middle ring), 7.27 (d, 4H, Ar-H, 8.2 Hz), 7.12 (d, 4H, Ar-H, 8.2 Hz), 4.72 (d, 4H, CH_2 , 5.5 Hz), 2.26 (s, 6H, CH_3)

^{13}C NMR (125 MHz, DMSO-d_6) δ 180.8, 139.2, 136.3, 133.6, 129.1, 128.2, 126.2, 125.9, 123.8, 47.2, 20.5

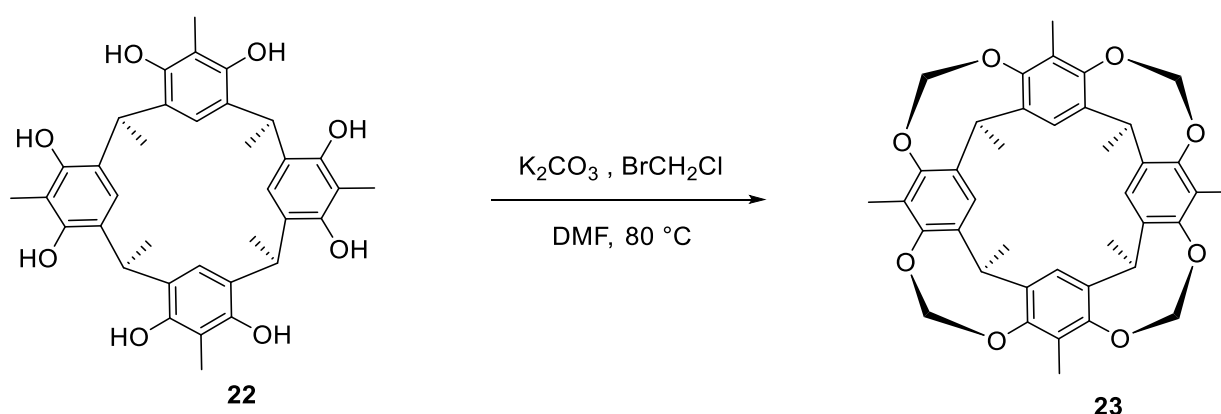
$[\text{M}+\text{Na}]^+ 547.1481$, $[\text{2M}+\text{Na}]^+ 891.3058$

10.16 Tetramethylcalix-[4]-resorcinarene **22**Scheme 10.16. Synthesis procedure for compound **22**

2,6-Dihydroxytoluene **20** (9.801 g, 79.0 mmol) was dissolved in a solution containing 40 ml H₂O, 40 ml EtOH and 10 ml HCl (37 %) (Scheme 10.16). To this stirring solution, acetaldehyde **21** (4.0 g, 90.0 mmol, 5.13 ml, 1.15 eq.) was added gradually during 15 min. The reaction mixture was refluxed overnight at 80 °C. Formed orange precipitate was washed with cold EtOH/H₂O solution. After drying 3.441 g yellowish orange powder was obtained 29.0%.

¹H NMR (500 MHz, DMSO-*d*₆) δ 8.64 (s, 8H, Ar-OH), 7.38 (s, 4H, Ar-H), 4.43 (q, 4H, CH₃CH, 7.2 Hz), 1.94 (s, 12H, Ar-CH₃), 1.69 (d, 12H, CH₃CH, 7.3 Hz)

¹³C NMR (125 MHz, DMSO-*d*₆) δ 148.6, 125.7, 120.9, 111.5, 28.6, 20.1, 9.9

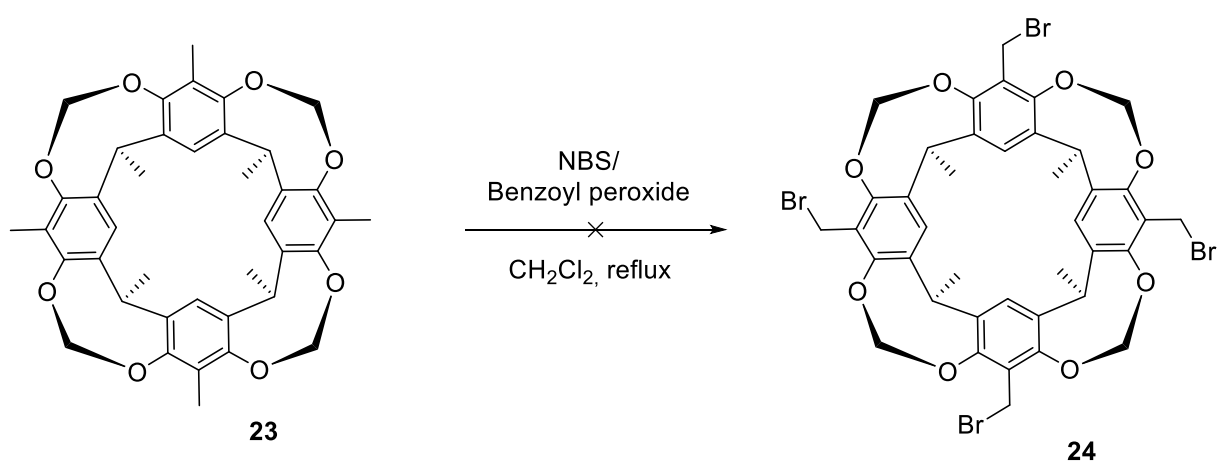
10.17 Tetramethylcalix-[4]-resorcinarene **23**Scheme 10.17. Synthesis procedure for compound **23**

Cavitand **22** (1.612 g, 2.68 mmol) and K₃CO₃ (7.40 g, 53.6 mmol, 20 eq.) were dissolved in 40 ml of dimethyl formamide and reaction mixture heated to 60 °C (Scheme 10.17). To this stirring

mixture bromochloromethane (20.8 g, 0.161 mol, 10.5 ml, 60 eq) was added gradually during 10 min. The mixture was refluxed overnight at 80 °C. The formed white precipitate was filtrated, and the remained solution added to 100 ml of 2 M HCl. The resulted orange precipitate was filtrated and washed with H₂O. After column chromatography (CH₂Cl₂) purification 0.736 g of white powder was obtained 42.3%.

¹H NMR (500 MHz, CDCl₃) δ 7.07 (s, 4H, Ar-H), 5.83 (d, 4H, outer of OCH₂O, 6.6 Hz), 4.94 (q, 4H, CH₃CH, 7.4 Hz), 4.21 (d, 4H, inner of OCH₂O, 6.8 Hz), 1.92 (s, 12H, Ar-CH₃), 1.69 (d, 12H, CH₃CH, 7.4 Hz)

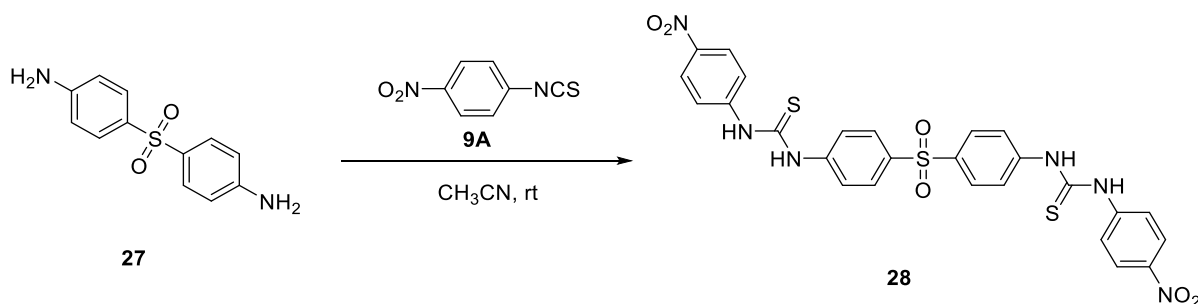
10.18 Tetramethylcalix-[4]-resorcinarene **24**



Scheme 10.18. Synthesis procedure for compound **24**

To the stirring solution of tetramethylcalix-[4]-resorcinarene **23** (0.250 g, 0.42 mmol) in dichloromethane *N*-bromosuccinimide (0.313 g, 1.76 mmol, 4.2 eq) and benzoyl peroxide (3.4 mg, 0.014 mmol, 1/30 eq) were added gradually during 1 hour (Scheme 10.18). The reaction mixture was refluxed overnight forming a white precipitate, which was filtrated over Celite and washed with hexane:EtOAc (80:20) solution. After the solvent evaporation product was purified with hexane:EtOAc (80:20) column chromatography with a small amount of dichloromethane to enhance solubility. Analyzed fractions contained either starting reagent or monosubstituted product. No desired product was obtained.

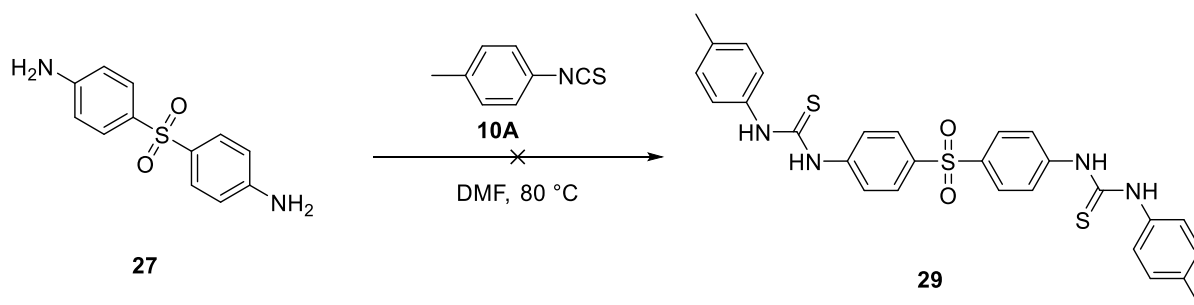
10.19 1,1'-(Sulfonylbis(4,1-phenylene))bis(3-(4-nitrophenyl)thiourea)

Scheme 10.19. Synthesis procedure for compound **28**

To the stirring solution of bis(4-aminophenyl)sulfone **27** (0.502 g, 2.01 mmol) in acetonitrile 4-nitrophenyl isothiocyanate **9A** (0.798 g, 4.43 mmol, 2.2 eq) was added (Scheme 10.19). The reaction mixture was left stirring overnight at room temperature. The formed pale-yellow precipitate was centrifuged (2 x 3500 rpm, 10 min) and washed with acetonitrile. After drying, 0.270 g of a pale-yellow powder was obtained 31.4 %.

^1H NMR (500 MHz, CD_3COCD_3) δ 9.83 (s, 2H, NH), 9.76 (s, 2H, NH), 8.23 (d, 4H, Ar-H, 9.1 Hz), 7.98 (d, 4H, Ar-H, 8.8 Hz), 7.92 (d, 4H, Ar-H, 9.1 Hz), 7.86 (d, 4H, Ar-H, 8.8 Hz)

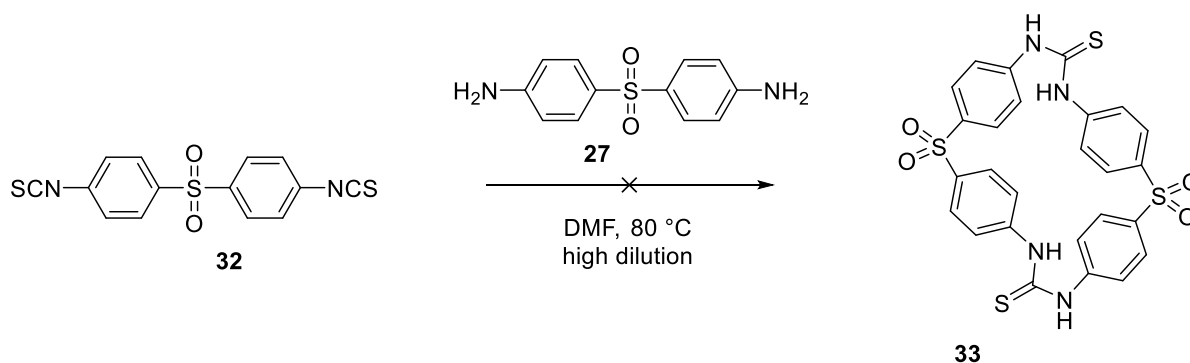
^{13}C NMR (125 MHz, CD_3COCD_3) δ 180.8, 146.5, 144.7, 138.7, 129.4, 125.2, 124.4, 123.6, 114.4

10.20 1,1'-(Sulfonylbis(4,1-phenylene))bis(3-(*p*-tolyl)thiourea)Scheme 10.20. Synthesis procedure for compound **29**

To the stirring solution of bis(4-aminophenyl)sulfone **27** (0.462 g, 1.86 mmol) in dimethylformamide *p*-tolylisothiocyanate **10A** (0.74 g, 4.9 mmol, 2.6 eq) was added (Scheme 10.20). The reaction mixture was stirred overnight at 80 °C. After the evaporation most of the dimethylformamide, H_2O was added to the reaction mixture. The formed oily precipitate was filtrated and washed with H_2O and EtOAc. The recrystallization from EtOH

gave small amount of a white powder. According to NMR analysis neither powder nor oil contained the desired product.

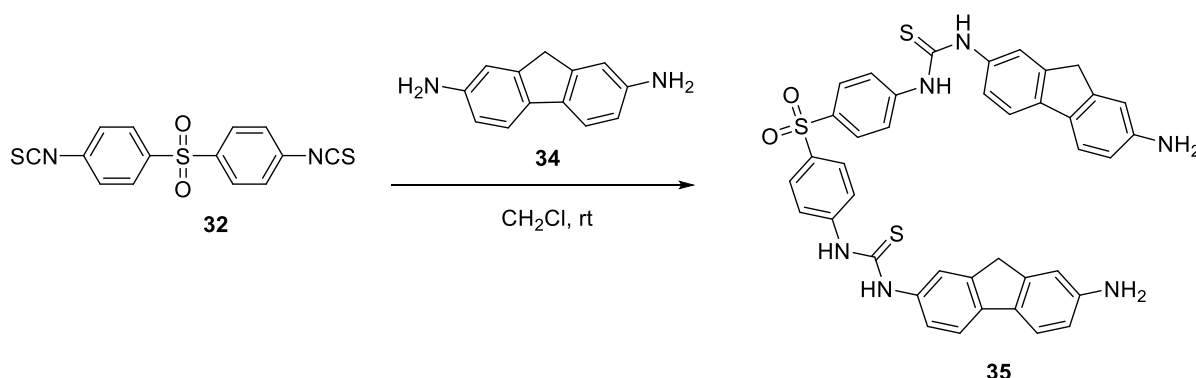
10.21 2,8-Dithia-4,6,10,12-tetraaza-1,3,7,9(1,4)- tetrabenzenacyclododecaphane-5,11-dithione 2,2,8,8-tetraoxide



Scheme 10.21. Synthesis procedure for compound **33**

To the reaction flask 15 ml of dimethylformamide was added. Isothiocyanatophenyl sulfone **32** (0.150 g, 0.06 mmol, 1 eq.) and bis(4-aminophenyl)sulfone **27** (0.201 g, 0.06 mmol, 1 eq.) were dissolved in 23 ml of DMF (Scheme 10.21). The reaction mixture was heated to 80 °C and the addition of reagents was performed gradually within 24 hours. After 1.5 days of stirring no reaction was observed. The desired product was not obtained.

10.22 1,1'-(Sulfonylbis(4,1-phenylene))bis(3-(7-amino-9H-fluoren-2-yl)thiourea)



Scheme 10.22. Synthesis procedure for compound **35**

2,7-Fluorenediamine **34** (0.177 g, 0.90 mmol, 2 eq.) was diluted in 25 ml of dichloromethane to the reaction flask. Isothiocyanatophenyl sulfone **32** (0.150 g, 0.45 mmol) was diluted in 20 ml of dichloromethane and added gradually to the reaction mixture within 20 hours

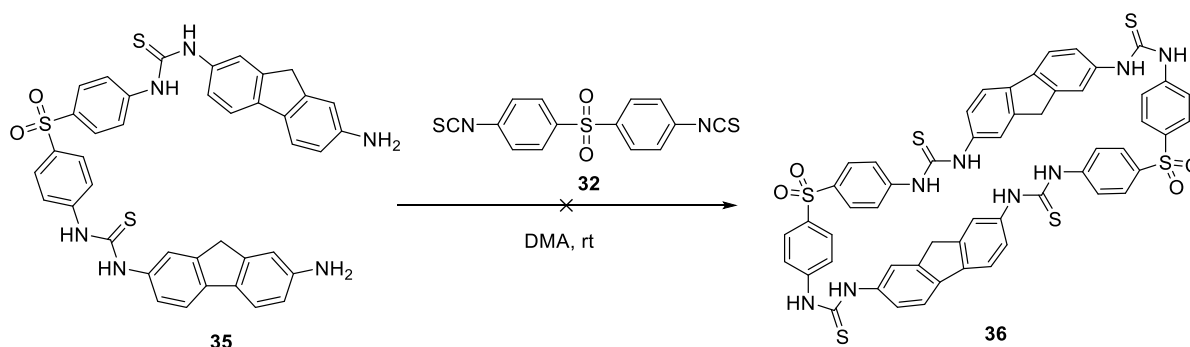
(Scheme 10.22). After stirring the mixture overnight, the formed dark brown precipitate was filtrated and washed with dichloromethane. Drying the precipitate gave 0.142 g of dark brown powder 43.6%. According to NMR spectra product contained traces of **34**.

^1H NMR (500 MHz, **DMSO-d6**) δ 10.09 (s, 2H, NH), 10.06 (s, 2H, NH), 7.42-6.75 (20H, Ar-H), 5.19 (4H, NH₂), 3.73 (s, 4H, CH₂ of fluorene)

^{13}C NMR (125 MHz, **DMSO-d6**) δ 179.2, 148.2, 144.7, 143.5, 141.9, 139.5, 137.6, 135.4, 129.2, 127.8, 122.7, 122.5, 120.6, 120.3, 117.7, 112.8, 110.4, 36.2

$[\text{M}+\text{H}]^+$ 725.1833, $[\text{M}+\text{Na}]^+$ 747.1653

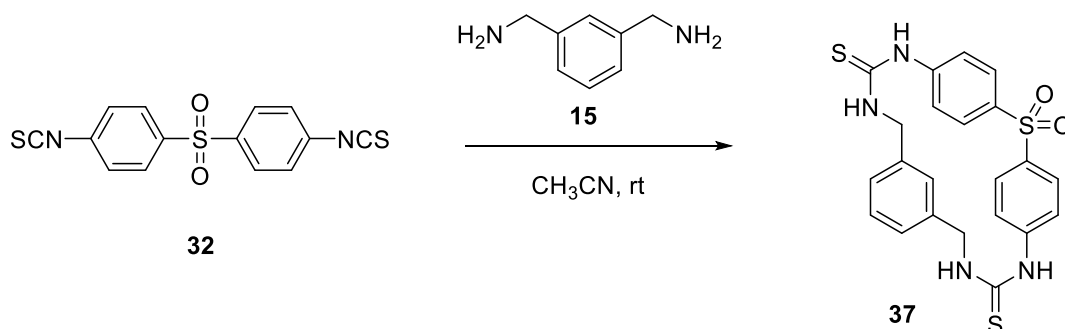
10.23 7H,17H-2,12-Dithia-4,6,8,10,14,16,18,20-octaaza-7,17(2,7)-difluorena-1,3,11,13(1,4)-tetrabenzenacycloicosaphane-5,9,15,19-tetrathione 2,2,12,12-tetraoxide



Scheme 10.23. Synthesis procedure for compound **36**

To the reaction flask, 15 ml of dimethylacetamide was added. Compound **35** (0.030 g, 0.042 mmol, 1 eq.) and isothiocyantophenyl sulfone **32** (0.014 g, 0.042 mmol, 1 eq.) were dissolved separately in 20 ml of DMA (Scheme 10.23). The equal addition of reagents was performed within 7 hours. Reaction mixture was stirred overnight at room temperature. The reaction solvent was evaporated until the formation of a dark precipitate, which was filtrated and washed with cold DMA. Formed product was poorly soluble in organic solvents, which prevented characterization of the compound **36**.

10.24 2-Thia-4,6,10,12-tetraaza-1,3(1,4),8(1,3)-tribenzenacyclododecaphane-5,11-dithione 2,2-dioxide



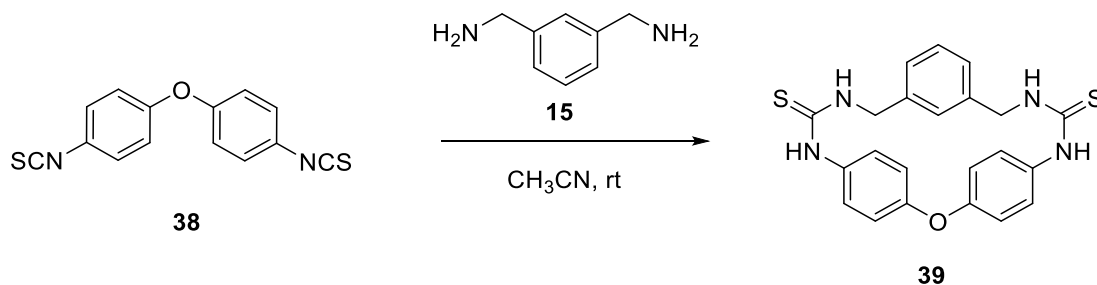
Scheme 10.24. Synthesis procedure for compound **37**

To the reaction flask, 10 ml of acetonitrile was added. Isothiocyanatophenyl sulfone **32** (0.150 g, 0.45 mmol, 1eq.) and 3-(aminomethyl)-benzylamine **15** (0.061 g, 0.45 mmol, 0.06 ml, 1eq.) were separately dissolved in 60 ml of ACN (Scheme 10.24). The equal addition of reagents was performed within 3 hours. The reaction mixture was stirred overnight at room temperature. The formed pink precipitate was filtrated, washed with ACN and dried, giving 0.127 g of pale red powder 60.2%.

^1H NMR (500 MHz, **DMSO-d₆**) δ 10.0 (s, 2H, NH), 8.60 (s, 2H, NH), 7.22-7.82 (12H, Ar-H), 4.72 (s, 4H, CH₂)

^{13}C NMR (125 MHz, **DMSO-d₆**) δ 180.4, 144.2, 143.0, 138.5, 135.2, 128.0, 126.3, 125.8, 121.6, 47.2

10.25 2-Oxa-4,6,10,12-tetraaza-1,3(1,4),8(1,3)-tribenzenacyclododecaphane-5,11-dithione



Scheme 10.25. Synthesis procedure for compound **39**

4-Isothiocyanatophenyl ether **38** (0.150g, 0.53 mmol, 1eq.) and 3-(aminomethyl)-benzylamine **15** (0.072 g, 0.53 mmol, 0.07 ml, 1eq.) were separately dissolved in 30 ml ACN ([Scheme 10.25](#)). The equal addition of reagents was performed within 1 hour. The reaction mixture was stirred overnight at the room temperature forming pale white precipitate in the solution. After filtration and wash with ACN 0.161 g of crema white powder was obtained 72.2%.

^1H NMR (500 MHz, **DMSO-d6**) δ 9.56 (s, 2H, NH), 8.08 (s, 2H, NH), 6.87-7.40 (12H, Ar-H), 4.73 (s, CH₂)

^{13}C NMR (125 MHz, **DMSO-d6**) δ 181.0, 153.6, 144.0, 139.5, 139.1, 134.4, 128.2, 125.8, 118.6, 47.2

11 References

1. Goodman, M. S.; Jubian, V.; Linton, B. and Andrew D., H., A Combinatorial Library Approach to Artificial Receptor Design, *J. Am. Chem. Soc.*, **1995**, *117*, 11610–11611.
2. Lehn, J.-M., Towards Complex Matter: Supramolecular Chemistry and Self-organization, *Eur. Rev.*, **2009**, *17*, 263–280.
3. Clayden, J.; Nick, G.; Warren, S. and Wothers, P., *Organic Chemistry*, Oxford University Press, 1st edition., 2001.
4. Steed, J. and Atwood, J., *Supramolecular Chemistry*, Wiley, 2nd edition., 2009.
5. Albrecht, M., Supramolecular chemistry - General principles and selected examples from anion recognition and metallocsupramolecular chemistry, *Naturwissenschaften*, **2007**, *94*, 951–966.
6. Steed, J.; Turner, D. and Wallace, K., *Core Concepts in Supramolecular Chemistry and Nanochemistry*, Wiley, 2nd edition., 2007.
7. Weber, E. and Vögtle, F., Classification and nomenclature of coronands, cryptands, podands, and of their complexes, *Inorganica Chim. Acta*, **1980**, *45*, L65–L67.
8. Lindoy, L.; Park, K.-M. and Sung Lee, S., Cryptands and Spherands, *Supramol. Chem.*, **2012**.
9. Marsault, E. and Peterson, M. L., Macrocycles Are Great Cycles: Applications, Opportunities, and Challenges of Synthetic Macrocycles in Drug Discovery, *J. Med. Chem.*, **2011**, *54*, 1961–2004.
10. Frank, A. T.; Farina, N. S.; Sawwan, N.; Wauchope, O. R.; Qi, M.; Brzostowska, E. M.; Chan, W.; Grasso, F. W.; Haberfield, P. and Greer, A., Natural macrocyclic molecules have a possible limited structural diversity, *Mol. Divers.*, **2007**, *11*, 115–118.
11. Frausto da Silva, J. J. R., The chelate effect redefined, *J. Chem. Educ.*, **2009**, *60*, 390.
12. Cram, D. J.; Karbach, S.; Kim, H. E.; Knobler, C. B.; Maverick, E. F.; Ericson, J. L. and Helgeson, R. C., Host-Guest Complexation. 46. Cavitands as Open Molecular Vessels Form Solvates, *J. Am. Chem. Soc.*, **1988**, *110*, 2229–2237.
13. Merrifield, R. B., The Design of Molecular Hosts, Guests, and Their Complexes, *Angew.*

Chemie Int. Ed. English, **1985**, *24*, 799–810.

14. Martí-Centelles, V.; Pandey, M. D.; Burguete, M. I. and Luis, S. V., Macrocyclization Reactions: The Importance of Conformational, Configurational, and Template-Induced Preorganization, *Chem. Rev.*, **2015**, *115*, 8736–8834.
15. Li, Y.; Wang, Y.; Huang, G. and Gao, J., Cooperativity Principles in Self-Assembled Nanomedicine., *Chem. Rev.*, **2018**, *118*, 5359–5391.
16. Khaliullin, R. Z.; Cobar, E. A.; Lochan, R. C.; Bell, A. T. and Head-Gordon, M., Unravelling the origin of intermolecular interactions using absolutely localized molecular orbitals, *J. Phys. Chem. A*, **2007**, *111*, 8753–8765.
17. Herschlag, D. and Pinney, M. M., Hydrogen Bonds: Simple after All?, *Biochemistry*, **2018**, *57*, 3338–3352.
18. Cavallo, G.; Metrangolo, P.; Milani, R.; Pilati, T.; Priimagi, A.; Resnati, G. and Terraneo, G., The halogen bond, *Chem. Rev.*, **2016**, *116*, 2478–2601.
19. Arunan, E.; Desiraju, G. R.; Klein, R. A.; Sadlej, J.; Scheiner, S.; Alkorta, I.; Clary, D. C.; Crabtree, R. H.; Dannenberg, J. J.; Hobza, P.; Kjaergaard, H. G.; Legon, A. C.; Mennucci, B. and Nesbitt, D. J., Definition of the hydrogen bond (IUPAC Recommendations 2011), *Pure Appl. Chem.*, **2011**, *83*, 1637–1641.
20. Barth, A. and Zscherp, C., What vibrations tell about proteins, *Q. Rev. Biophys.*, **2002**, *35*, 369–430.
21. Metrangolo, P.; Meyer, F.; Pilati, T.; Resnati, G. and Terraneo, G., Halogen bonding in supramolecular chemistry, *Angew. Chemie - Int. Ed.*, **2008**, *47*, 6114–6127.
22. Clark, T.; Hennemann, M.; Murray, J. S. and Politzer, P., Halogen bonding: The σ -hole: Proceedings of 'Modeling interactions in biomolecules II', Prague, September 5th-9th, 2005, *J. Mol. Model.*, **2007**, *13*, 291–296.
23. Wang, H.; Wang, W. and Jin, W. J., σ -Hole Bond vs π -Hole Bond: A Comparison Based on Halogen Bond, *Chem. Rev.*, **2016**, *116*, 5072–5104.
24. Riley, K. E.; Murray, J. S.; Fanfrlík, J.; Řezáč, J.; Solá, R. J.; Concha, M. C.; Ramos, F. M. and Politzer, P., Halogen bond tunability I: The effects of aromatic fluorine substitution on the strengths of halogen-bonding interactions involving chlorine, bromine, and

- iodine, *J. Mol. Model.*, **2011**, *17*, 3309–3318.
25. Politzer, P.; Murray, J. S. and Clark, T., Halogen bonding: An electrostatically-driven highly directional noncovalent interaction, *Phys. Chem. Chem. Phys.*, **2010**, *12*, 7748–7757.
 26. Priimagi, A.; Cavallo, G.; Metrangolo, P. and Resnati, G., The Halogen Bond in the Design of Functional Supramolecular Materials: Recent Advances, *Acc. Chem. Res.*, **2013**, *46*, 2686–2695.
 27. Lu, Y.; Li, H.; Zhu, X.; Zhu, W. and Liu, H., How does halogen bonding behave in solution? A theoretical study using implicit solvation model, *J. Phys. Chem. A*, **2011**, *115*, 4467–4475.
 28. Parker, A. J.; Stewart, J.; Donald, K. J. and Parish, C. A., Halogen bonding in DNA base pairs, *J. Am. Chem. Soc.*, **2012**, *134*, 5165–5172.
 29. Custelcean, R., Crystal engineering with urea and thiourea hydrogen-bonding groups, *Chem. Commun.*, **2008**, 295–307.
 30. Desiraju, G. R., Supramolecular Synthons in Crystal Engineering—A New Organic Synthesis, *Angew. Chemie Int. Ed. English*, **1995**, *34*, 2311–2327.
 31. Braga, D.; Brammer, L. and Champness, N. R., New trends in crystal engineering, *CrystEngComm*, **2005**, *7*, 1–19.
 32. Abboud, J. L. M.; Ballesteros, E.; Herreros, M.; Homan, H.; Lopez-Mardomingo, C.; Notario, R.; Mó, O.; de Paz, J. L. G.; Yáñez, M.; Esseffar, M.; Bouab, W.; El-Mouhtadi, M. and Mokhlisse, R., Thiocarbonyl versus Carbonyl Compounds: A Comparison of Intrinsic Reactivities, *J. Am. Chem. Soc.*, **1993**, *115*, 12468–12476.
 33. Wiberg, K. B. and Rablen, P. R., Why Does Thioformamide Have a Larger Rotational Barrier Than Formamide?, *J. Am. Chem. Soc.*, **1995**, *117*, 2201–2209.
 34. Choudhary, A. and Raines, R. T., An Evaluation of Peptide-Bond Isosteres, *ChemBioChem*, **2011**, *12*, 1801–1807.
 35. Artis, D. R. and Lipton, M. A., Conformations of thioamide-containing dipeptides: A computational study, *J. Am. Chem. Soc.*, **1998**, *120*, 12200–12206.
 36. Kim, W.; Lee, H. J.; Choi, Y. S.; Choi, J. H. and Yoon, C. J., The nature of rotational barriers

- of the C-N bond in thioamides and the origin of the nonplanarity for thiourea, *J. Chem. Soc. - Faraday Trans.*, **1998**, *94*, 2663–2668.
37. Bordwell, F. G.; Algrim, D. J. and Harrelson, J. A., The relative ease of removing a proton, a hydrogen atom, or an electron from carboxamides versus thiocarboxamides, *J. Am. Chem. Soc.*, **1988**, *110*, 5903–5904.
 38. Ozturk, T.; Ertas, E. and Mert, O., Use of Lawesson's reagent in organic syntheses, *Chem. Rev.*, **2007**, *107*, 5210–5278.
 39. Cao, X. T.; Qiao, L.; Zheng, H.; Yang, H. Y. and Zhang, P. F., A efficient protocol for the synthesis of thioamides in [DBUH][OAc] at room temperature, *RSC Adv.*, **2018**, *8*, 170–175.
 40. Zbruyev, O. I.; Stiasni, N. and Kappe, C. O., Preparation of thioamide building blocks via microwave-promoted three-component kindler reactions, *J. Comb. Chem.*, **2003**, *5*, 145–148.
 41. Verma, H.; Khatri, B.; Chakraborti, S. and Chatterjee, J., Increasing the bioactive space of peptide macrocycles by thioamide substitution, *Chem. Sci.*, **2018**, *9*, 2443–2451.
 42. Inoue, Y.; Kanbara, T. and Yamamoto, T., Preparation of a new receptor for anions, macrocyclic polythiolactam - Structure and high anion-binding ability, *Tetrahedron Lett.*, **2003**, *44*, 5167–5169.
 43. Hossain, M. A.; Kang, S. O.; Llinares, J. M.; Powell, D. and Bowman-James, K., Elite new anion ligands: Polythioamide macrocycles, *Inorg. Chem.*, **2003**, *42*, 5043–5045.
 44. No, K.; Lee, J. H.; Yang, S. H.; Yu, S. H.; Cho, M. H.; Kim, M. J. and Kim, J. S., Syntheses and conformations of tetrahomodioxacalix[4]arene tetraamides and tetrathioamides, *J. Org. Chem.*, **2002**, *67*, 3165–3168.
 45. Gómez, D. E.; Fabbrizzi, L.; Licchelli, M. and Monzani, E., Urea vs. thiourea in anion recognition, *Org. Biomol. Chem.*, **2005**, *3*, 1495–1500.
 46. Masunov, A. and Dannenberg, J. J., Theoretical Study of Urea and Thiourea. 2. Chains and Ribbons, *J. Phys. Chem. B*, **2002**, *104*, 806–810.
 47. Scheerder, J.; Engbersen, J. F. J.; Casnati, A.; Ungaro, R. and Reinhoudt, D. N., Complexation of Halide Anions and Tricarboxylate Anions by Neutral Urea-Derivatized

- P-tert-Butylcalix[6]arenes, *J. Org. Chem.*, **1995**, *60*, 6448–6454.
48. Arman, H. D.; Giesecking, R. L.; Hanks, T. W. and Pennington, W. T., Complementary halogen and hydrogen bonding: Sulfur···iodine interactions and thioamide ribbons, *Chem. Commun.*, **2010**, *46*, 1854–1856.
 49. Yudin, A. K., Macrocycles: Lessons from the distant past, recent developments, and future directions, *Chem. Sci.*, **2015**, *6*, 30–49.
 50. Sasaki, S. ichi; Mizuno, M.; Naemura, K. and Tobe, Y., Synthesis and anion-selective complexation of cyclophane-based cyclic thioureas, *J. Org. Chem.*, **2000**, *65*, 275–283.
 51. Matsumura, N.; Tomura, M.; Mori, O.; Yuko, T.; Yoneda, S. and Toriumi, K., Synthesis and Structure of 6,7-Dihydro-2,3-disubstituted 5H-2a-Thia(2a-S)-2,3,4a,7a-tetraazacyclopent[cd]indene-1,4(2H,3H)-dithione, *Chem. Soc. Japan*, **1988**, *61*, 2419–2424.
 52. Matsumura, N.; Konishi, T.; Hayashi, H.; Yasui, M.; Iwasaki, F. and Mizuno, K., Synthesis and Properties of Novel Macrocyclic Compounds Bearing Thiourea Moieties by Use of Chemical Feature of Hypervalent Sulfur., *ChemInform*, **2010**, *33*, 189–202.
 53. Boerrigter, H.; Grave, L.; Nissink, J. W. M.; Christoffels, L. A. J.; Van der Maas, J. H.; Verboom, W.; De Jong, F. and Reinhoudt, D. N., (Thio)urea Resorcinarene Cavitands. Complexation and Membrane Transport of Halide Anions, *J. Org. Chem.*, **1998**, *63*, 4174–4180.
 54. Boerrigter, H.; Verboom, W. and Reinhoudt, D. N., Novel Resorcinarene Cavitand-Based CMP(O) Cation Ligands: Synthesis and Extraction Properties, *J. Org. Chem.*, **1997**, *62*, 7148–7155.
 55. Hamon, M.; Menand, M.; Gac, S. Le; Luhmer, M.; Dalla, V. and Jabin, I., Calix [6] tris (thio) ureas : Heteroditopic Receptors for the Cooperative Binding of Organic Ion Pairs, *J. Org. Chem.*, **2008**, *73*, 7067–7071.
 56. Le Gac, S.; Zeng, X.; Girardot, C. and Jabin, I., Efficient synthesis and host-guest properties of a new class of calix[6]azacryptands, *J. Org. Chem.*, **2006**, *71*, 9233–9236.
 57. Casnati, A.; Fochi, M.; Minari, P.; Pochini, A.; Reggiani, M.; Ungaro, R. and Reinhoudt, D. N., Upper-rim urea-derivatized calix[4]arenes as neutral receptors for

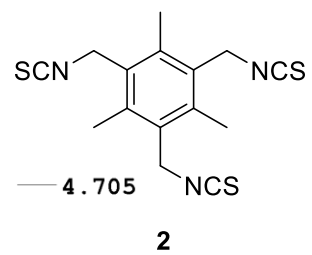
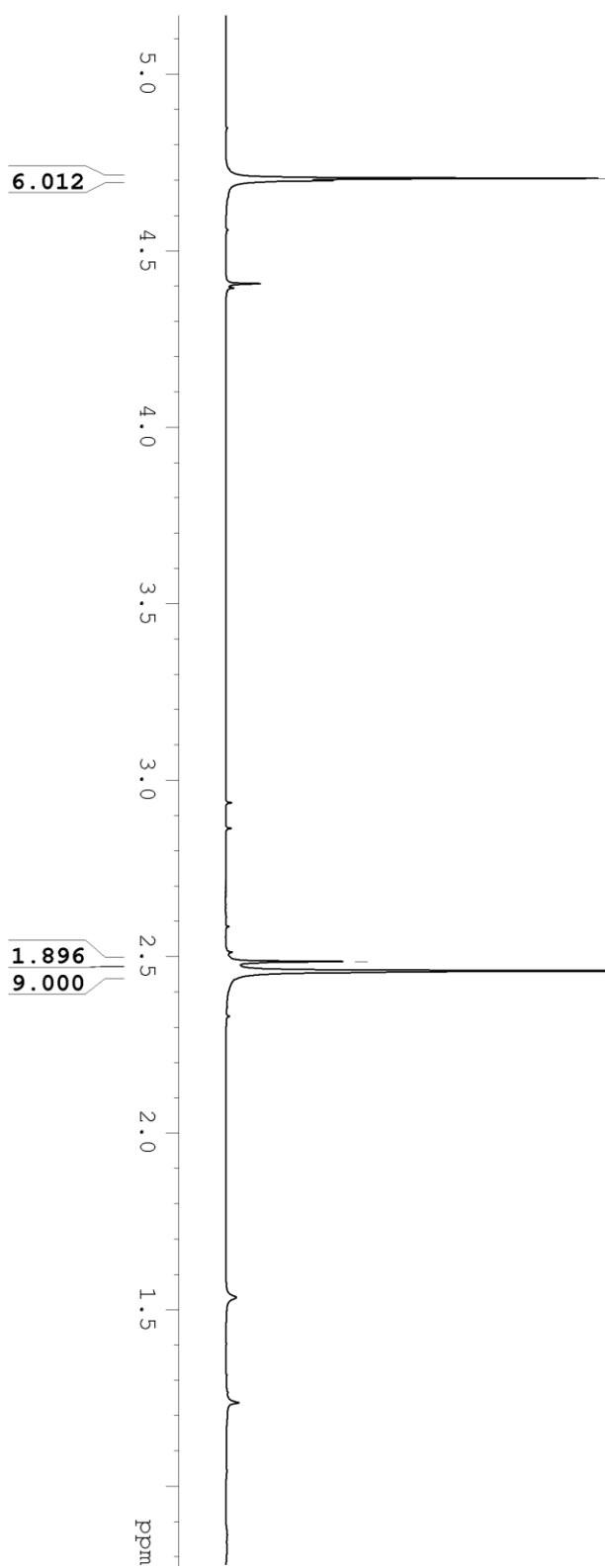
- monocarboxylate anions, *Gazz. Chim. Ital.*, **1996**, *126*, 99–106.
58. Pelizzi, N.; Casnati, A.; Friggeri, A. and Ungaro, R., Synthesis and properties of new calixarene-based ditopic receptors for the simultaneous complexation of cations and carboxylate anions, *J. Chem. Soc. Perkin Trans. 2*, **1998**, 1307–1312.
59. Fernandez, G.; Blanco, J.; Mellet, O. and Fuentes, J., Synthesis, Conformational Flexibility and Preliminary Complexation Behavior of α,α' -Trehalose-Based Macrocycles Containing Thiourea Spacers., *ChemInform*, **1995**, *26*, 57–58.
60. Amendola, V.; Esteban-Gómez, D.; Fabbrizzi, L.; Licchelli, M.; Monzani, E. and Sancenón, F., Metal-enhanced H-bond donor tendencies of urea and thiourea toward anions: Ditopic receptors for silver(I) salts, *Inorg. Chem.*, **2005**, *44*, 8690–8698.
61. Okumura, Y.; Murakami, S.; Maeda, H.; Matsumura, N. and Mizuno, K., Synthesis and dual binding character of novel macrocyclic thiourea derivatives, *Tetrahedron Lett.*, **2003**, *44*, 8183–8185.
62. Huang, G.; Valkonen, A.; Rissanen, K. and Jiang, W., Endo -Functionalized molecular tubes: Selective encapsulation of neutral molecules in non-polar media, *Chem. Commun.*, **2016**, *52*, 9078–9081.
63. Prusinowska, N.; Szymkowiak, J. and Kwit, M., Enantiopure Tertiary Urea and Thiourea Derivatives of Trianglamine Macrocyclic: Structural Studies and Metallogel Properties, *J. Org. Chem.*, **2018**, *83*, 1167–1175.
64. Sindt, A. J.; Smith, M. D.; Pellechia, P. J. and Shimizu, L. S., Thioureas and Squaramides: Comparison with Ureas as Assembly Directing Motifs for *m*-Xylene Macrocycles, *Cryst. Growth Des.*, **2018**, *18*, 1605–1612.
65. Akhtar, N.; Pradhan, N.; Saha, A.; Kumar, V.; Biswas, O.; Dey, S.; Shah, M.; Kumar, S. and Manna, D., Tuning the solubility of ionophores: glutathione-mediated transport of chloride ions across hydrophobic membranes, *Chem. Commun.*, **2019**, *55*, 8482–8485.
66. Zoller, T.; Uguen, D.; De Cian, A. and Fischer, J., Efficient preparation of *E*- β -iodovinyl phenylsulfone by Finkelstein reaction at a vinylic center, *Tetrahedron Lett.*, **1998**, *39*, 8089–8092.
67. Cant, A. A.; Bhalla, R.; Pimlott, S. L. and Sutherland, A., Nickel-catalysed aromatic

- Finkelstein reaction of aryl and heteroaryl bromides, *Chem. Commun.*, **2012**, *48*, 3993–3995.
68. Tobe, Y.; Sasaki, S. I.; Mizuno, M.; Hirose, K. and Naemura, K., Novel self-assembly of *m*-xylylene type dithioureas by head-to-tail hydrogen bonding, *J. Org. Chem.*, **1998**, *63*, 7481–7489.
69. Pingaew, R.; Sinthupoom, N.; Mandi, P.; Prachayasittikul, V.; Cherdtrakulkiat, R.; Prachayasittikul, S.; Ruchirawat, S. and Prachayasittikul, V., Synthesis, biological evaluation and in silico study of bis-thiourea derivatives as anticancer, antimalarial and antimicrobial agents, *Med. Chem. Res.*, **2017**, *26*, 3136–3148.
70. Pingaew, R.; Tongraung, P.; Worachartcheewan, A.; Nantasenamat, C.; Prachayasittikul, S.; Ruchirawat, S. and Prachayasittikul, V., Cytotoxicity and QSAR study of (thio)ureas derived from phenylalkylamines and pyridylalkylamines, *Med. Chem. Res.*, **2013**, *22*, 4016–4029.
71. Nimse, S. B. and Kim, T., Biological applications of functionalized calixarenes, *Chem. Soc. Rev.*, **2013**, *42*, 366–386.
72. Moussaoui, S. A.; Damaj, Z.; Wehbie, M.; Rostaing, S. P. and Karamé, I., Alternative and Eco-Friendly Synthesis of Tetrakis(Aminomethyl)Calix-[4]-Resorcinarene, *Int. J. Org. Chem.*, **2017**, *07*, 403–411.
73. Hu, Y. J.; Yang, J.; Liu, Y. Y.; Song, S. and Ma, J. F., A Family of Capsule-Based Coordination Polymers Constructed from a New Tetrakis(1,2,4-triazolylmethyl)resorcin[4]arene Cavitand and Varied Dicarboxylates for Selective Metal-Ion Exchange and Luminescent Properties, *Cryst. Growth Des.*, **2015**, *15*, 3822–3831.
74. Djerassi, C., Brominations with *N*-Bromosuccinimide and Related Compounds. The Wohl–Ziegler Reaction, *Chem. Rev.*, **1948**, *43*, 271–317.
75. Ghorab, M. M.; Radwan, M. A. A.; Taha, N. M. H.; Amin, N. E.; Shehab, M. A. and Faker, I. M. I., Dapsone in heterocyclic chemistry, part II: Antimicrobial and antitumor activities of some novel sulfone biscompounds containing biologically active thioureido, carbamothioate, quinazoline, imidazolidine, and thiazole moieties, *Phosphorus, Sulfur Silicon Relat. Elem.*, **2008**, *183*, 2906–2917.
76. Yang, L.; Zhao, L.; Zhou, Z.; He, C.; Sun, H. and Duan, C., A thiourea-functionalized metal-

- organic macrocycle for the catalysis of Michael additions and prominent size-selective effect, *Dalt. Trans.*, **2017**, *46*, 4086–4092.
77. Carlsson, A. C. C.; Uhrbom, M.; Karim, A.; Brath, U.; Gräfenstein, J. and Erdélyi, M., Solvent effects on halogen bond symmetry, *CrystEngComm*, **2013**, *15*, 3087–3092.
78. Le Questel, J. Y.; Laurence, C. and Graton, J., Halogen-bond interactions: A crystallographic basicity scale towards iodoorganic compounds, *CrystEngComm*, **2013**, *15*, 3212–3221.
79. Corban, G. J.; Hadjikakou, S. K.; Hadjiliadis, N.; Kubicki, M.; Tiekink, E. R. T.; Butler, I. S.; Drougas, E. and Kosmas, A. M., Synthesis, structural characterization, and computational studies of novel diiodine adducts with the heterocyclic thioamides N-methylbenzothiazole-2-thione and benzimidazole-2-thione: Implications with the mechanism of action of antithyroid drugs, *Inorg. Chem.*, **2005**, *44*, 8617–8627.
80. Lin, G. H.-Y. and Hope, H., The crystal structure of bis(thiourea)iodine(I) iodide, *Acta Crystallogr. Sect. B*, **1972**, *28*, 643–646.
81. Tamilselvi, A. and Muges, G., Interaction of heterocyclic thiols/thiones eliminated from cephalosporins with iodine and its biological implications, *Bioorganic Med. Chem. Lett.*, **2010**, *20*, 3692–3697.
82. Biesiada, M.; Kourkoumelis, N.; Kubicki, M.; Owczarzak, A. M.; Balas, V. and Hadjikakou, S. K., Fundamental chemistry of iodine. the reaction of di-iodine towards thiourea and its methyl-derivative: Formation of aminothiazoles and aminothiadiazoles through dicationic disulfides, *Dalt. Trans.*, **2014**, *43*, 4790–4796.

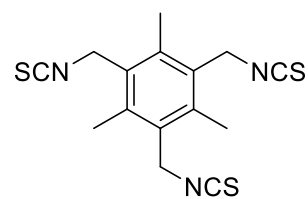
Appendix – NMR and MS spectra

APPENDIX 1
¹H-NMR 500 MHz CDCl₃



APPENDIX 2

^{13}C -NMR 125 MHz CDCl_3

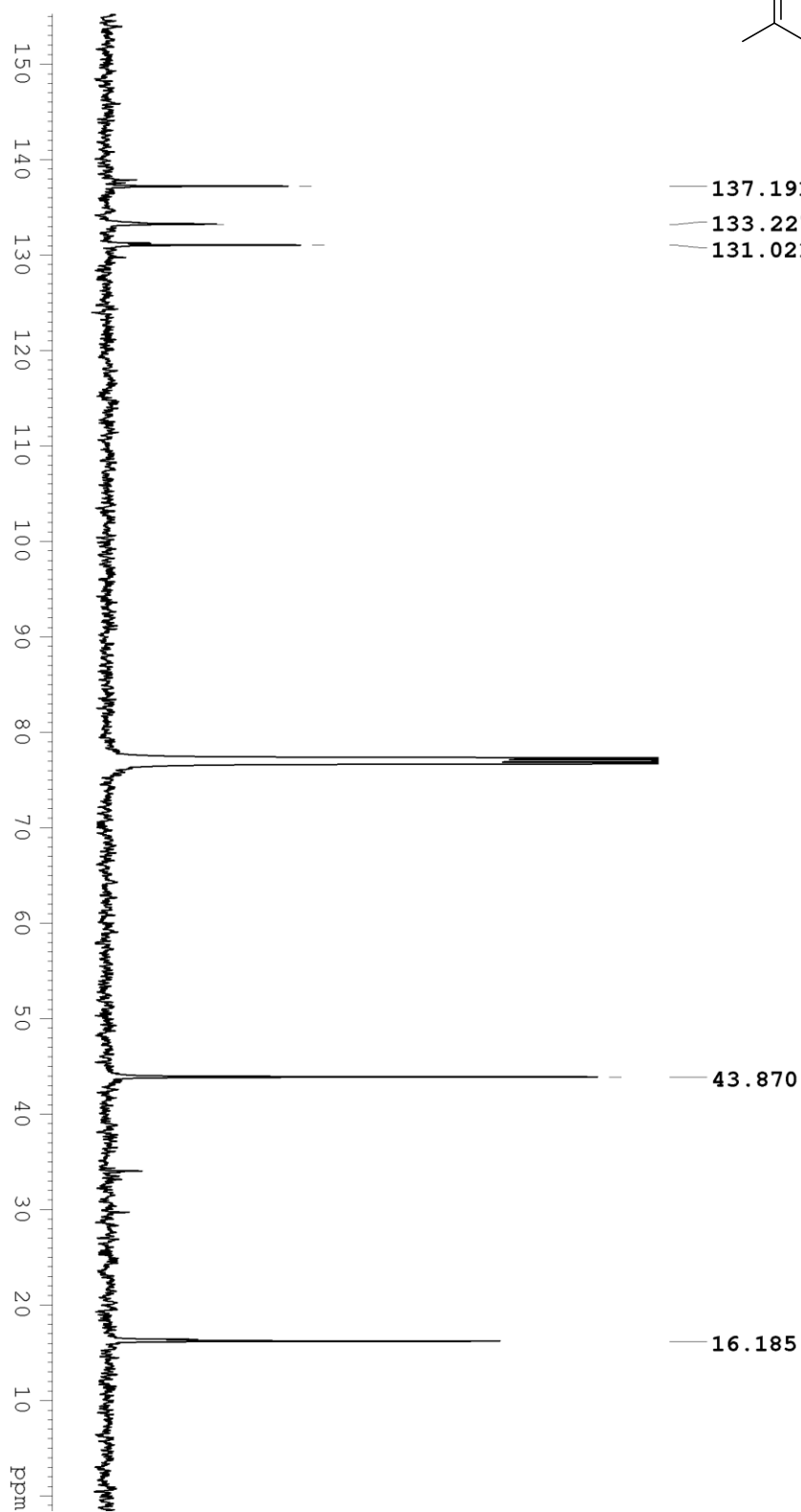


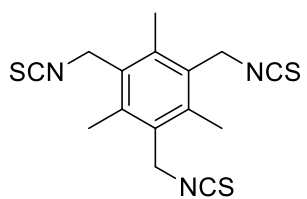
2

— 137.191

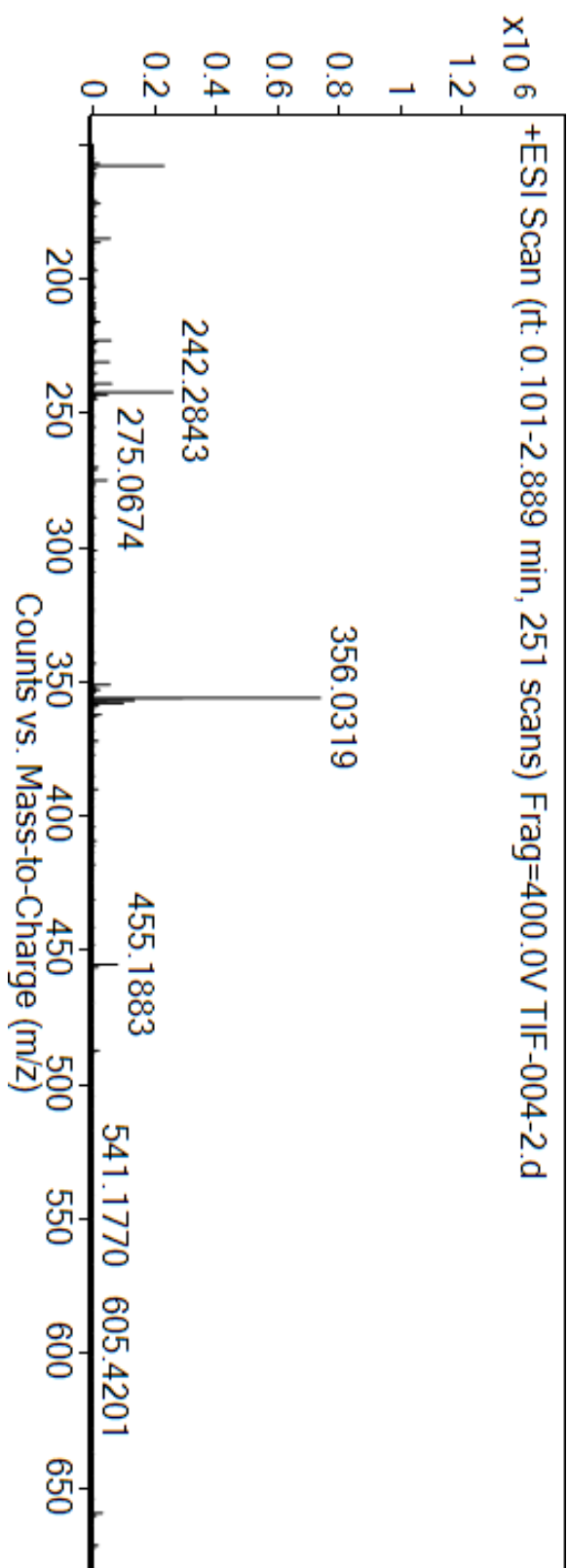
— 133.227

— 131.021



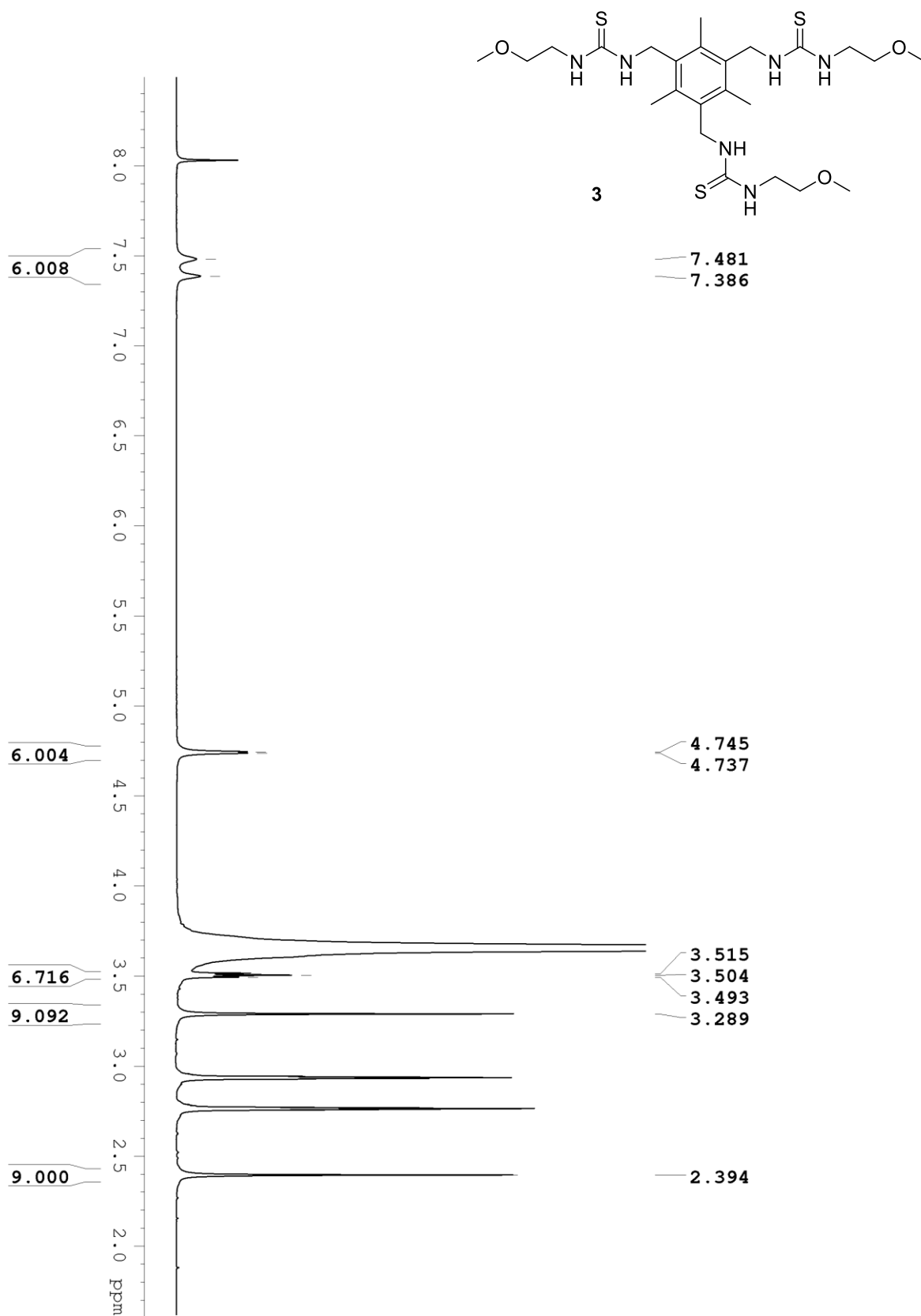


2



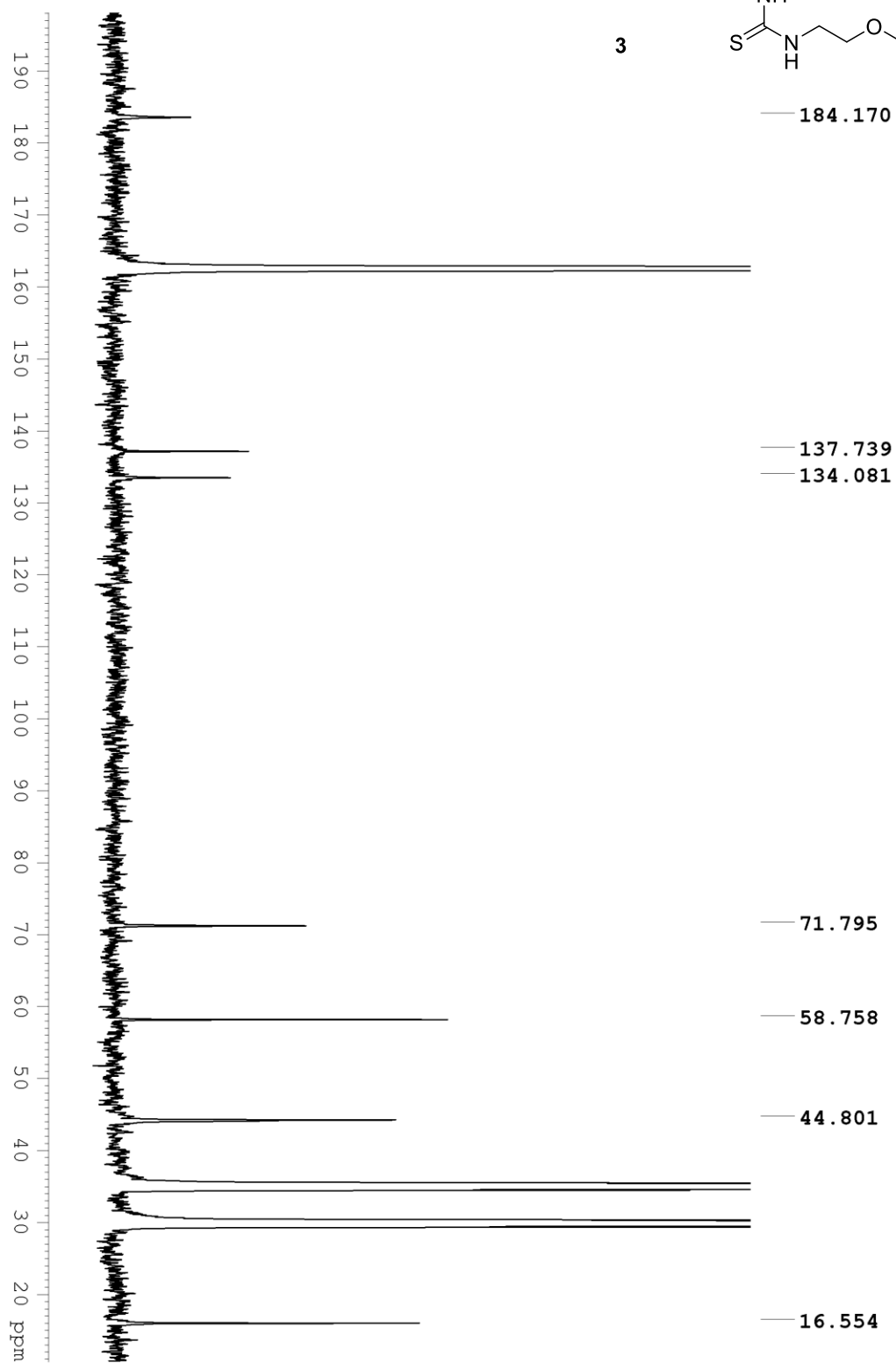
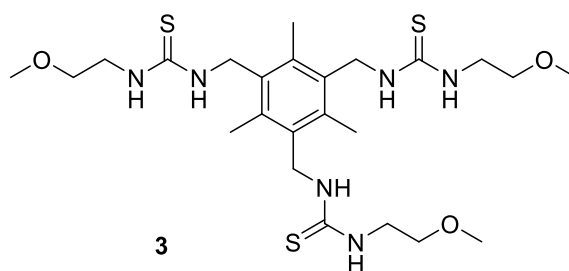
APPENDIX 4

¹H-NMR 500 MHz DMF-d7

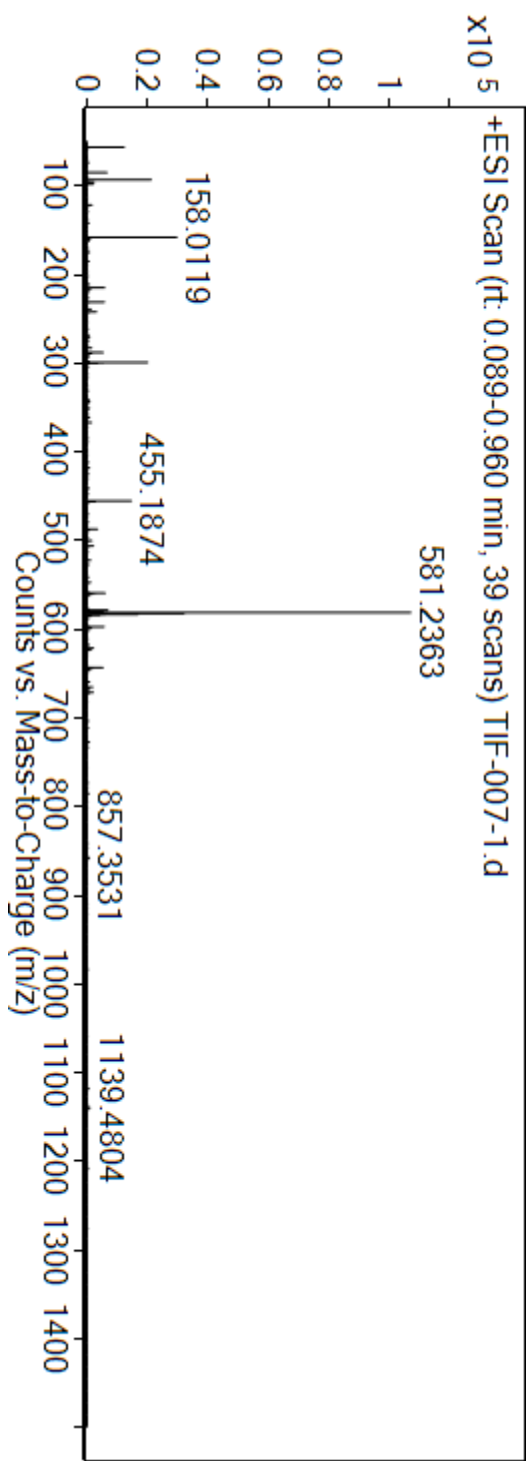
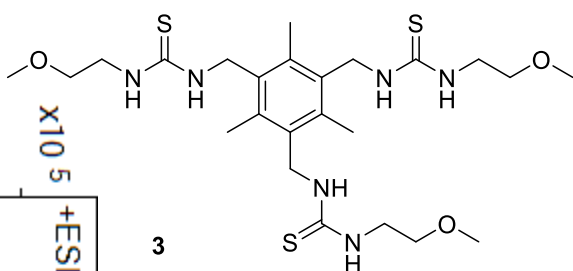


APPENDIX 5

^{13}C -NMR 125 MHz DMF-d7

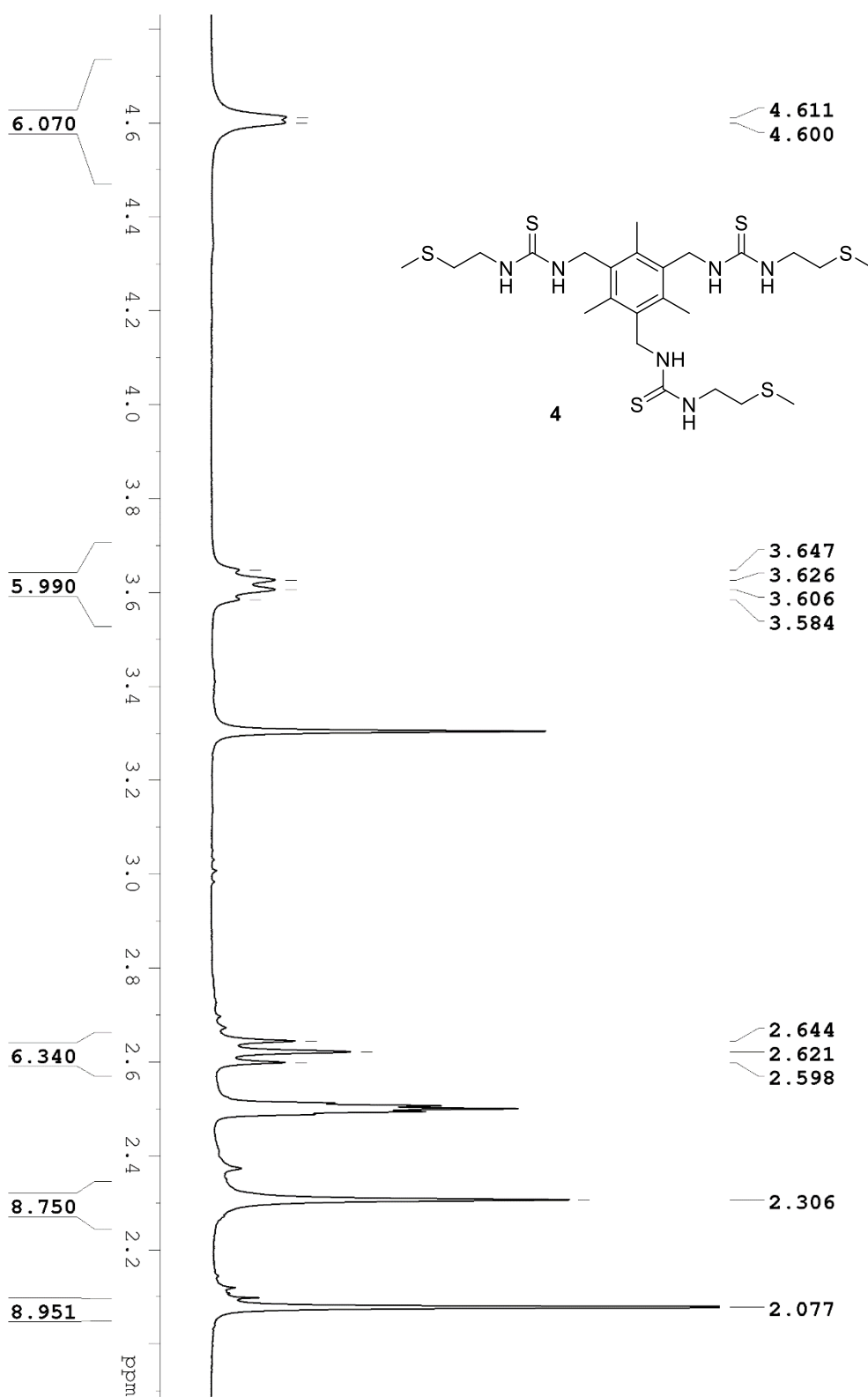


APPENDIX 6
MS



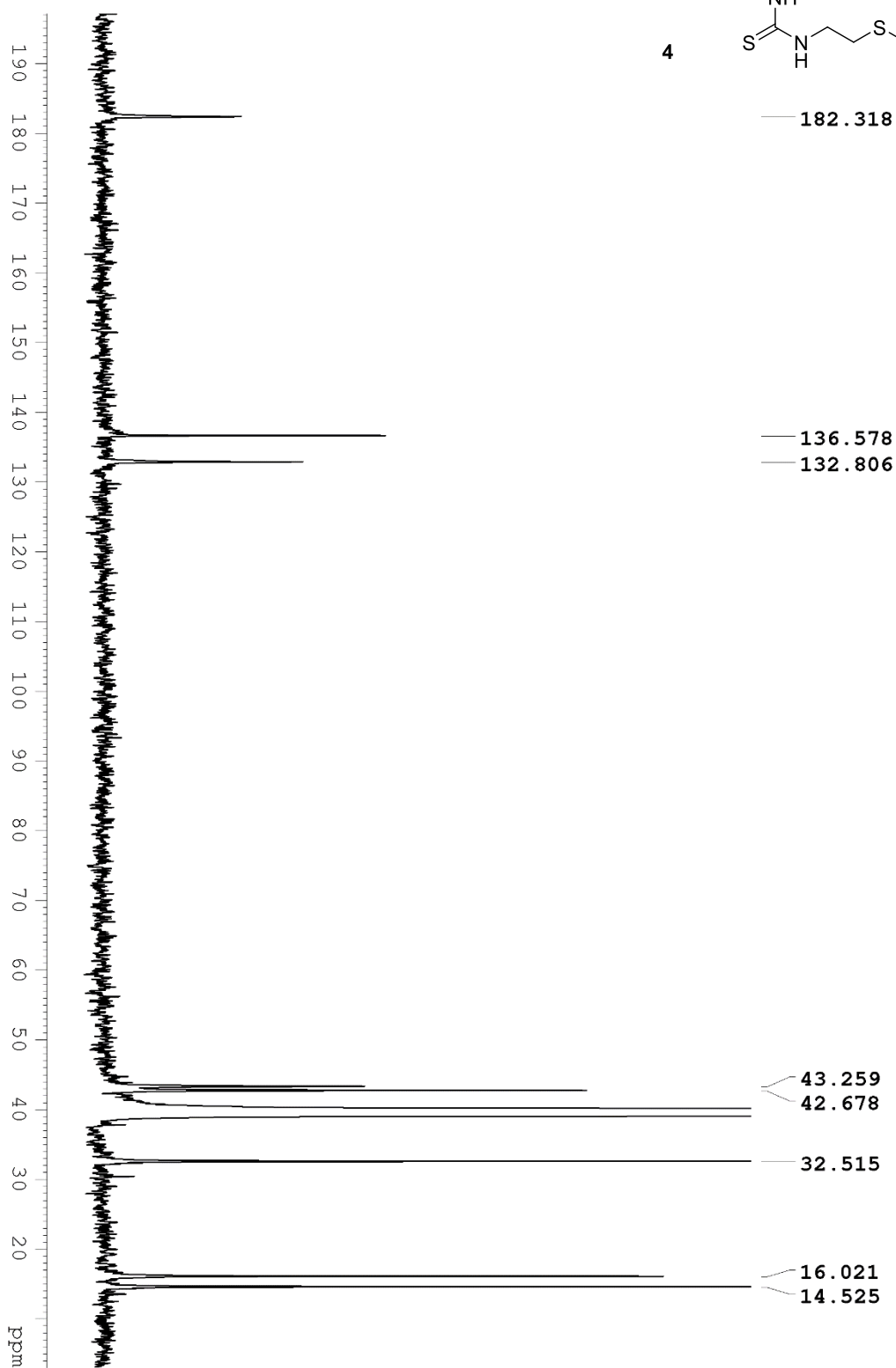
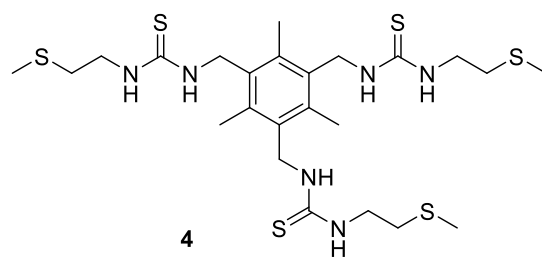
APPENDIX 7

¹H-NMR 500 MHz DMSO-d6

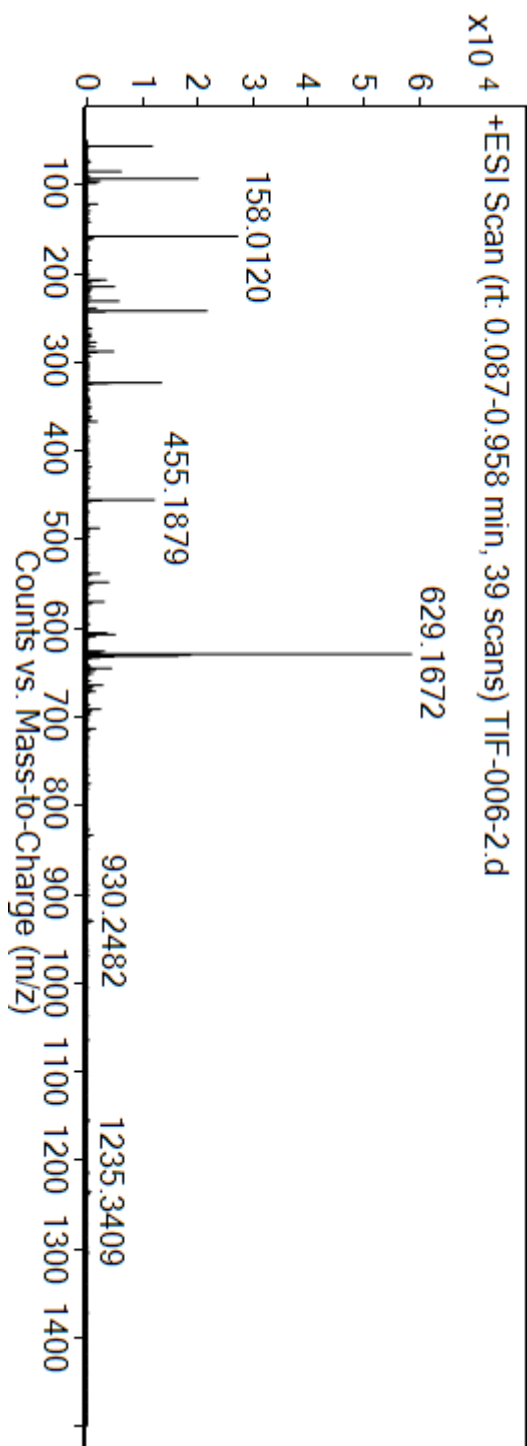
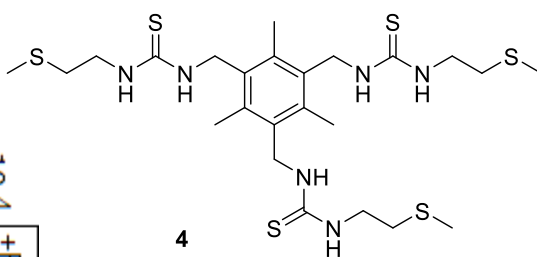


APPENDIX 8

$^{13}\text{C-NMR}$ 125 MHz DMSO-d₆

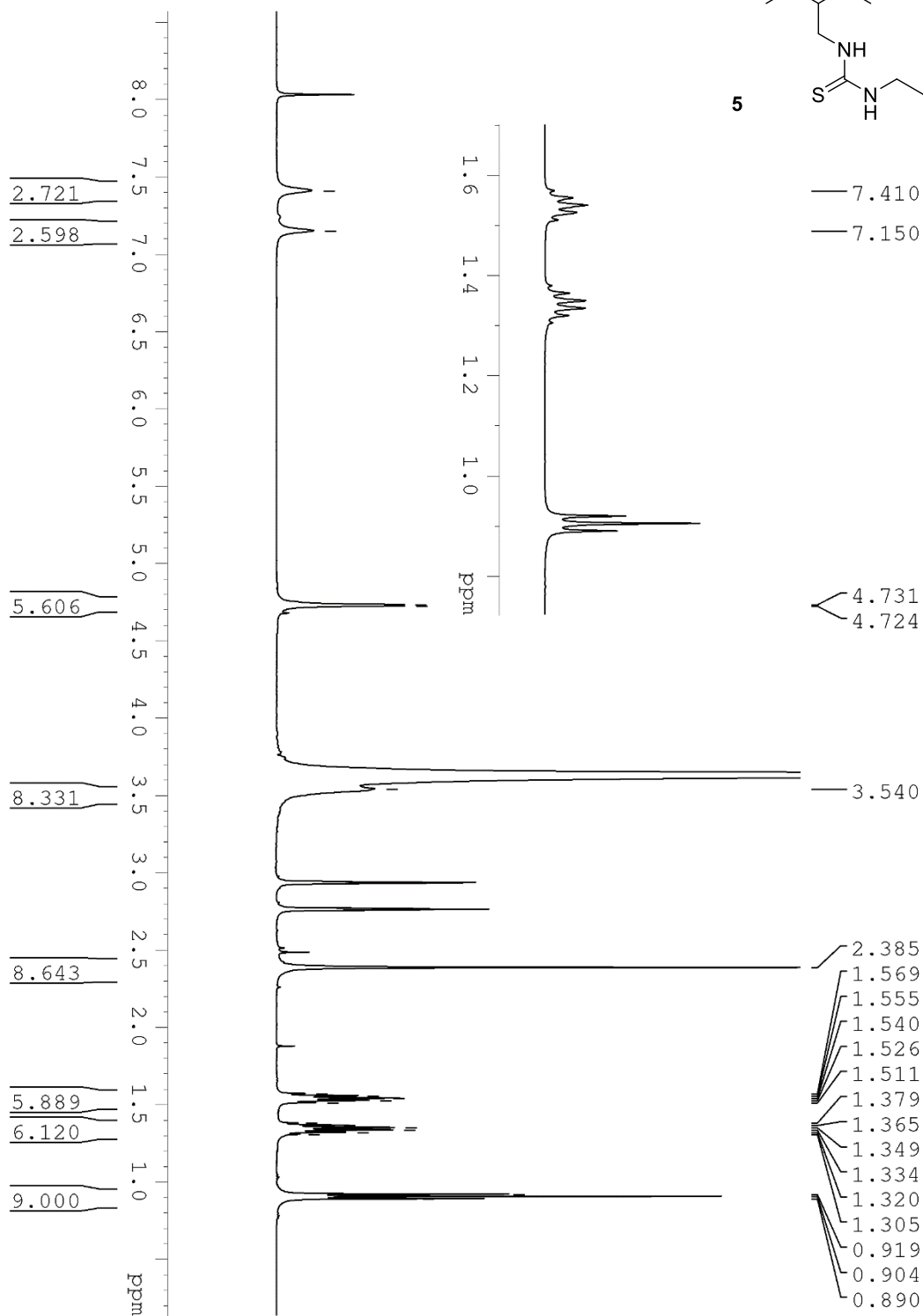
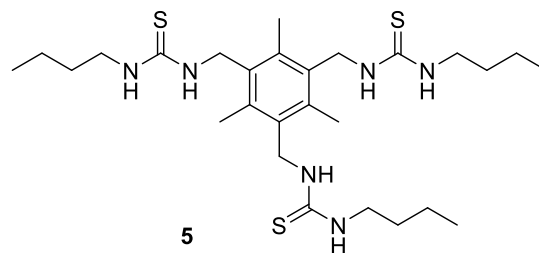


APPENDIX 9
MS



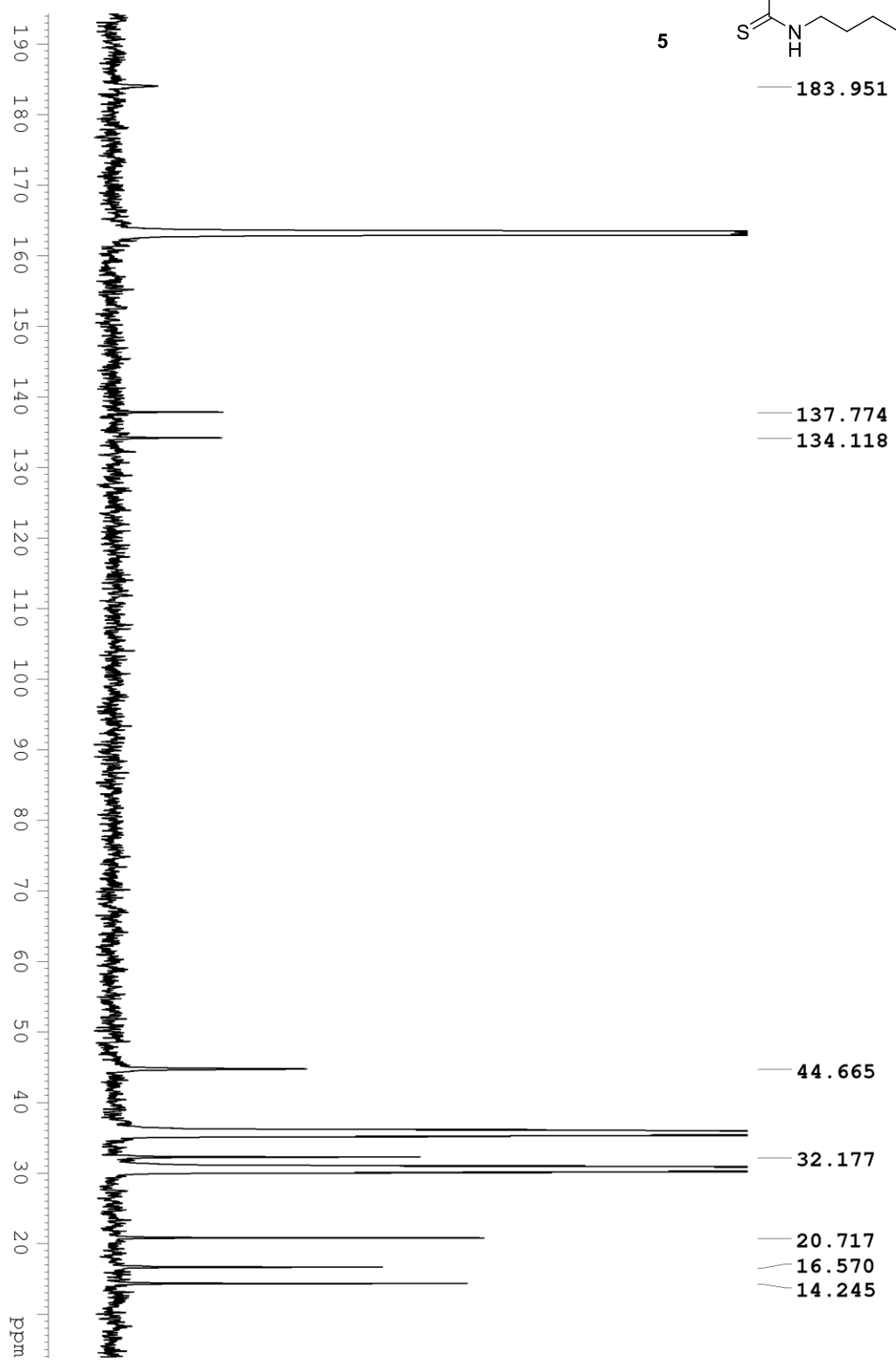
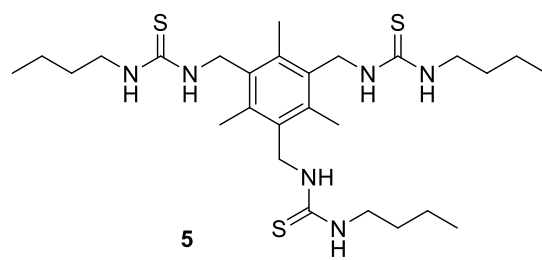
APPENDIX 10

¹H-NMR 500 MHz DMF-d7

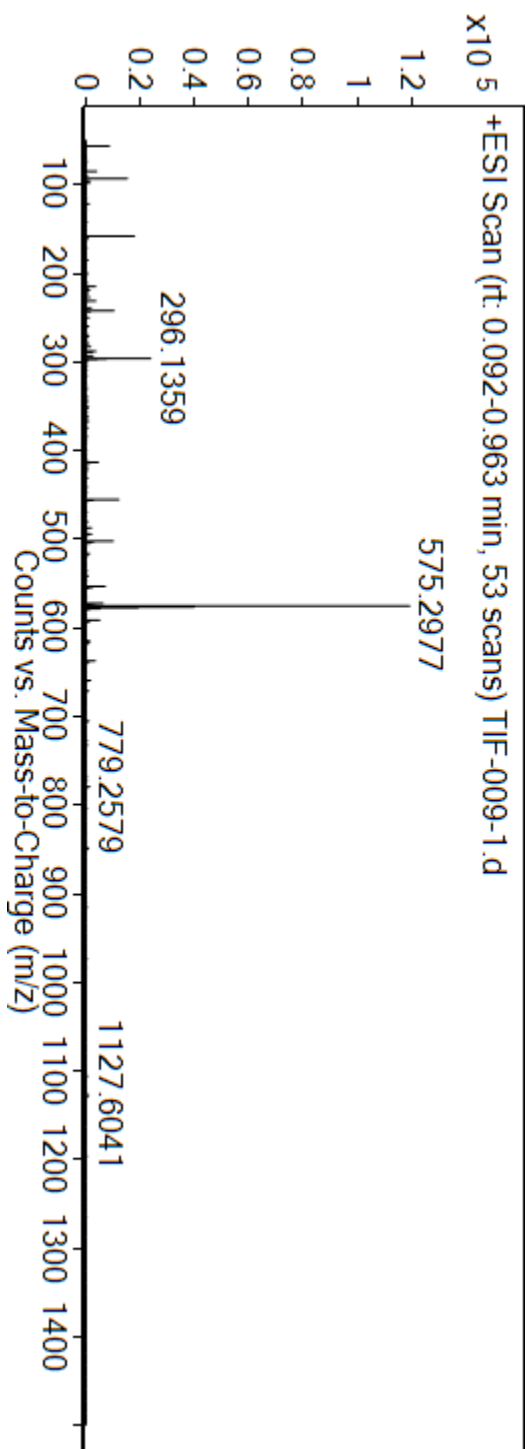
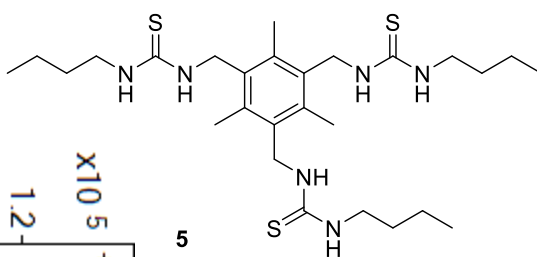


APPENDIX 11

^{13}C -NMR 125 MHz DMF-d₇

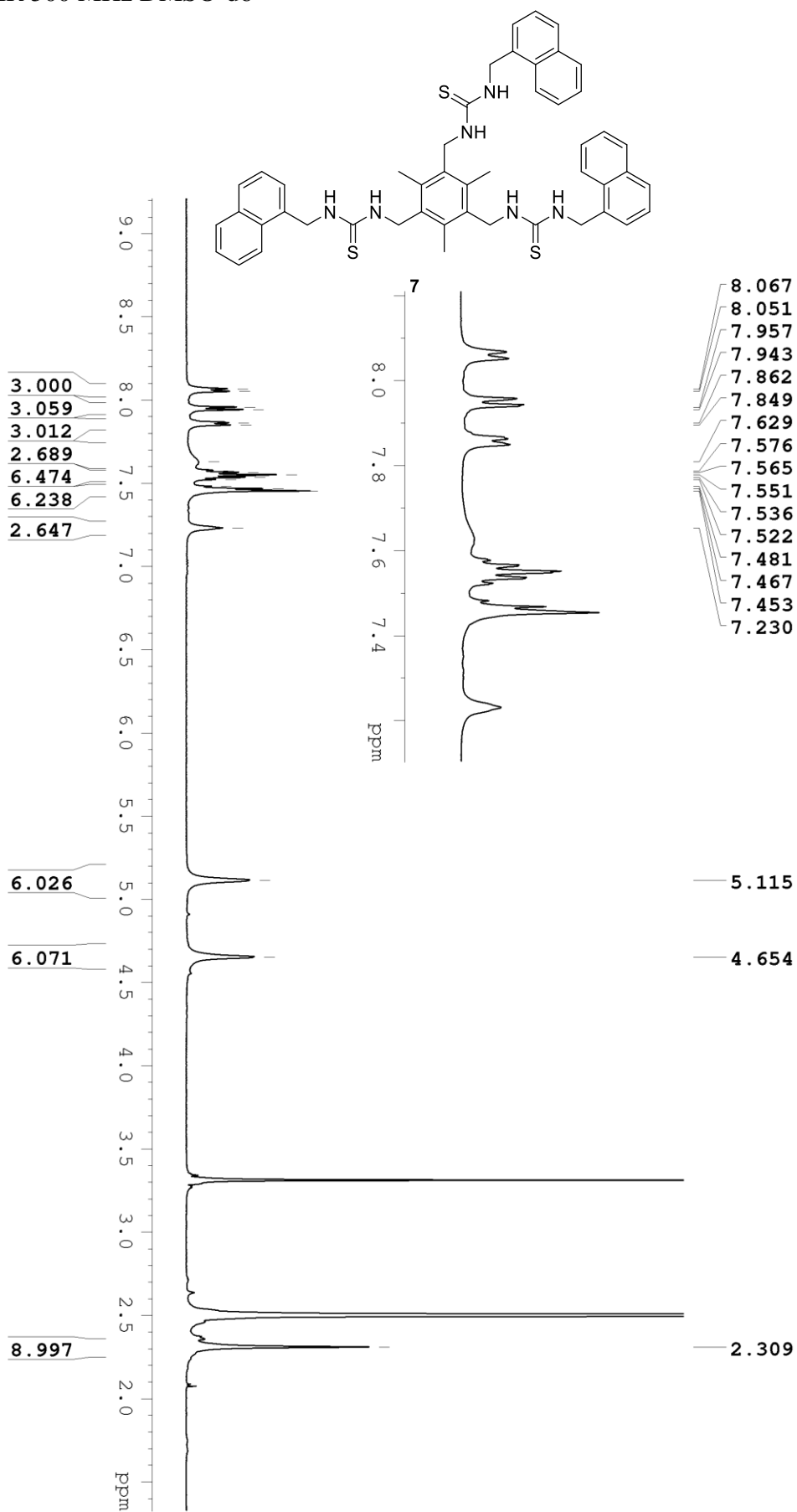


APPENDIX 12
MS



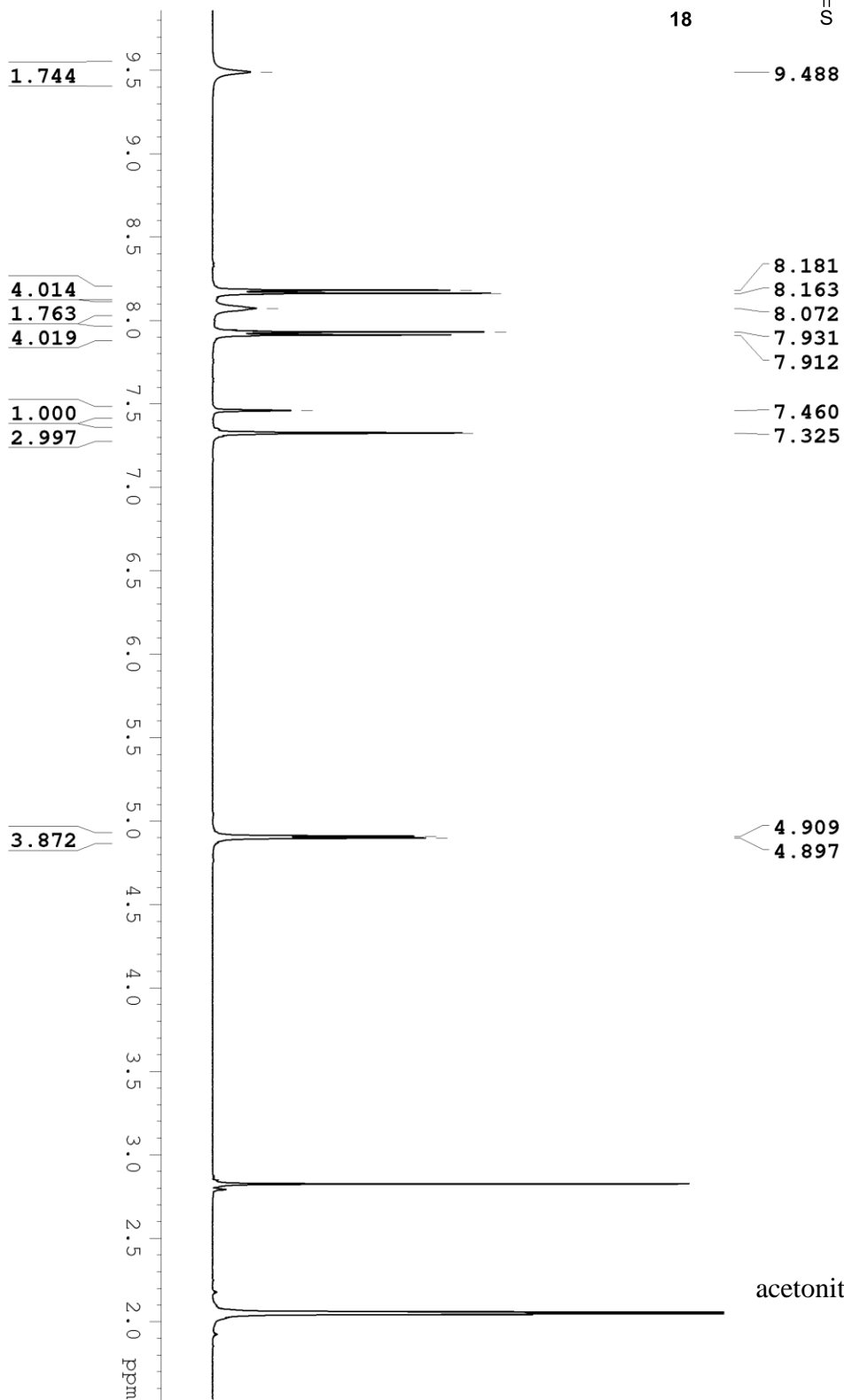
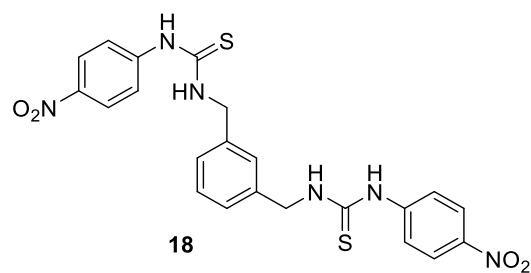
APPENDIX 13

¹H-NMR 500 MHz DMSO-d6



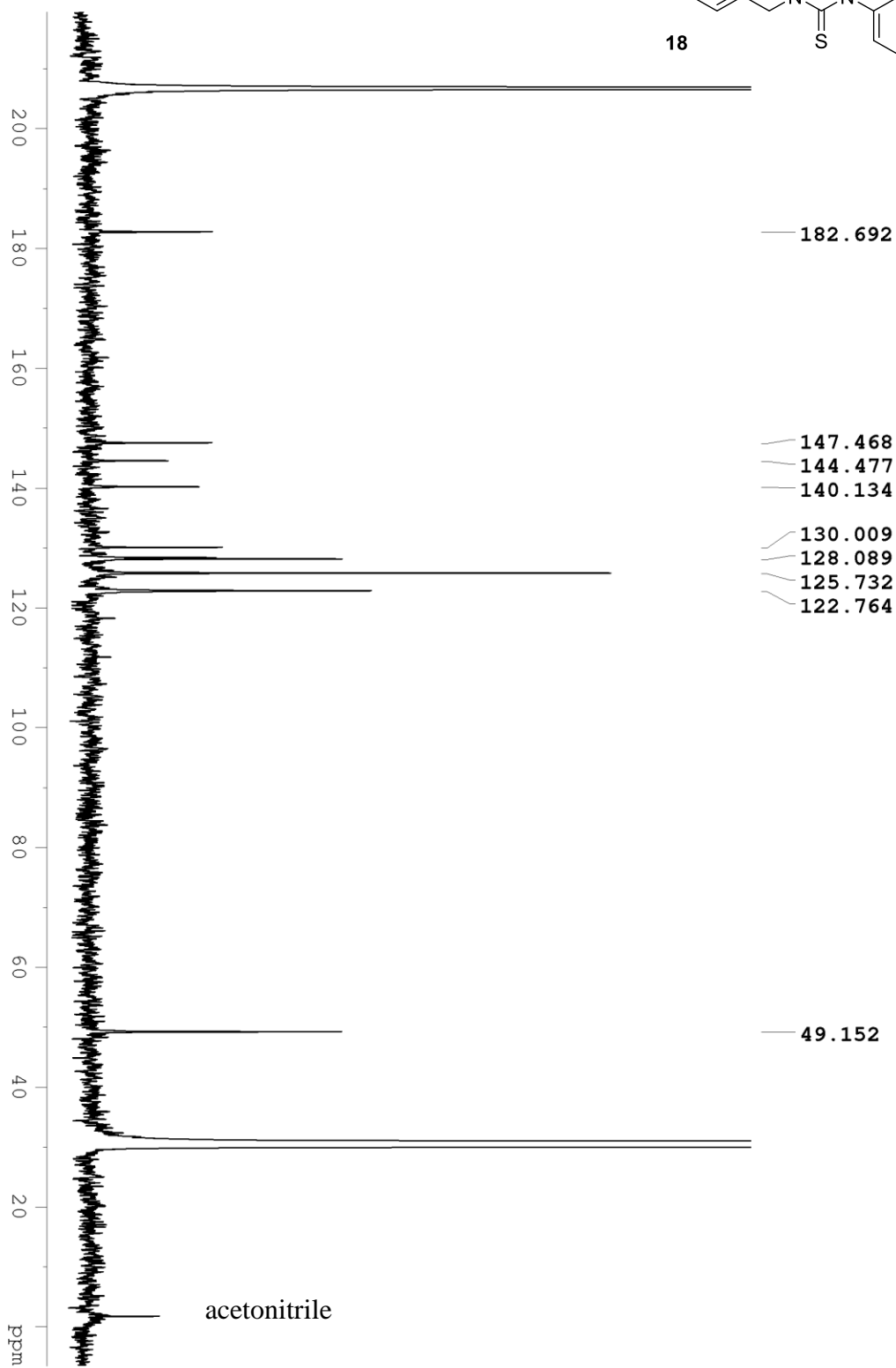
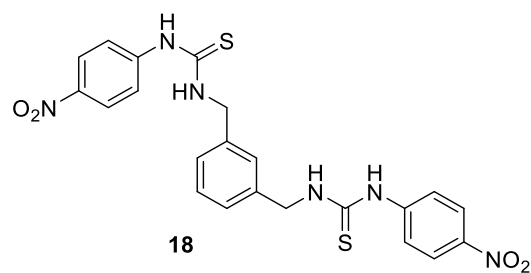
APPENDIX 14

¹H-NMR 500 MHz CD₃COCD₃

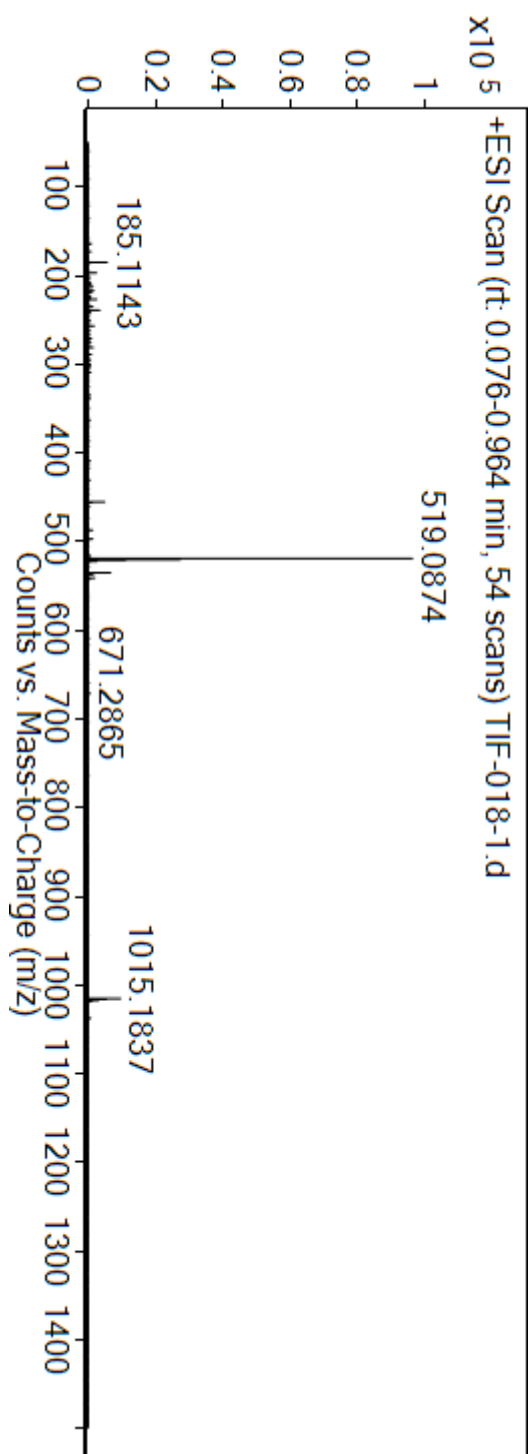
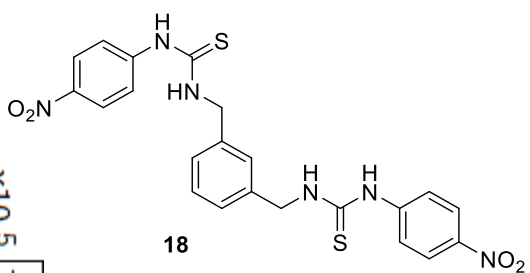


APPENDIX 15

^{13}C -NMR 125 MHz CD_3COCD_3

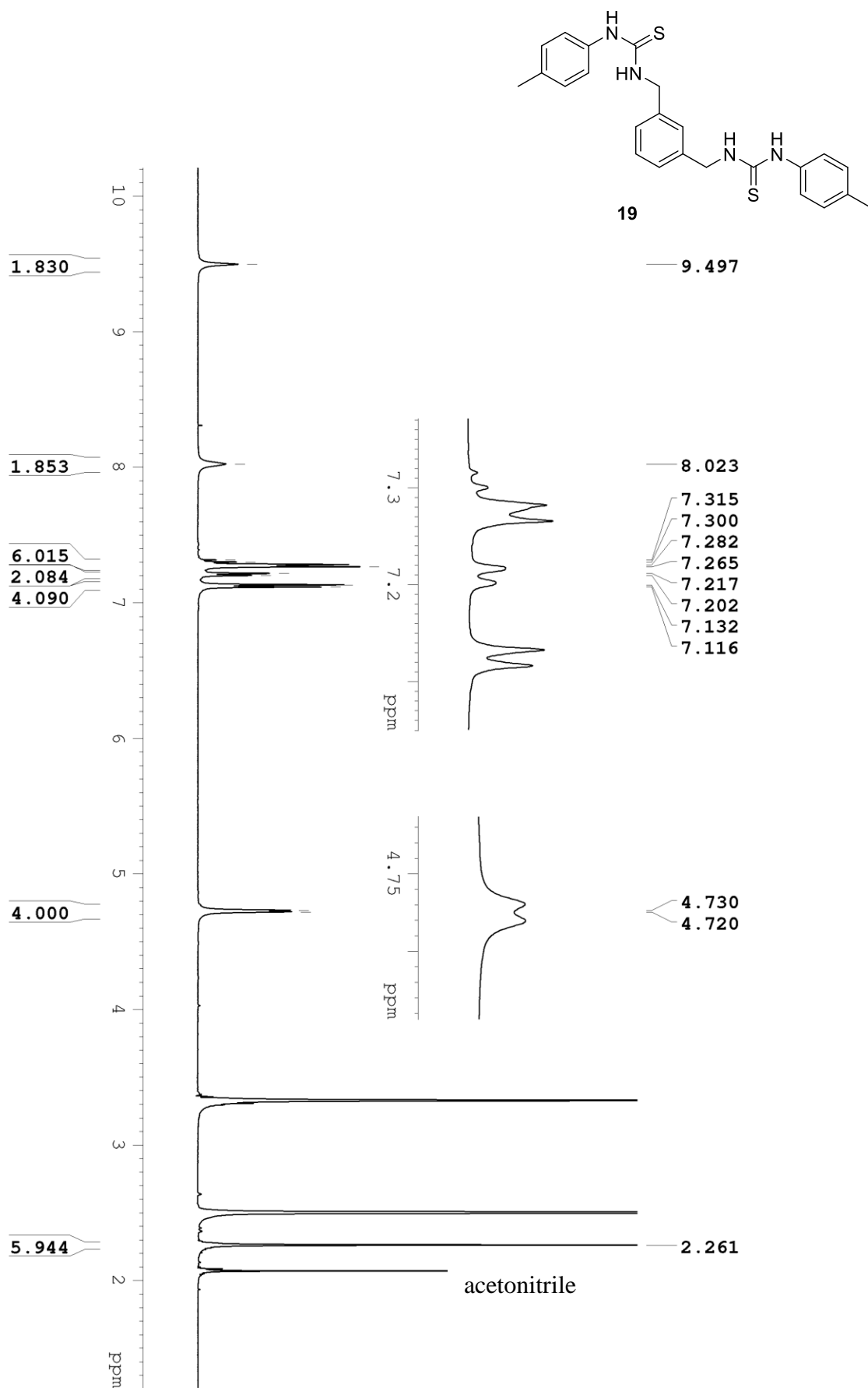


APPENDIX 16
MS



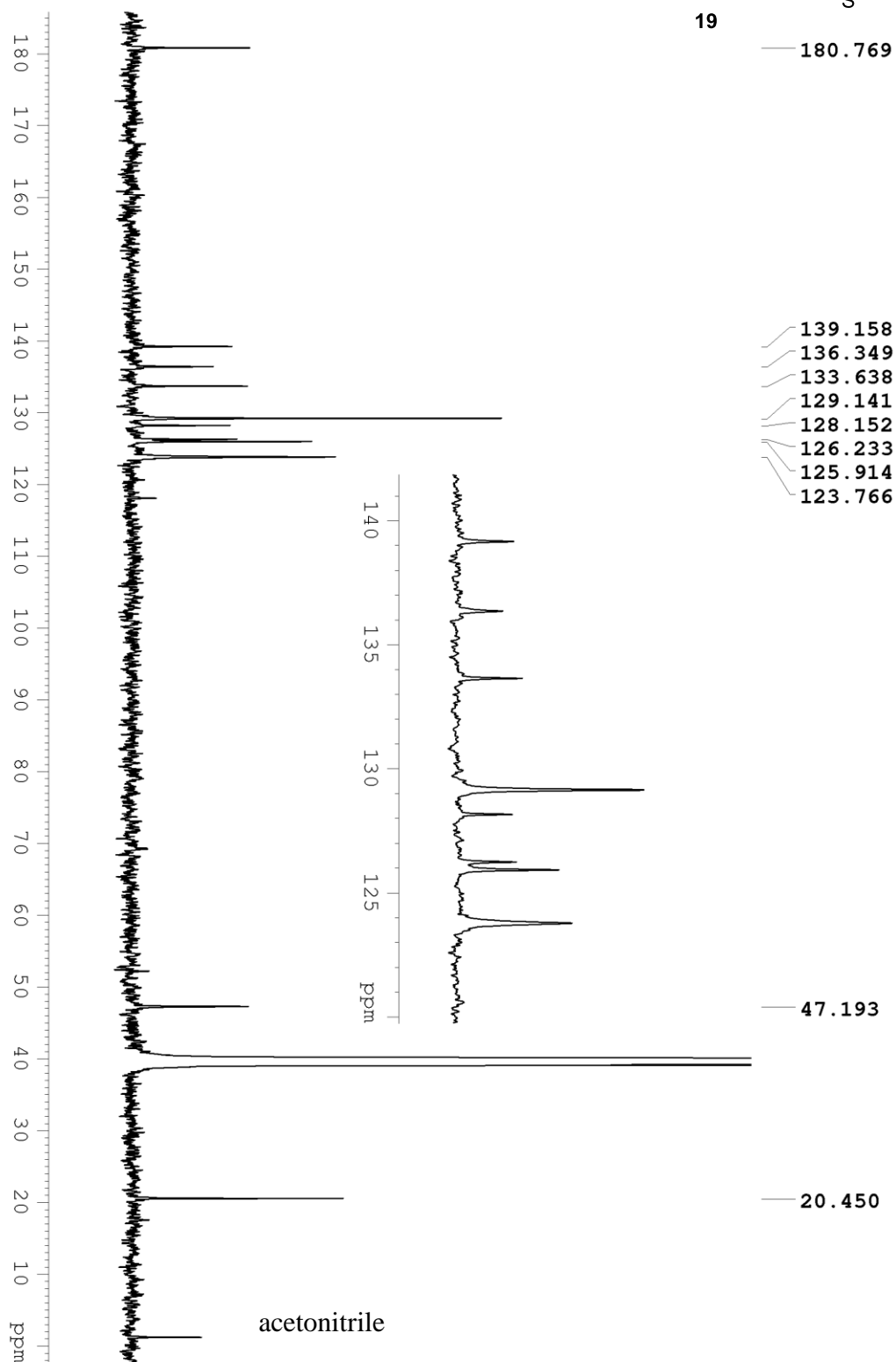
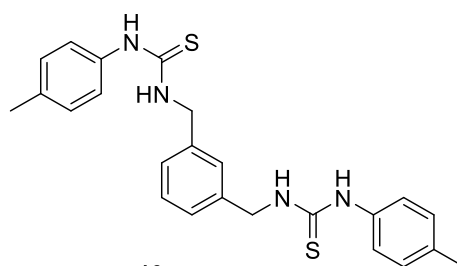
APPENDIX 17

¹H-NMR 500 MHz DMSO-d₆

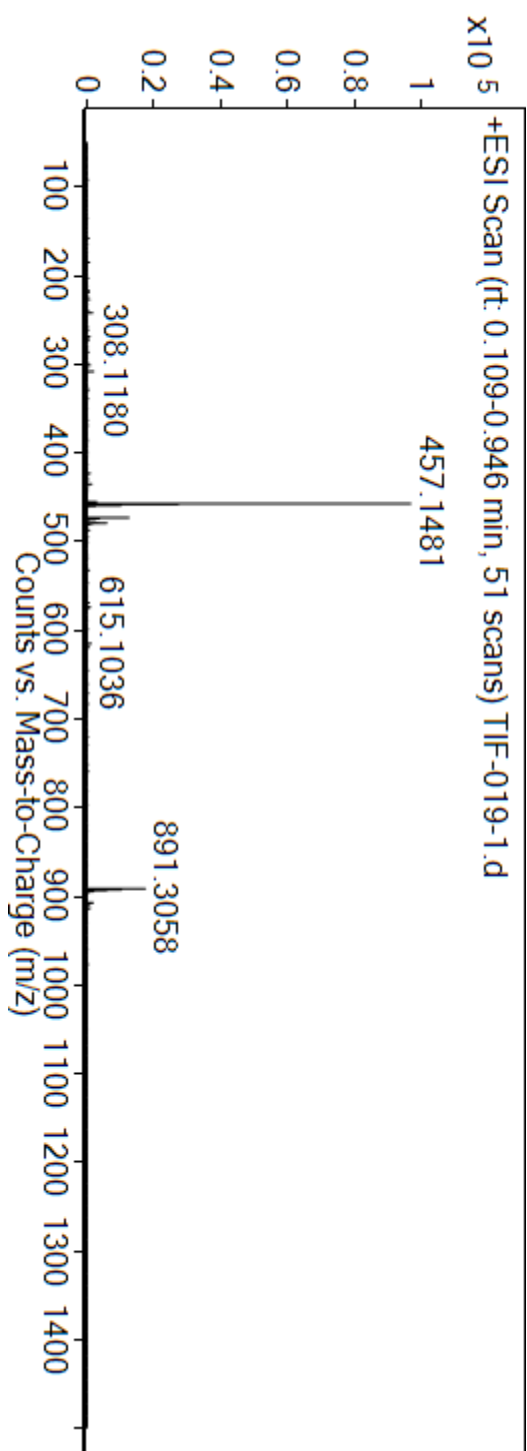
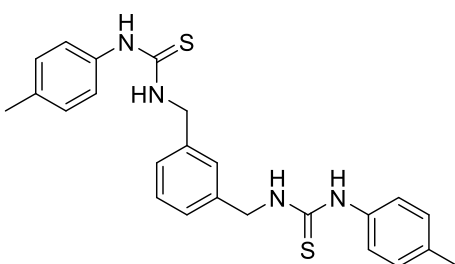


APPENDIX 18

^{13}C -NMR 125 MHz DMSO-d₆

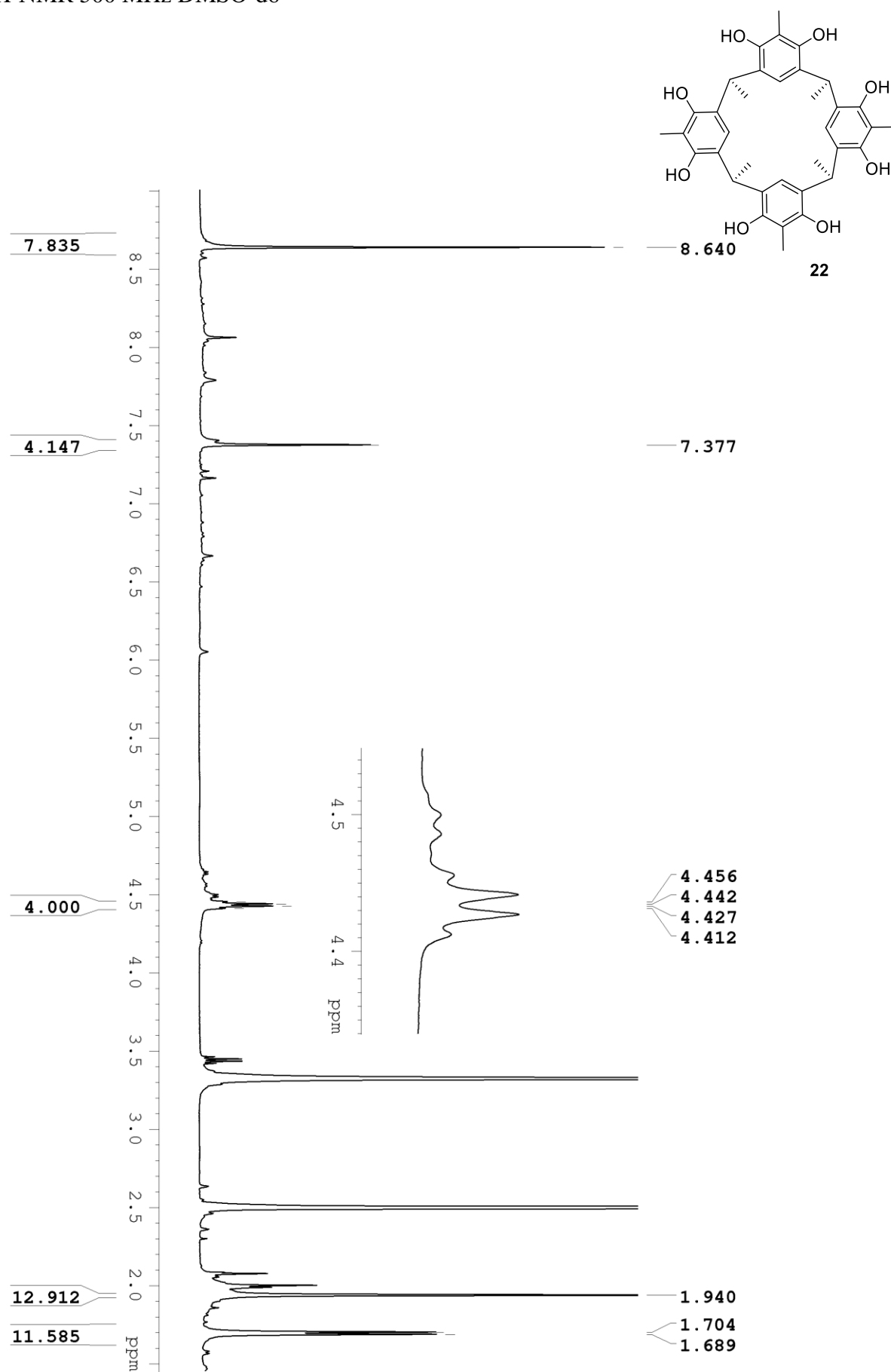


APPENDIX 19
MS



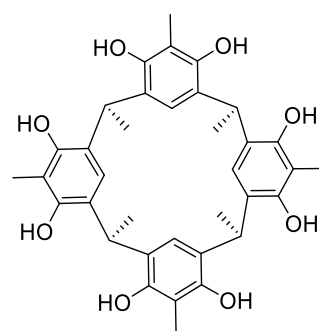
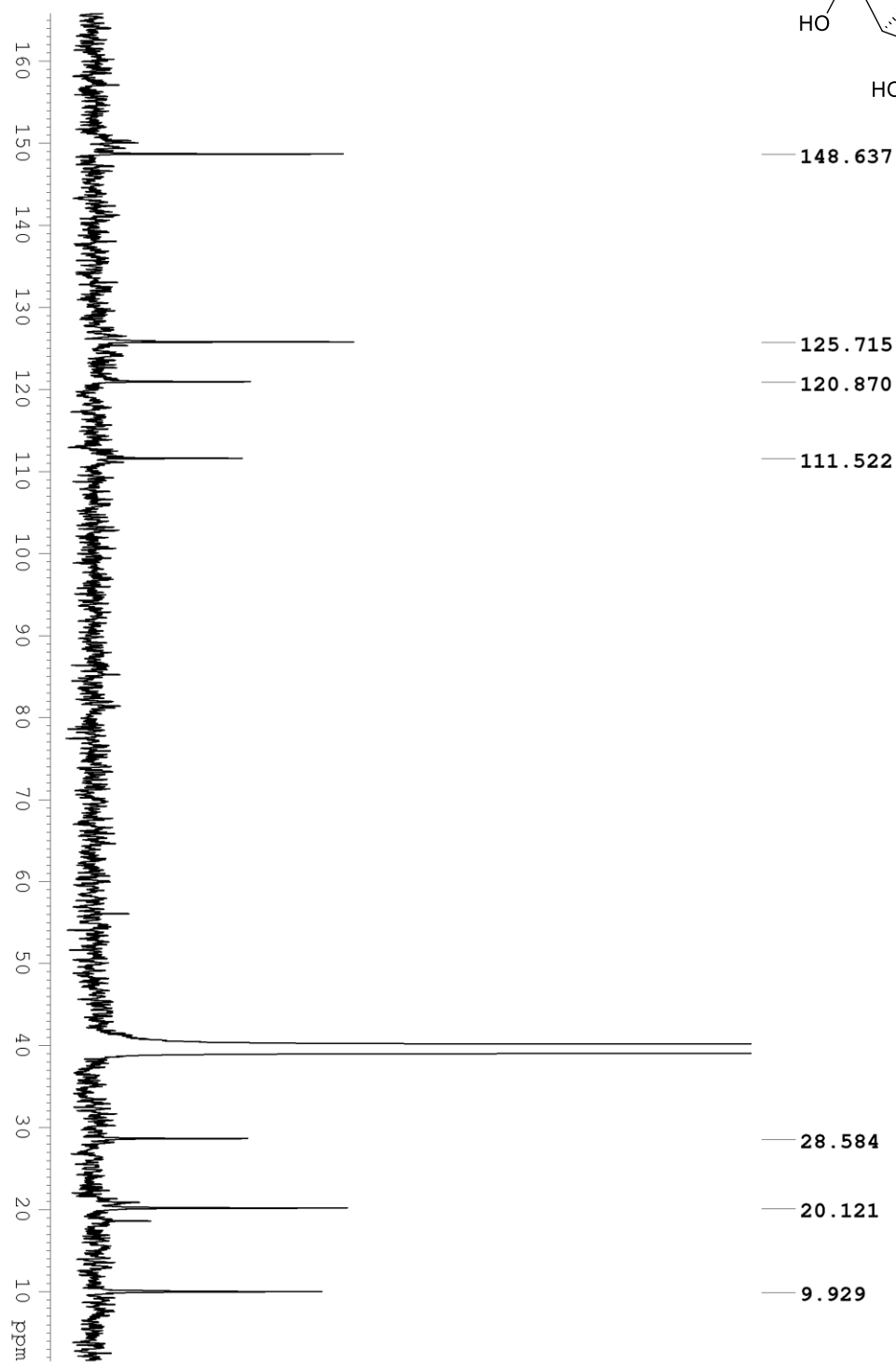
APPENDIX 20

¹H-NMR 500 MHz DMSO-d₆



APPENDIX 21

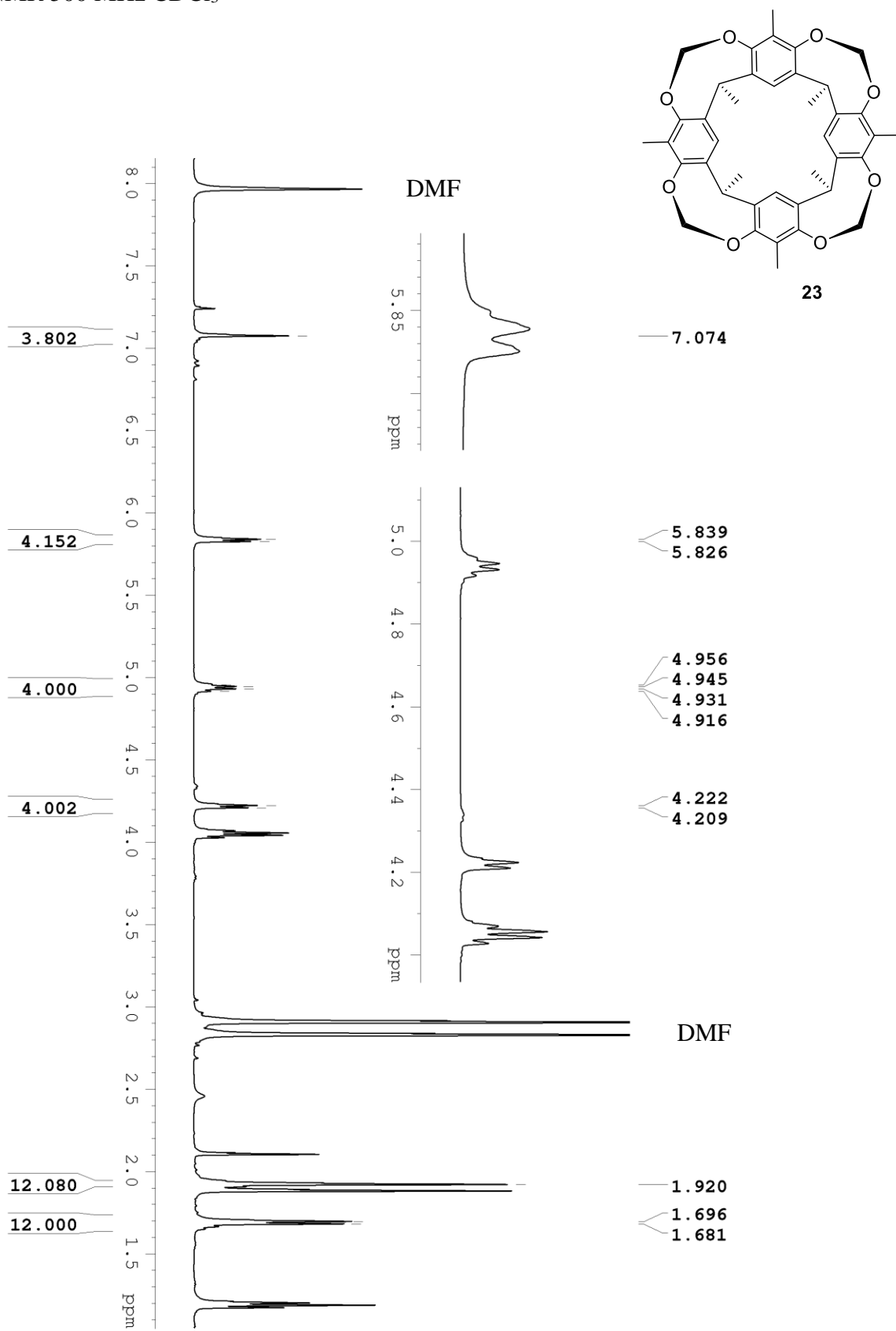
^{13}C -NMR 125 MHz DMSO-d₆



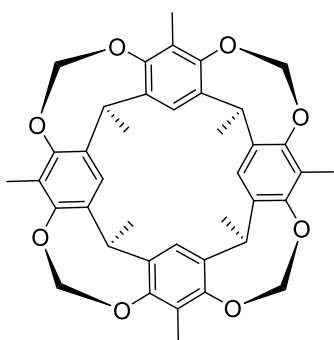
— 148.637 **22**

APPENDIX 22

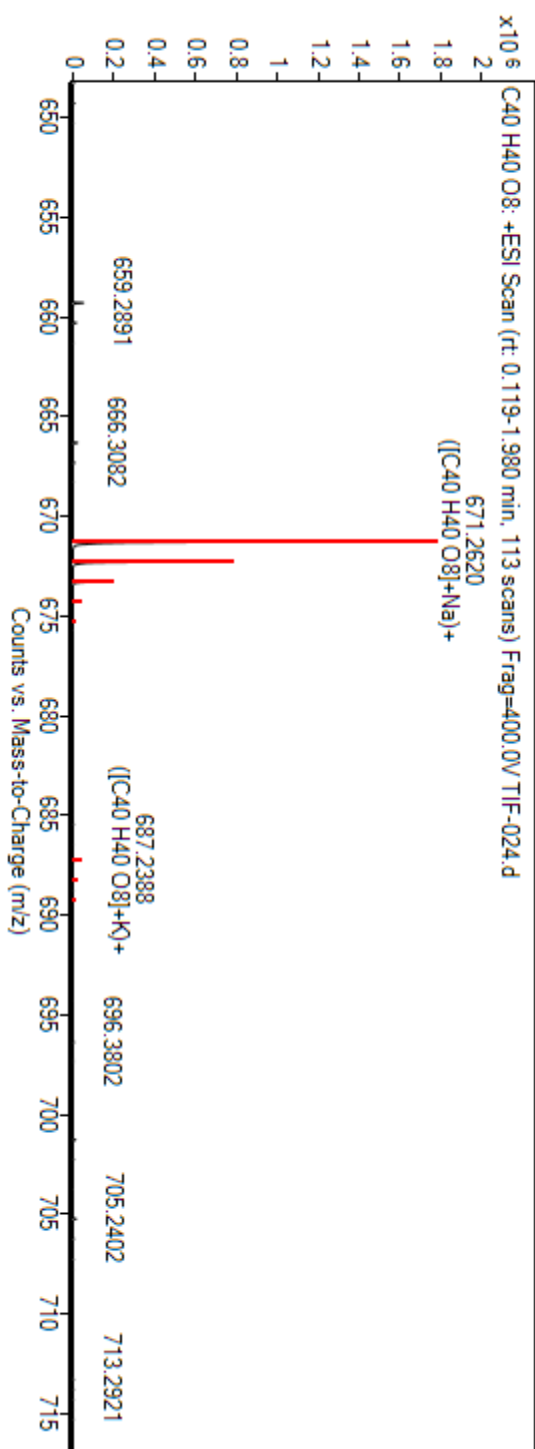
¹H-NMR 500 MHz CDCl₃



APPENDIX 23
MS

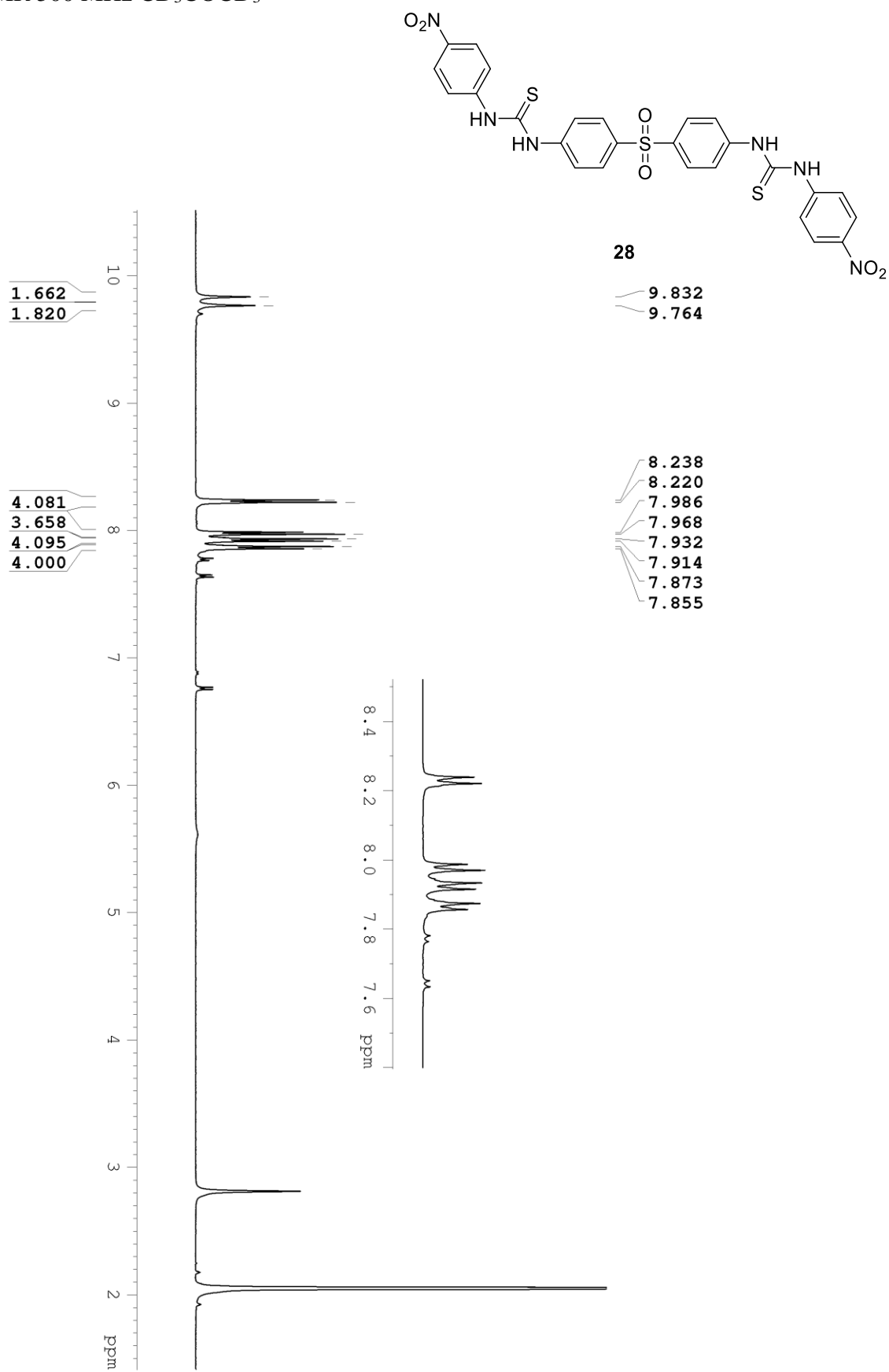


23



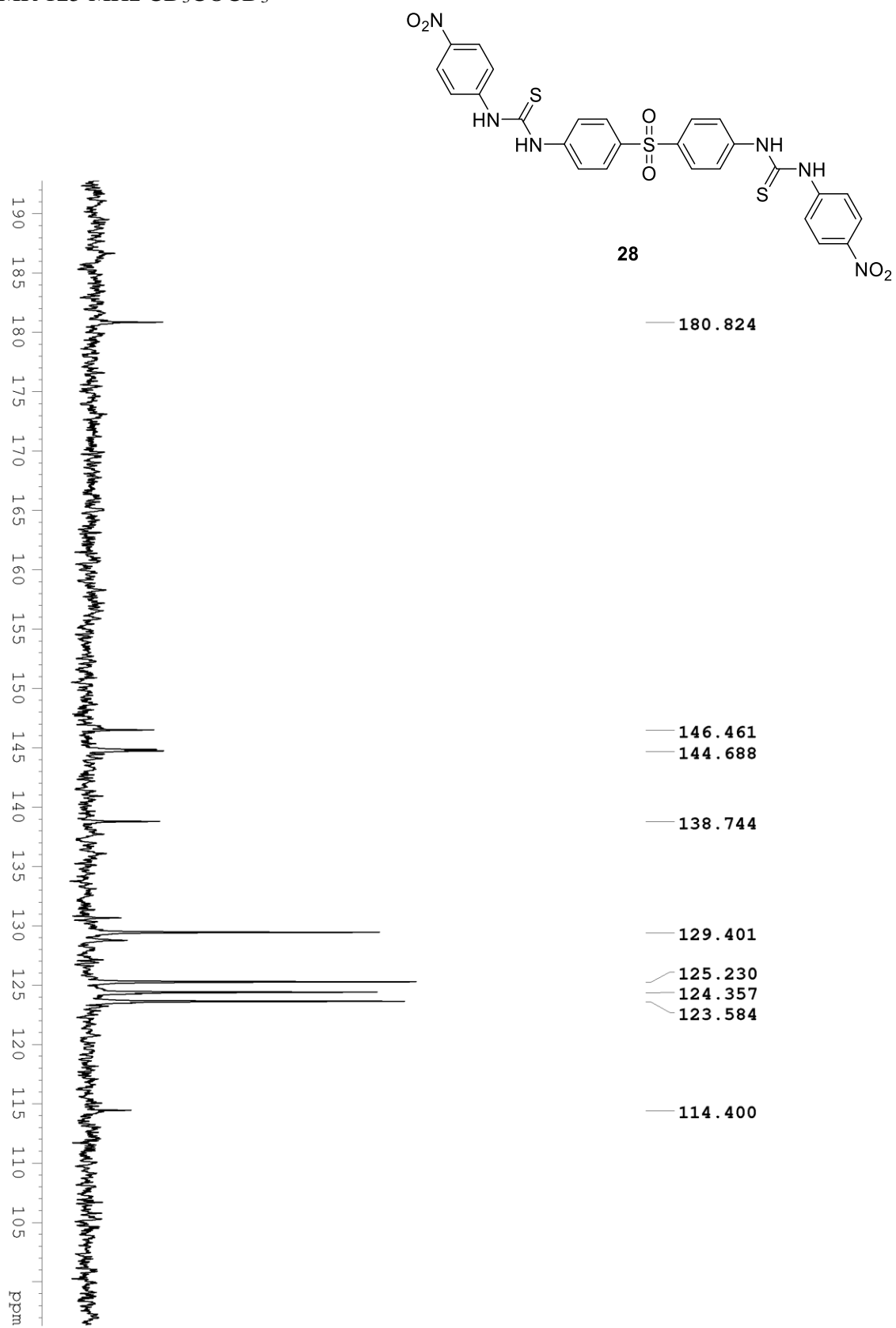
APPENDIX 24

¹H-NMR 500 MHz CD₃COCD₃



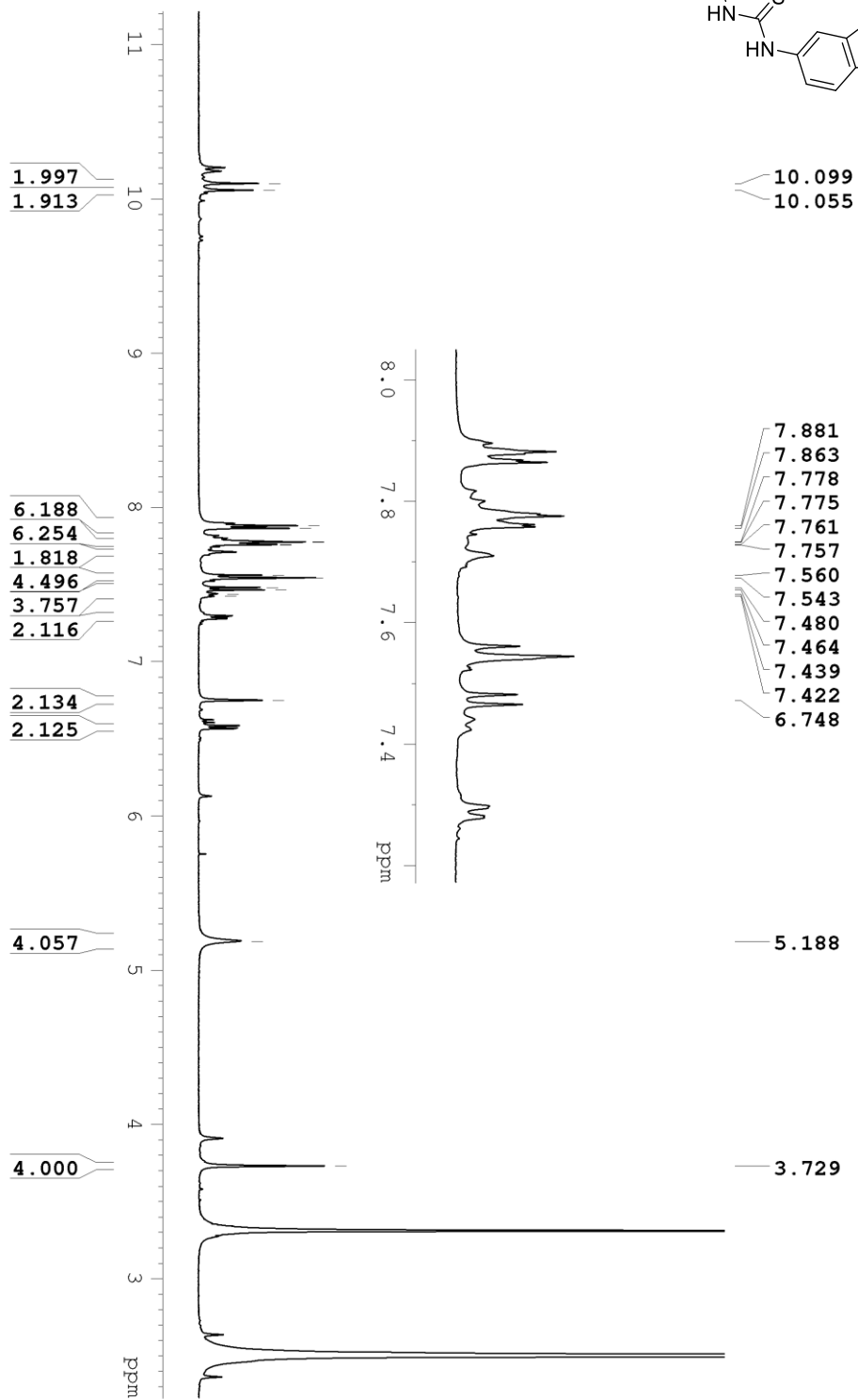
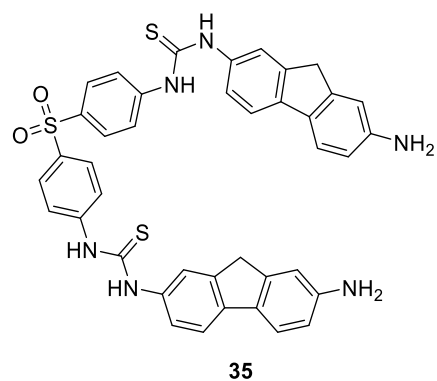
APPENDIX 25

^{13}C -NMR 125 MHz CD_3COCD_3



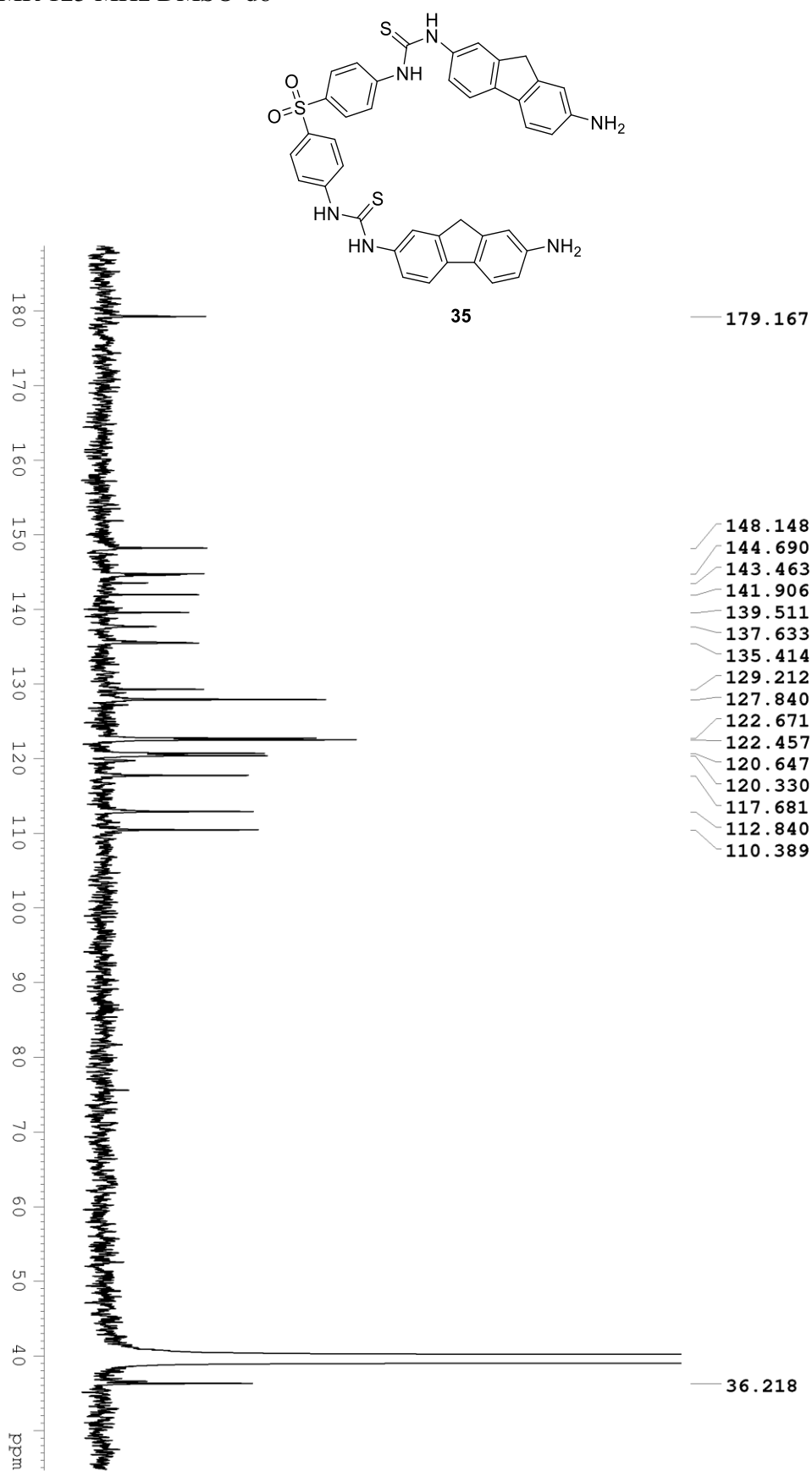
APPENDIX 26

¹H-NMR 500 MHz DMSO-d₆

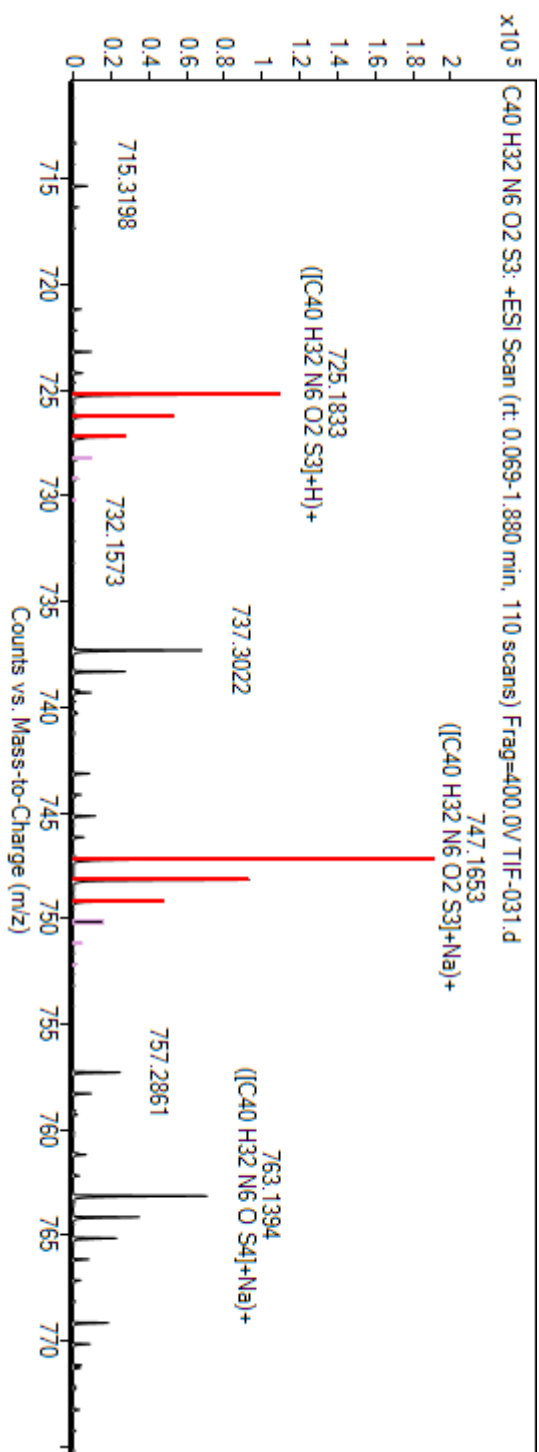
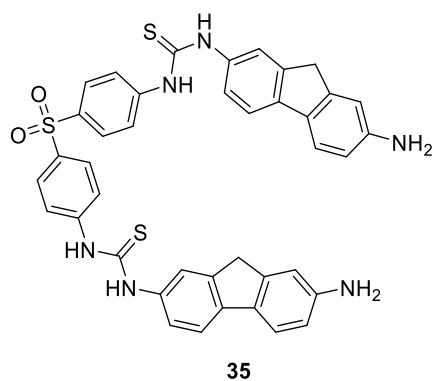


APPENDIX 27

^{13}C -NMR 125 MHz DMSO-d₆

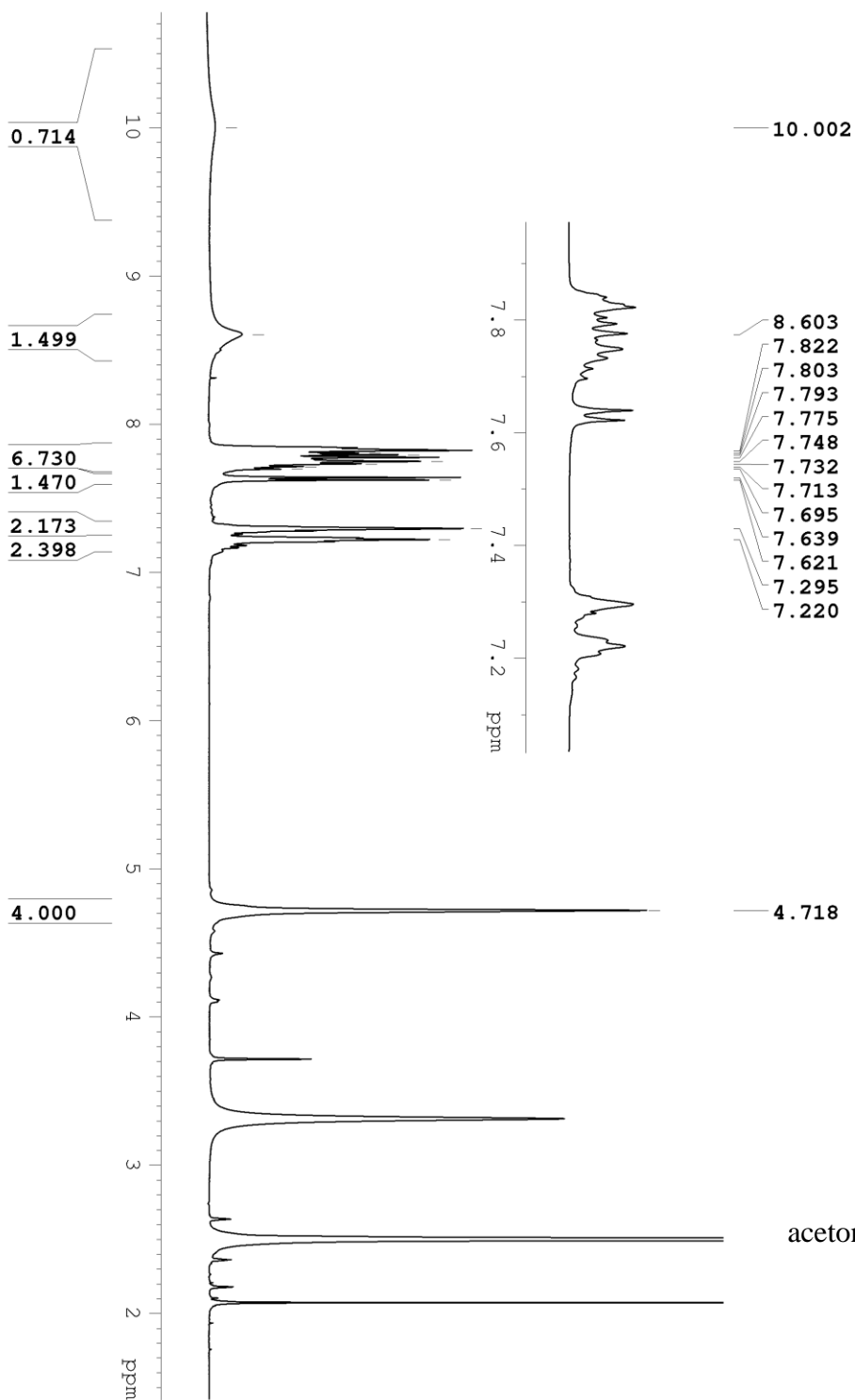
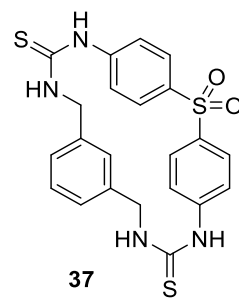


APPENDIX 28
MS



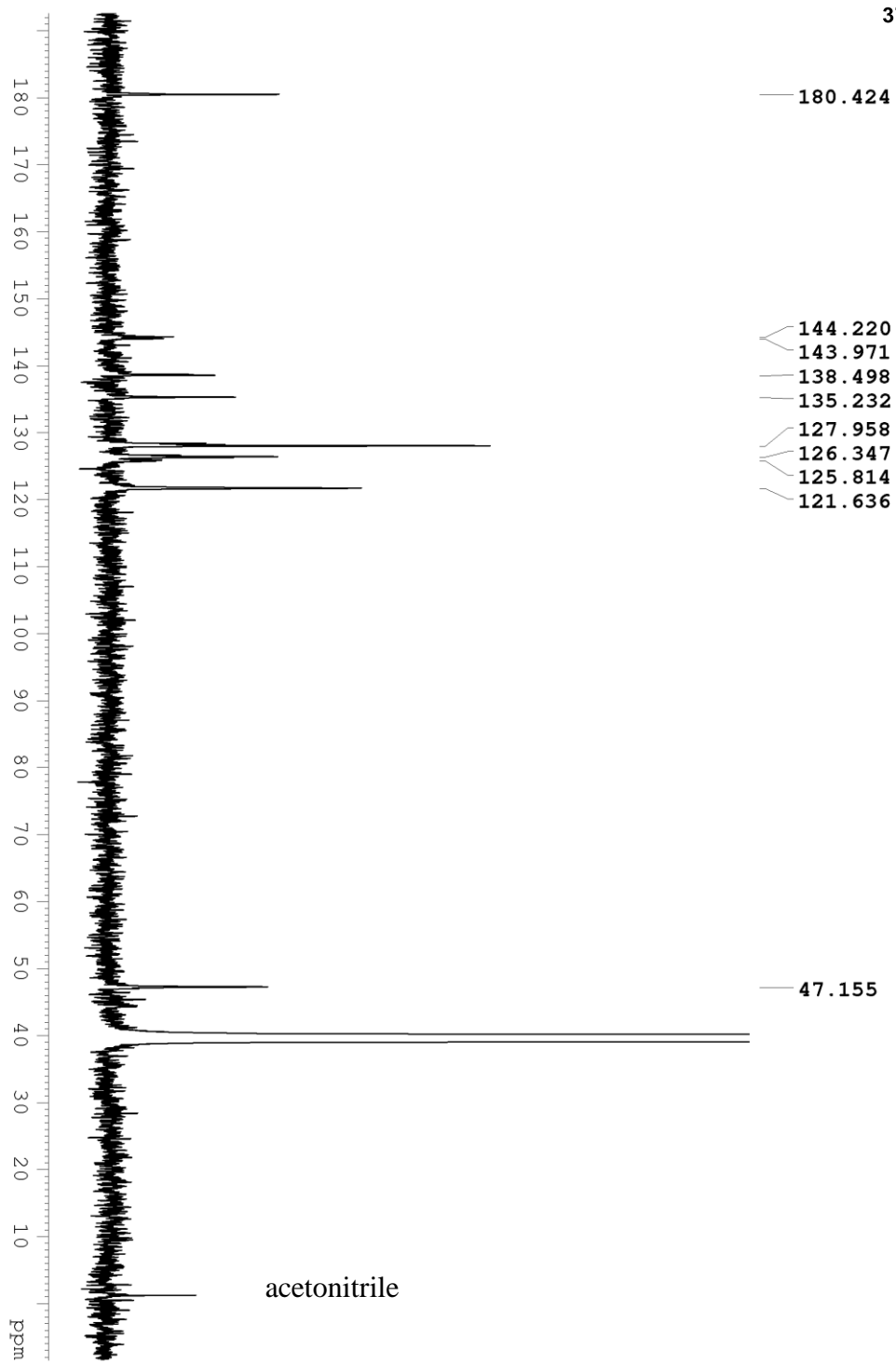
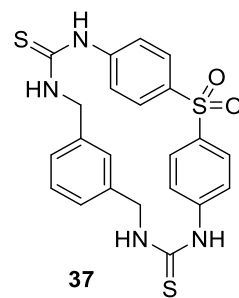
APPENDIX 29

¹H-NMR 500 MHz DMSO-d6



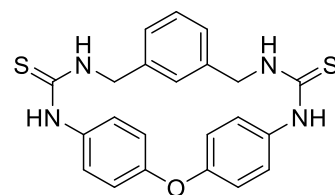
APPENDIX 30

¹³C-NMR 125 MHz DMSO-d₆

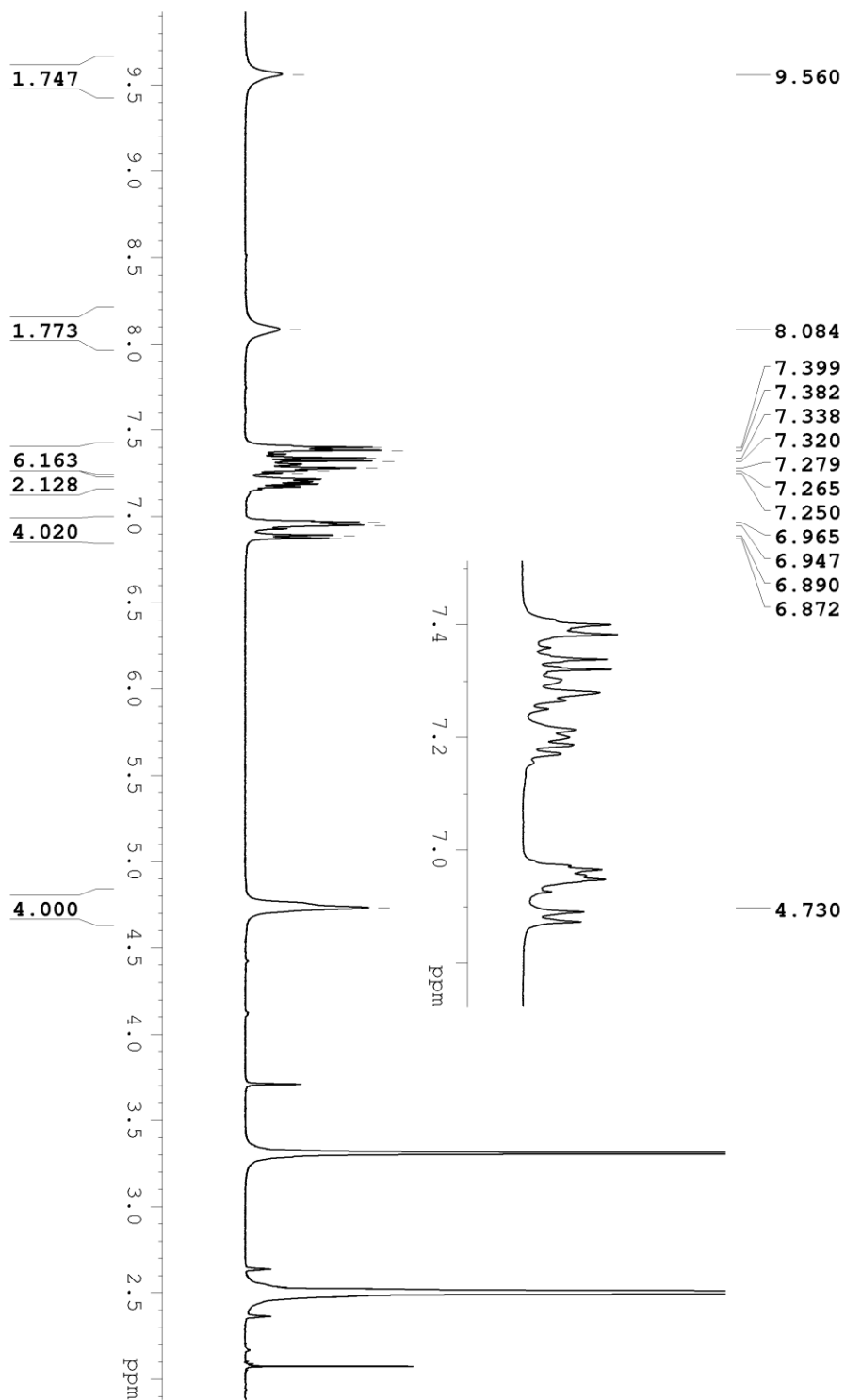


APPENDIX 31

¹H-NMR 500 MHz DMSO-d₆

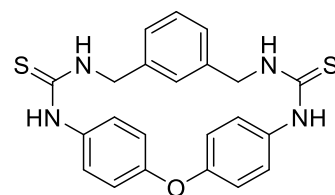


39

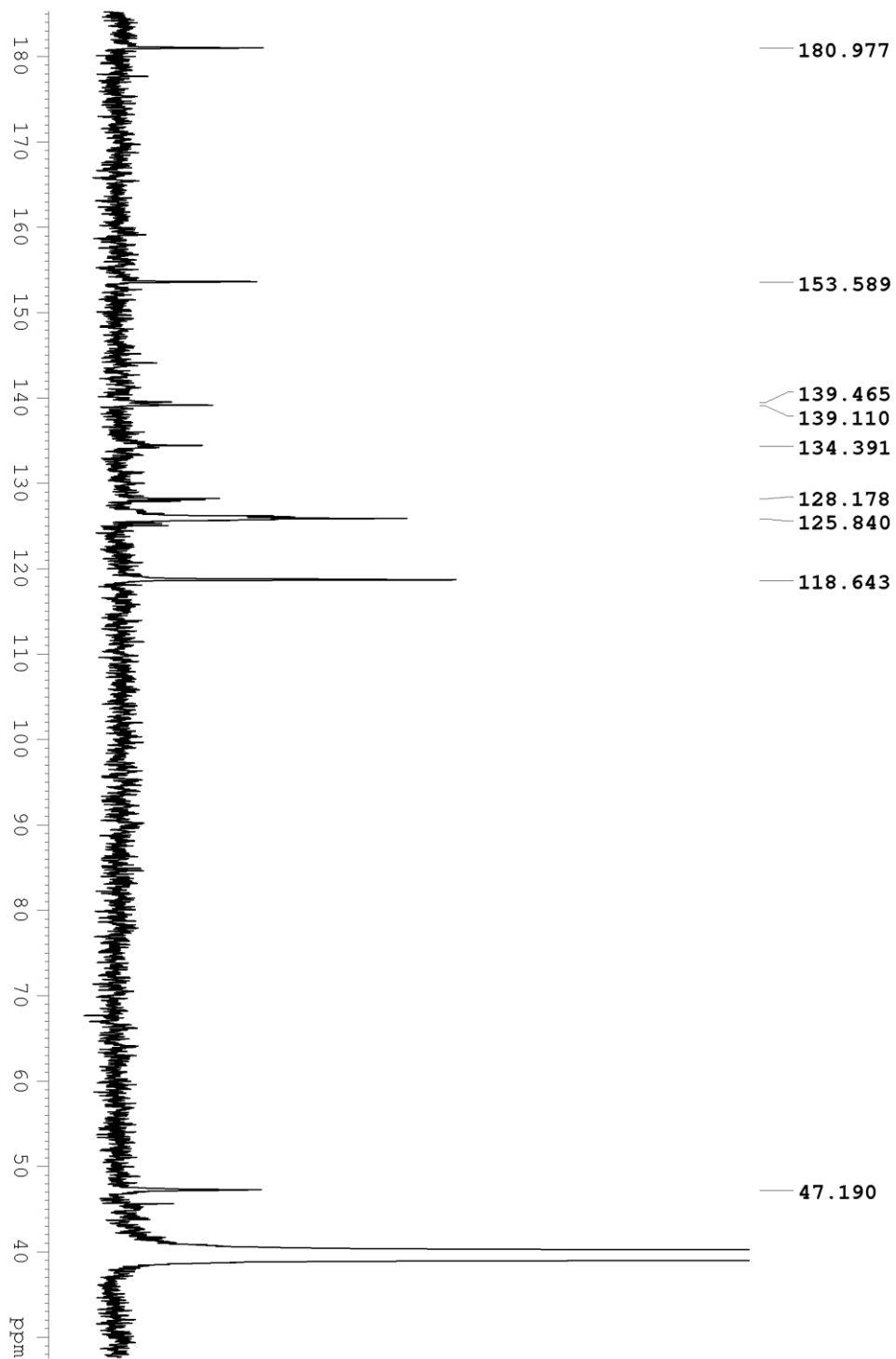


APPENDIX 32

^{13}C -NMR 125 MHz DMSO-d₆



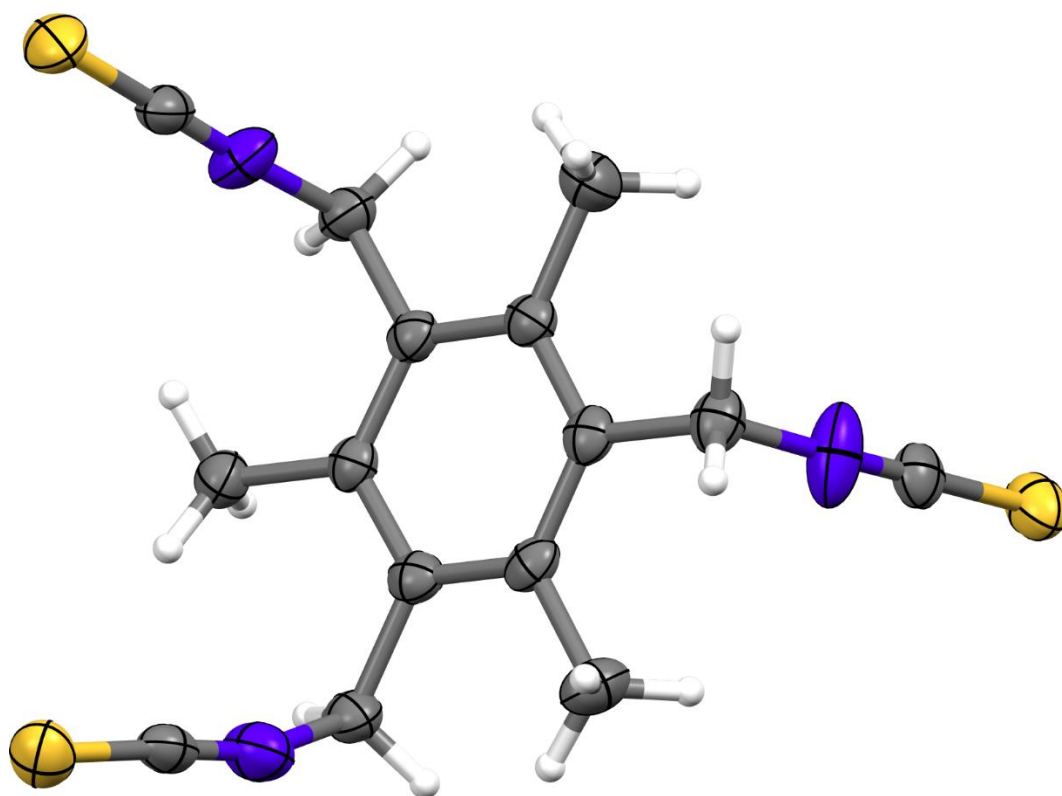
39



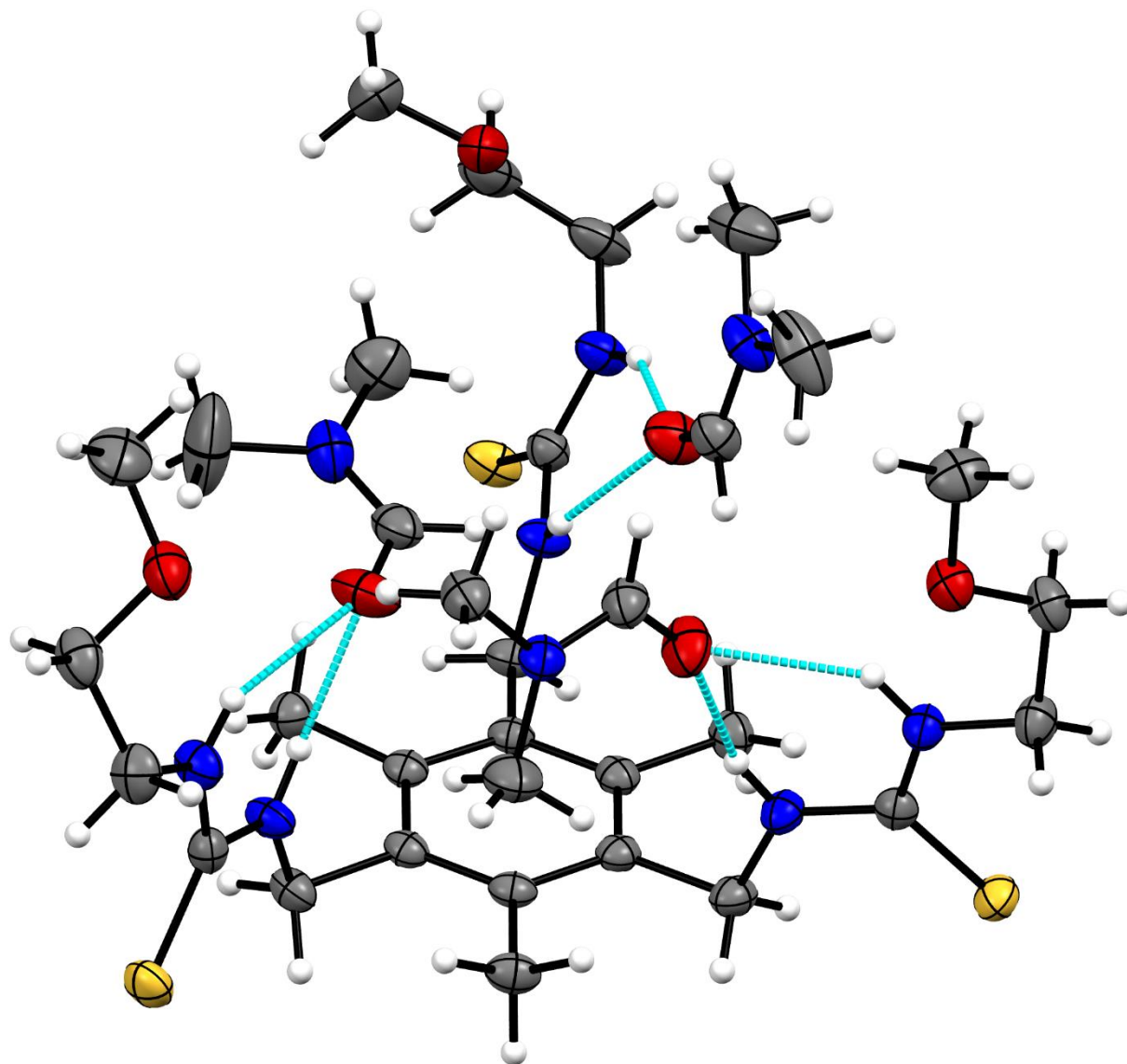
Appendix – Crystal structures

APPENDIX 33

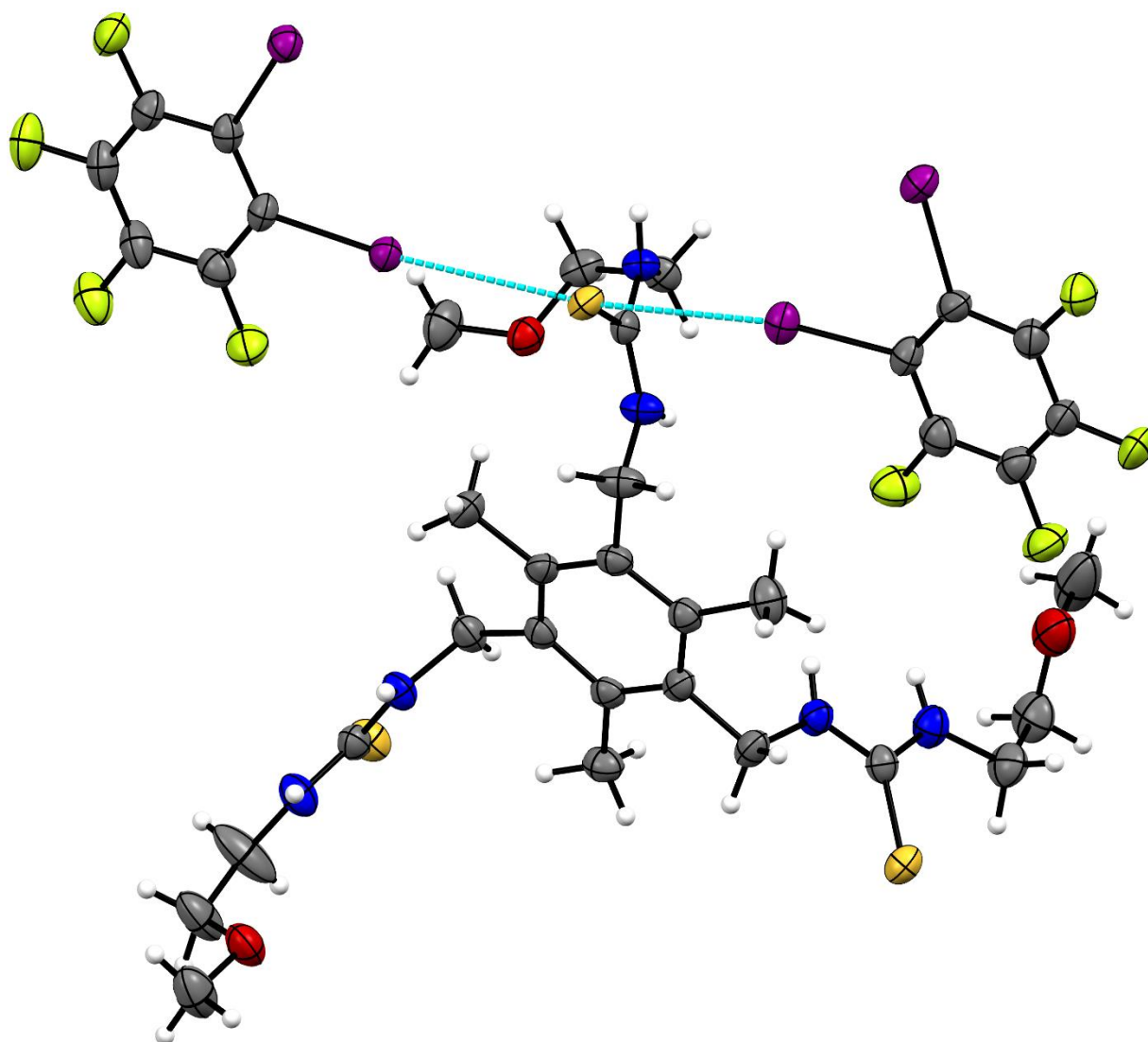
Compound 2



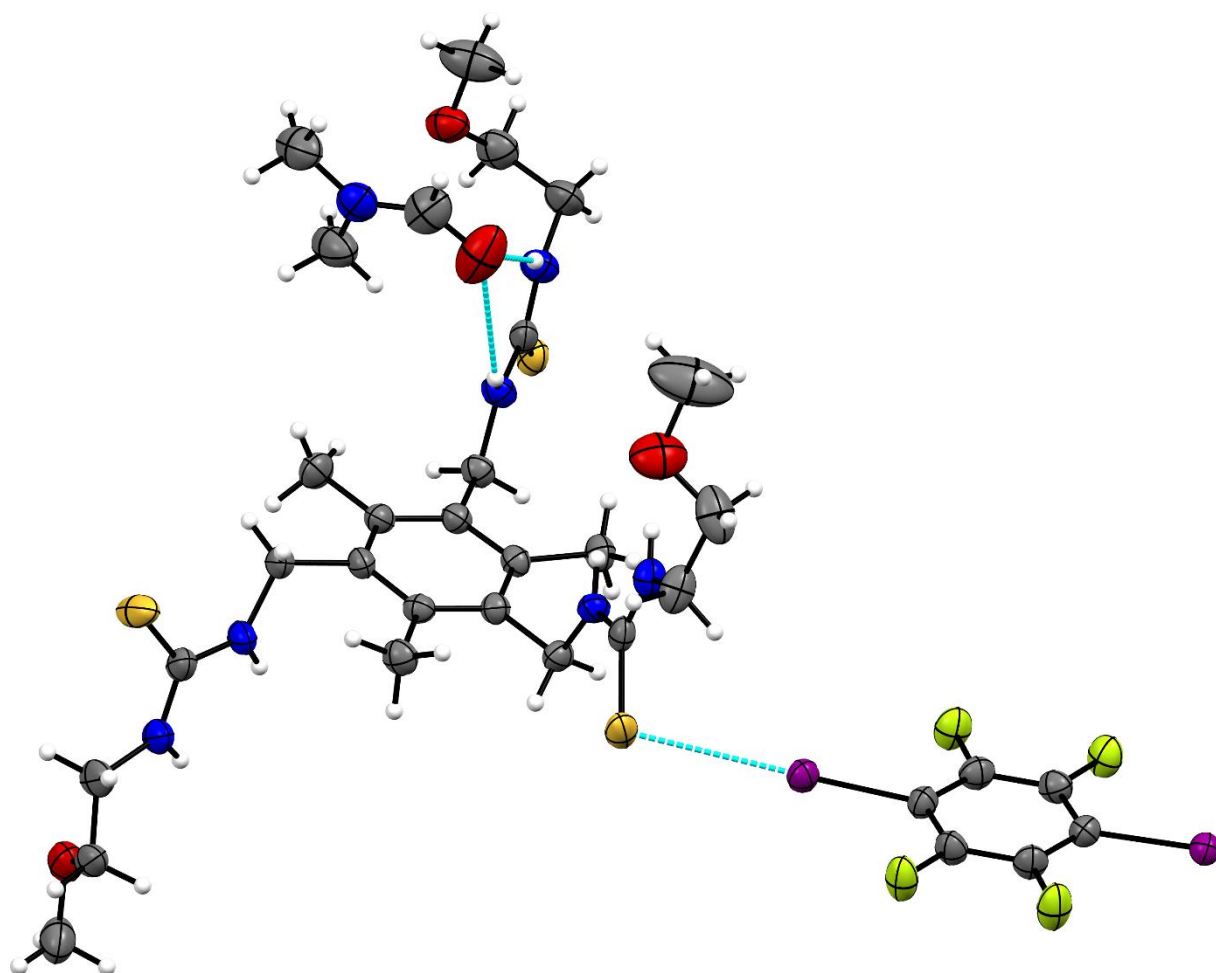
APPENDIX 34
Receptor **3** with three DMF molecules enclosed



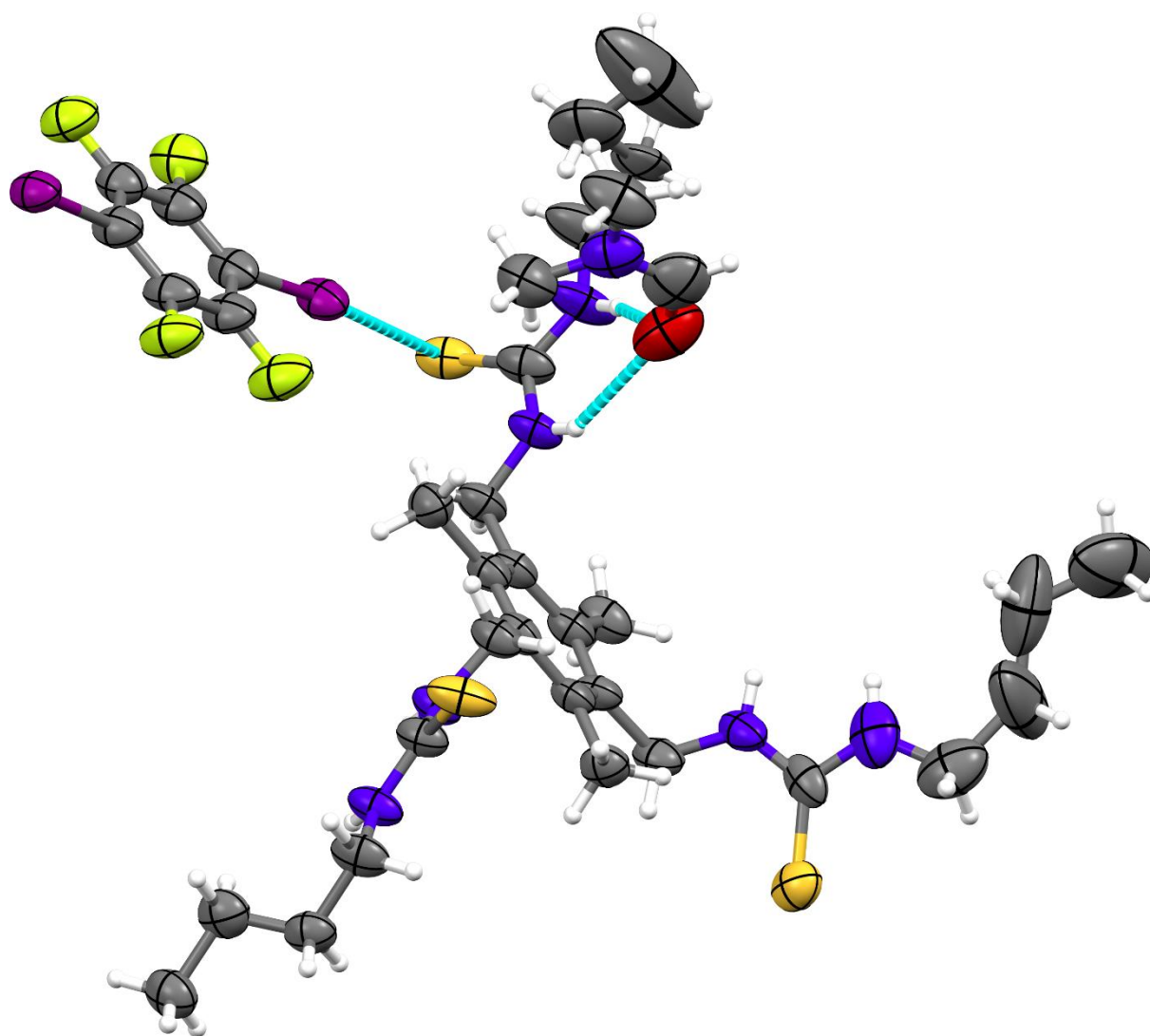
APPENDIX 35
Receptor **3** with 1,2-diodotetrafluorobenzene



APPENDIX 36
Receptor **3** with 1,4-diodotetrafluorobenzene



APPENDIX 37
Receptor **5** with 1,4-diodotetrafluorobenzene



APPENDIX 38
Compound **23** with two CHCl₃ molecules

